Studies on the structure and role of Mge1, a mitochondrial co chaperone of Hsp70 in abiotic stresses adaptation

A Thesis

Submitted to the University of Hyderabad for the award of a Ph.D degree

in Department of Biochemistry, School of Life Sciences

By

Srinivasu Karri

(Regd No. 13LBPH06)

Supervisor
Prof. Dorairajan Balasubramanian
Distinguished Scientist and Director Emeritus,
Prof Brien Holden Eye Research Centre
L.V Prasad Eye Institute
Hyderabad-500034
India

Co-Supervisor
Prof. Naresh Babu V Sepuri
Department of Biochemistry
University of Hyderabad-500046

University of Hyderabad
Hyderabad- 500 046, India

CERTIFICATE

This is to certify that this thesis entitled **"studies on the structure and role of Mge1, a mitochondrial co-chaperone in abiotic stresses adaptation"** submitted by **Mr. Srinivasu Karri** bearing registration number **13LBPH06** in partial fulfilment of the requirements for award of Doctor of Philosophy in the Department of Biochemistry, School of Life Sciences, is a bonafide work carried out by him under my supervision and guidance.

This thesis is free from plagiarism and has not been submitted previously in part or in full to this or any other University or Institution for award of any degree or diploma.

Parts of this thesis have been:

A. Published in the following publications:

1. Karri, S., Singh, S., Paripati, A. K., Marada, A., Krishnamoorthy, T., Guruprasad, L., ... & Sepuri, N. B. V. (2018). Adaptation of Mge1 to oxidative stress by local unfolding and altered Interaction with mitochondrial Hsp70 and Mxr2. *Mitochondrion*.Chapter-5.

2 Marada, A., **Karri, S**., Singh, S., Allu, P. K., Boggula, Y., Krishnamoorthy, T.,. & V Sepuri, N. B. (2016). A Single Point Mutation in Mitochondrial Hsp70 Cochaperone Mge1 Gains Thermal Stability and Resistance. *Biochemistry*, *55*(51), 7065-7072 (equally contributed).

B. Presented in the following conferences:

Karri S, Paripati AK, Marada A, Krishnamoorthy T, Balasubramanian D, Sepuri NBV Mge1 , nucleotide exchange factor of Hsp70 response to global stress by regulating Hsp70 chaperone cycle and helps in cell survival by inducing mitochondrial unfolded protein response. *Stress Proteins in Growth, Development & Disease (Gordon Research Conferences)*, Grand Summit Hotel at Sunday River in Newry ME United States.

Further, the student has passed the following courses towards fulfilment of coursework requirement for Ph.D.

Course code	Name	Pass/Fail
REM	Research ethics and management	Pass
AT	Analytical techniques	Pass
BS	Biostatistics	Pass

Supervisor **Co-guide** **Head of Department** **Dean of School**

University of Hyderabad
Hyderabad- 500 046, India

DECLARATION

I, **Srinivasu Karri**, hereby declare that this thesis entitled **"Studies on the structure and role of Mge1, a mitochondrial co-chaperone in abiotic stresses adaptation"** submitted by me under the guidance and supervision of **Professor Dorairajan Balasubramanian**, is an original and independent research work. I also declare that it has not been submitted previously in part or in full to this University or any other University or Institution for the award of any degree or diploma.

Date:

Signature of the student

Name: Srinivasu Karri

Regd No. 13LBPH06

Signature of the Supervisor

Signature of the Co-guide

Dedicated to

Prof. Balu Sir

ACKNOWLEDGEMENTS

First and foremost I would like to thank **Prof. Dorairajan Balasubramanian**, Distinguished Scientist and Director Emeritus, Prof Brien Holden Eye Research Centre, for giving me an opportunity to work in his lab. Though in the beginning it was scary but afterwards especially when I was playing around with the fluorescence spectroscopy, it was always motivating and encouraging meeting him in the corridors and discussing new results. I heartily thank for his patience and faith in me to work. His scholarly guidance and inspiring suggestions have helped me in carrying out the present research work. Words are inadequate to express my deep sense of gratitude to him for his valuable guidance.

I cannot dream about this thesis without the strong support, guidance and co-operation of **Prof. Naresh Babu V. Sepuri**, Professor, Department of Biochemistry, and University of Hyderabad. In fact, I have learnt a great deal from Prof. Naresh Babu regarding research methodology, particularly the tools and techniques used in the present study. Without his valuable guidance and suggestions, this research project would not have been possible.

I thank University of Hyderabad for providing me a very good infrastructure, resources for laboratory work, informative lectures and seminars and a chance to meet eminent scholars from various fields.

I would like to thank Council for Scientific and Industrial Research (India) and Hyderabad Eye Research Foundation for the funding support throughout my PhD. I truly thank the Department of Science and Technology (ITS) for giving international travel grants to attend the Gordon Research Conference on Stress Chaperones and Diseases, Maine (ME), Newry, USA.

I would like to thank Dr. GN Rao, Dr. G Chandrasekhar and Dr. Shivaji for providing wonderful laboratory and infrastructure facilities at LVPEI, granting me the permission and opportunity to carry out my research here.

I am thankful to Prof. Lalitha Guruparasad and swati singh, school of chemistry, university of Hyderabad for helped me in compoutational aspects.

I am thankful to Dean of life sciences and Head of the Biochemistry department, School of life sciences, Hyderabad Central University. It was really kind of Mr. Chary for taking care of my PhD related matters, helping me a lot starting from the registration of PhD till the submission.

I am grateful to faculty members from LVPEI, Dr. Chitra, Dr. Indumathi, Dr Inderjeet Kaur, Dr.Subhabrata Chakrabarti, Dr. Vivek, Dr. Sachin, Dr. Sanhita, Dr. Savitri and all the other research faculties for providing me valuable comments and suggestions during research seminars.

I thank Jai ganesh, Elena, Moddin, Divya, and Preeti and Srinivas for providing me administrative support. I truly thank Savitri for supporting in scientific and non-scientific issues. I also thank Bhanu, Sudhakar for helping in getting photocopies of research articles.

I am greatful to Sridhar for sharing rare chemical and Prasad for allowing me the use the CD manchine.

I would like to thank my seniors Pulla rao, Ramesh Babu, Aadinarayana, Anjineylu, Praveen Kumar, Prasad, Madhavi, Pulla Reddy, Samuel and Usha for helping me in learning Methodologies.

I am fortunate to have Verma, Shanmukha, Mohan Raj, Kiran, Santosh, Brahmmi, Somashekar and many others were always there to share the ups and downs of PhD life and to chat for hours to forget everything. I also thank Praveen J, Meha, Shahna, Satish, Vinay, and sonika for their support and help during my stay in LVPEI.

I have to thank other labmates, Amita, Arun, Fareed, Prasad, Yerranna, Venkata Ramana, Arpan, Dr. Usha, Dr. Noble, Vandana, Dr. Aritra, Priyanka, Nayana, and Bharathi with whom I had spent nice times chatting science and non-science (sometimes non-sense like Indian marriages and hierarchy of Hindu Gods) which were perfect stress-relievers. Specially, I thank Narasimha for timely providing glassware.

During the course of my work, I had the pleasure of working with several project students, Nidula, Shijisha, Deepanshi, and Deeksha. Their assistance during the presented work is gratefully acknowledged.

I specially thank Deeksha, for being the reason I smiled. I will be greatful forever.

I also specially thank Amita, Mohan Raj and Meha for her valuable support and shaping up this thesis in the present format.

I am lucky to have amazing roommates Naidu babu, Yerranna, I am grateful to thank neighbor Lakshmi aunty, for sharing homemade food.

This was a long journey starting from a very small town in Andhra Pradesh (Anakapalli) to do my PhD in basic science after getting a graduate degree. This would never have been possible without the support and patience of my parents and sister.

Srinivasu.K

List of abbreviations

5FOA	5' Fluro-orotic acid
µg	Microgram
µl	Microlitre
µM	Micomolar
ANS	Anilinonaphthalene 8-sulfonate
ATG	Autophagy related genes
ADP	Adeninosine diphosphate
AFM	Atomic force microscope
ATP	Adeninosine triphosphate
BN	Blue native
CLS	Chronological life span
COX	Cytochrome Oxidase
CD	Circular Dichroism
cDNA	Complementary DNA
DMSO	Dimethylsulphoxide
DSS	Disuccinimidyl suberate
DTT	Dithiothreitol
dNTPs	Deoxy nucleotide triphosphates
ETC	Electron transport chain
EDTA	Ethylene diamine tetra acetic acid
GDH	Glutamate dehydrogenase
GFP	Green fluorescent protein
Hsp's	Heat shock proteins
H2O2	Hydrogen peroxide
IMS	Inter membrane space proteins
IgG	Immunoglobulin G
Kb	Kilobase
kDa	Kilodalton
KI	Potassium Iodide

M	Molar
Mito	Mitochondria
Msx	Methionine sulphoxide
MD	Molecular Dynamics
mtDNA	Mitochondrial DNA
ng	Nanogram
OD	Optical density
OCR	Oxygen consumption rate
OXPHOS	Oxidative phosphorylation
pM	Picomolar
PAM	Pre-sequence Associated Motor complex
PMSF	phenylmethylsulfonyl fluoride
PAGE	Polyacrylamide gel electrophoresis
PBS	Phosphate buffered saline
PCR	Polymerase chain reaction
rpm	Revolutions per minute
ROS	Reactive oxygen species
SDS	Sodium dodecyl sulphate
SS DNA	Single standard DNA
TAE	Tris acetate EDTA
Tris	Tris (hydroxymethyl) aminomethane
TE	Tris-EDTA
Val	Valinomycin
YPD	Yeast Peptone Dextrose
YPG	Yeast Peptone Glycerol

Chapter 1
Review of Literature

Introduction

1.1 Some aspects of mitochondria structure and functions

In eukaryotic cells mitochondria are important organelle involved in many fundamental processes. Mitochondria are the hub for various metabolic pathways like β-oxidation system of fatty acids, citric acid cycle, lipid biosynthesis pathways, as well as amino acid metabolism (Figure 1.1) (Friedman and Nunnari 2014). Mitochondria are also involved in metal metabolism, particularly in iron-sulfur clusters and heme biosynthesis (Lill and Muhlenhoff 2008). Further, mitochondria play a major role in apoptosis (Danial and Korsmeyer 2004), calcium homeostasis (Jacobson and Duchen 2004) and redox signaling (Droge 2002). And, mitochondria are most noted for ATP production.

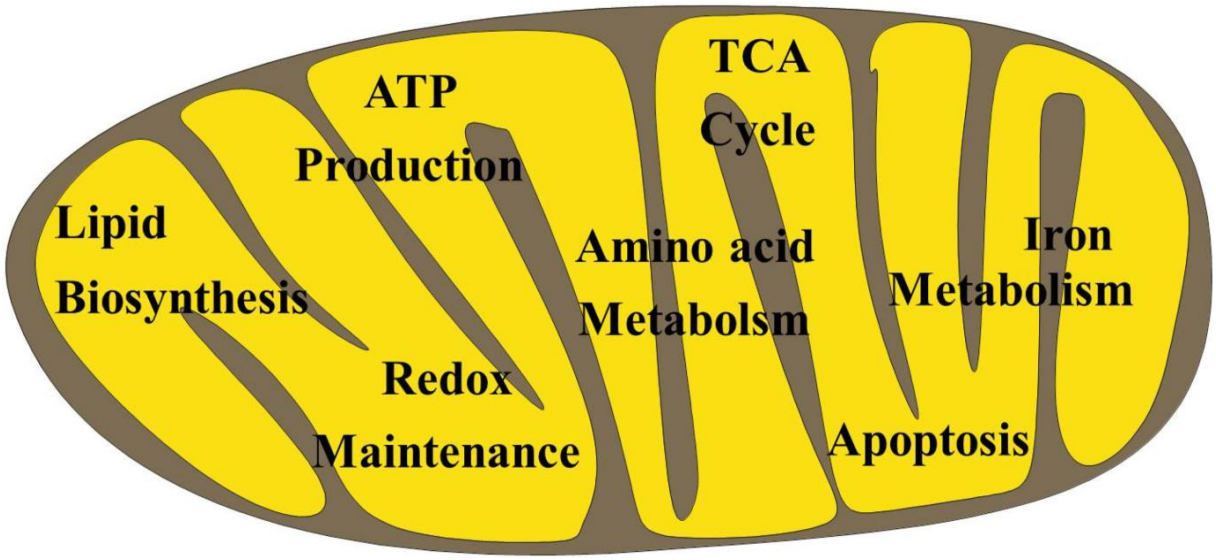

Figure 1.1: Mitochondria are involved in many functions. *Schematic representation of a mitochondrion illustrating the different functions*

Mitochondria are double membrane organelle which consists of outer membrane, inner membrane, two aqueous spaces called inner membrane space and matrix. Like other organelles, the outer membrane is involved in nonselective ion and lipid exchange and mainly comprises ion channels and protein translocation complexes. Inner membrane is impermeable to ions, helps in maintaining the membrane potential and also helps in cristae formation. Inner membrane is the hub for many oxidative phosphorylation (OXPHOS) complexes and tethered many assembly complexes. The membrane space and matrix contain many enzymes and chaperones involved in both folding and metabolism.

1.2 Mitochondrial functions and abiotic stresses adaptation

Yeast is a unicellular eukaryotic organism which is exposed to multiple abiotic stress conditions including oxidative, thermal and osmotic stress (Santos, Cheesman et al. 1999). The organism shows adaptation against these stresses by regulating many cell sensing processes like signal transduction, transcriptional and posttranscriptional control, protein-targeting, accumulation of protectants, increased activity of repair functions and metabolic pathways. There are several evidences supporting that the mitochondria in yeast cells are prime target for many abiotic stress conditions. Most of the transcriptional analysis from yeast exposed to different stresses (ethanol, osmotic and thermal) (Figure 1.2) has shown that they share common pathways and most of them converge to mitochondria (Lahtvee, Kumar et al. 2016).

Yeast cells, regularly exposed to ethanol stress, induce a response similar to those induced by heat shock (Auesukaree, Damnernsawad et al. 2009). Heat shock proteins like Hsp104, Hsp82, Hsp70, Hsp26, Hsp30 and Hsp12 have been shown to physiologically influence yeast tolerance to ethanol. Along with cytosolic chaperones, mitochondrial Hsp10 and Hsp70 are induced upon ethanol stress. Expressions studies have shown that the genes induced by ethanol stress are associated with cell energetics like glycolysis and TCA cycle, transport mechanisms, cell surface interactions, lipid metabolism, general stress response, trehalose metabolism, protein destination, ionic homoeostasis (Ding, Huang et al. 2009). Ethanol shock also causes imbalance in redox and shortage of NAD^+ which is a cofactor involved in lipid biosynthesis (Ma and Liu 2010, Vanegas, Contreras et al. 2012). Gene ontology studies have shown that ethanol stress downregulates aminoacid and nucleotide metabolisms and also causes impairment in RNA processing and protein synthesis.

Osmotic stress generally causes the opposing effects when cells are exposed to different concentration of salts like NaCl, or sugars like sorbitol. At lower salt concentrations, transcripts related to amino acid biosynthesis (arginine, methionine and proline), ornithine and ammonia transporters are downregulated. Higher salt concentrations results in up regulation of genes associated with trans membrane transport and TCA cycle. Typical osmotic stress induced genes like *STL1, SUC2, GPD1, GPP1 and CTT* are activated in oxidative stress along with antioxidants like *PRX1, MPR1, TRR1, TSA2, SOD2, DOT5, RSM26, SRX1, CCP1, CCS1, GLR1, and CTT1*).

Although osmotic stress differs from other stresses, it induces oxidative stress which impairs the proteins activity thereby increasing the maintenance of cells.

Thermal stress is studied well in terms of proteins folding and related diseases. Recent studies have been focused on changes in transcripts levels to understand the pathophysiology of cells

and development of industrial purpose strains (Gibson, Lawrence et al. 2007, Nevoigt 2008). Thermal stress causes the highest change in transcripts levels when compared to other stresses. And it also causes the significant loss of biomass and increases the ATP demand. Thermal stress down regulates the mitochondria based amino acid biosynthesis and translation. It also shares the pathways regarding mitochondrial respiration and antioxidant inducing with other stress like oxidative and osmotic stresses (Morano, Grant et al. 2012). And it induces many genes involved in proteins folding and its turnover along with the activation of a specialized machinery called autophagy to eliminate the damaged proteins.

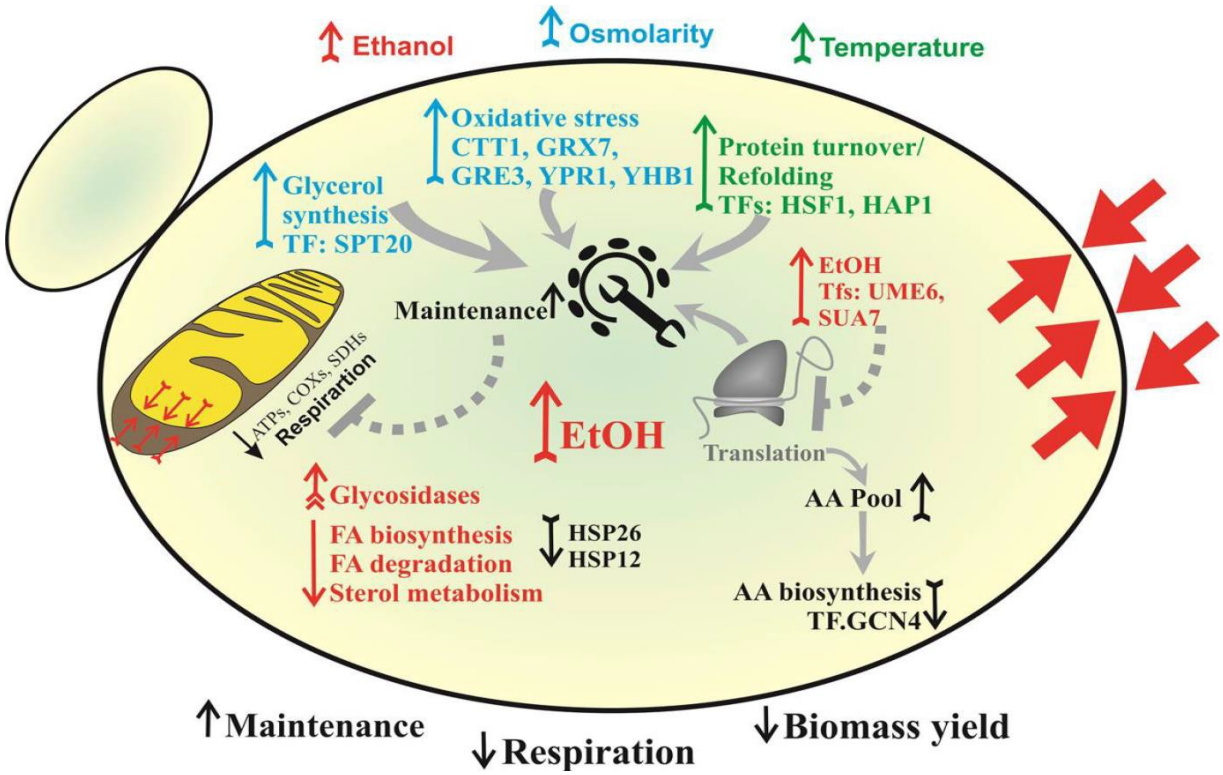

Figure 1.2: Multiple Abiotic stresses are converged to mitochondria functions.
Overview of effects and overlapped pathways studied upon three stress conditions. High ethanol concentrations induce the impairment of membrane potential and damage in membrane permeability. Osmotic stress, sharing most of pathways with oxidative induced damage results in increase in maintenance. ↑ Represnts up regulation, represents down regulation. (Adapted from Petri-Jaan Lahtvee et al., 2016)

1.3 Mitochondrial import

1.3.1 TOM complex— the general gateway for mitochondrial precursor proteins

Mitochondrial outer membrane translocase (TOM) is defined as a general import pore and adapter for many mitochondria precursor proteins after translation. It contains Tom40, which is an essential β-barrel protein that helps in pore forming and is indispensable for cell survival (Hill, Model et al. 1998). Tom22 is a receptor protein that binds with multiple Tom40 proteins and forms the 440 kDa complex. The complex is associated with Tom5, Tom6 (small Tom proteins).

1.3.2 The TOB Complex

Mitochondrial membrane proteins translocation and assembly is driven by TOB complex which is located in outer membrane. TOB complex contains two essential components, integral membrane protein Sam50, peripheral membrane protein Sam35 and non-essential Mas37 protein (Kozjak, Wiedemann et al. 2003, Wiedemann, Kozjak et al. 2003, Ishikawa, Yamamoto et al. 2004, Waizenegger, Habib et al. 2004)(Figure 1.3). Like all other precursor proteins, β-barrel precursors also cross the outer membrane through the TOM complex, then IMS where small Tim proteins guide them to TOB complex.

1.3.3 MIM — α-helical outer membrane proteins involved inimport and insertion assembly complex

The MIM complex is located in the mitochondrial outer membrane and is comprises of Mim1 and Mim2, forming 200 kDa complex, dedicated for efficient import and assembly of single-and multi-spanning α helices outer membrane proteins (Becker, Pfannschmidt et al. 2008, Hulett, Lueder et al. 2008, Becker, Wenz et al. 2011). MIM complex is associated with SAM complex, which contributes to membrane protein complex assembly (Figure 1.3).

1.3.4 TIM23 —innermembrane translocase for pre-sequence precursor proteins

A large number of mitochondrial targeted proteins bear an N-terminal presequence called MTS sequence (mitochondria targeting sequence), containing an amphipathic α-helix with polar residues on the one side and hydrophobic residues on the other side (Vogtle, Wortelkamp et al. 2009)(Figure 1.3). Most of the presequences with net positive charge in range of +3 to +6 have a length in range of 10 to 55 amino acids. These presequence containing proteins are initially recognised by TOM complex and further handed over to inner membrane TIM23 complex containing Tim50, Tim17 and Tim 23 membrane proteins (Mokranjac, Paschen et al. 2003).

TIM23, major inner membrane translocase complex, is involved in the translocation of both matrix targeted preproteins and some of the inner membrane proteins (Marom, Dayan et al. 2011). Import of preproteins across the inner membrane requires both inner mitochondrial membrane potential ($\Delta\psi$) and ATP as energy sources (Stuart, Gruhler et al. 1994). Outer membrane channel TOM complex is connected to TIM23 complex by Tim23 protein. Tim23 is a four helical spanning membrane protein forming translocase channel, cationic selective and activated by pre-sequence and membrane potential (Bauer, Sirrenberg et al. 1996). Part of N terminus residues of Tim23 are embedded in outer membrane and remaining parts are associated with Tim50 proteins. Tim17 is an important protein in Tim23 complex, serves multiple functions like stabilisation and voltage sensor. Tim17 is also involved in lateral sorting of single channel proteins and import of matrix target proteins (Martinez-Caballero, Grigoriev et al. 2007). Tim50 is a single spanning membrane receptor protein having a large C-terminal domain exposed into the inter-membrane space. This domain helps in preserving the membrane potential by closing the Tim23 channel in the inactive state. Tim21 is a single spanning membrane protein which is essential for stability of TIM23 complex. Both Tim17 and Tim21 are known to play role in two state theory of TIM23 translocase (Chacinska, Lind et al. 2005). One of the two states of TIM23 channel, import motor is involved in translocation of pre proteins.

1.3.5 PAM — motor complex associated with pre-sequence translocase

Precursor mitochondrial protein import into the mitochondrial matrix needs additional activity of the presequence translocase-associated motor (PAM) (Figure 1.3)(Hutu, Guiard et al. 2008) (ref). Mitochondrial Hsp70 is the central component of the PAM complex. Hsp70 has a C terminal substrate binding domain and a N terminal ATPase domain. Import motor contains mtHsp70 (Ssc1 in *S. cerevisiae*) as the main component and helps in both import and folding of matrix targeted proteins in ATP dependent cycles (Mapa, Sikor et al. 2010). Hsp70 is also involved in the assembly of respiratory chain complex, assisted by a number of co-chaperones. Tim44 acts as a co-chaperone and helps in recruiting chaperones and cochaperone of Hsp70 by forming complex which is ATP dependent (Hutu, Guiard et al. 2008). Tim14, Tim16 and Pam19 cochaperones are nonessential and are known to be involved in regulation of ATPase activity of Hsp70 (Mokranjac, Sichting et al. 2003). Other components of the PAM complex highly regulate and coordinate the import functions of mtHSP70. Tim44, J-domain containing protein which is bound peripherally to the inner mitochondrial membrane, is a fundamental organizer of the PAM complex. It has binding sites for mtHsp70 motor proteins and for Tim23 as well and has been shown to navigate the J-complex to the TIM23 translocase (Schiller, Cheng et al. 2008). Pam16 and Pam18 are two J

proteins influencing the ATPase activity of mtHsp70. Pam17 cooperates with the binding of Pam16 and Pam18 to the TIM23 complex (Frazier, Dudek et al. 2004, Hutu, Guiard et al. 2008). Mge1, mitochondrial matrix nucleotide exchanger, promotes the another cycle of ATPase cycle of mtHsp70 which helps in efficient import of precursor proteins in mitochondria, exchange of ADP to ATP on mtHsp70 and is essential for cell viability(Voos, Gambill et al. 1994, Westermann, Prip-Buus et al. 1995). Our focus in the thesis is to study the properties and role of Mge1.

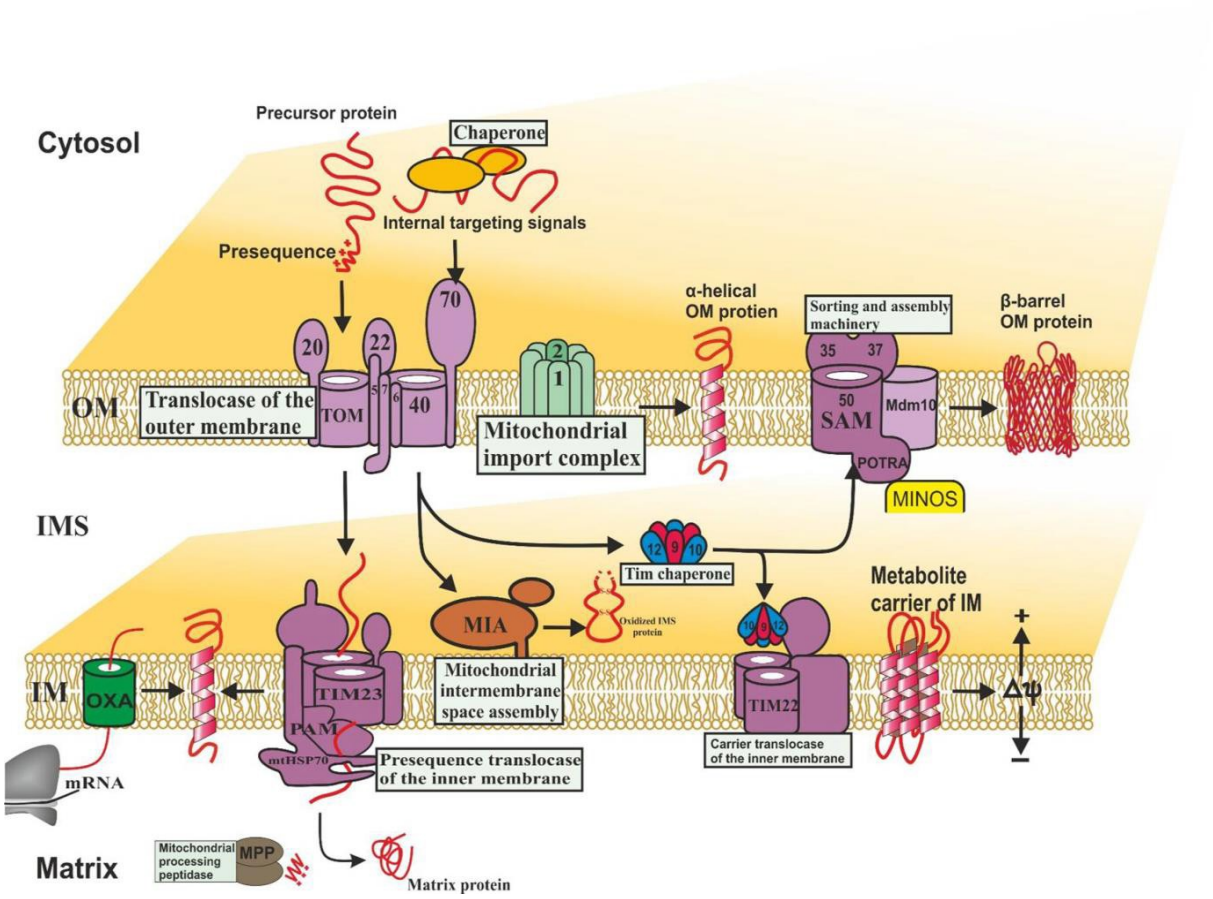

Figure 1.3: Mitochondrial import pathways *Mitochondria precursor proteins are translated in cytosol and imported with help of translocase of the outer membrane complex (TOM). Presequence carrying precursor proteins transferred from TOM complex to translocase of inner mitochondria membrane (TIM23) complex which is driven by membrane potential. PAM (presequence translocase assocaited motor) complex is involved in the import of matrix proteins with help of ATP. The pre-sequences are cleaved off by MPP (mitochondrial processing peptidases) proteases. Outer membrane β- barrel proteins are inserted into outer membrane through SAM (sorting and assembly machinery). The non-cleavable hydrophobic precursor proteins bound with cytosolic chaperones are translocated through Tom70. Inner membrane space small TIMs chaperone proteins are helping in insertion into inner membrane by TIM22 complex. Mitochondrial encoded proteins are inserted into inner mitochondrial proteins through OXA machinery. Cysteine -rich proteins destined for inner membrane space (IMS) are imported through TOM complex and folded with help of mitochondrial inner membrane space import and assembly (MIA) machinery. (Adapted from Pfanner et al., 2015)*

1.4 Mitochondrial import and Respiration complex are closely associated

Mostly, precursor proteins with hydrophobic transmembrane domains are inserted with help of membrane potential across the innermembrane. For such import events which are dependent membrane potential, the TIM23 complex associates with Tim21 which is a single spanning membrane protein. The C-terminal domain of Tim21 is exposes to the intermembrane space and it was known to interact with inter membrane space domain of Tom22 to ease the transfer of precursors from the TOM complex to the TIM23 complex in the inner membrane and also helps in preserving the membrane potential (Albrecht, Rehling et al. 2006). Moreover, Tim21 was involved in association of the TIM23 translocase to the respiratory supercomplexes formed by cytochrome c oxidase (COX) and cytochrome c reductase (complex III) (Dienhart and Stuart 2008). Thus, the association of the import machinery and respiratory supercomplex supports the membrane potential. This is the limiting factor for import of presequence proteins. This finding is believable with the idea of a localized higher membrane potential closely around proton pumping complexes of the respiratory chain. In this way, Tim21 subordinates the coupling of the presequence translocase to the respiratory chain which may be significant when the membrane potential is reduced. Mgr2 another subunit of Tim21-containig TIM23 complex helps in Tim21 and TIM23 association in inner membrane, bc1-COX super complexes in inner membrane and efficient binding of TIM23 to TOM translocase in outer membrane (Gebert, Schrempp et al. 2012). In addition, two import motor regulatory subunits, Pam16 and Pam18 are independently associated with the respiratory chain supercomplex (Wiedemann, van der Laan et al. 2007) (Figure 1.4).

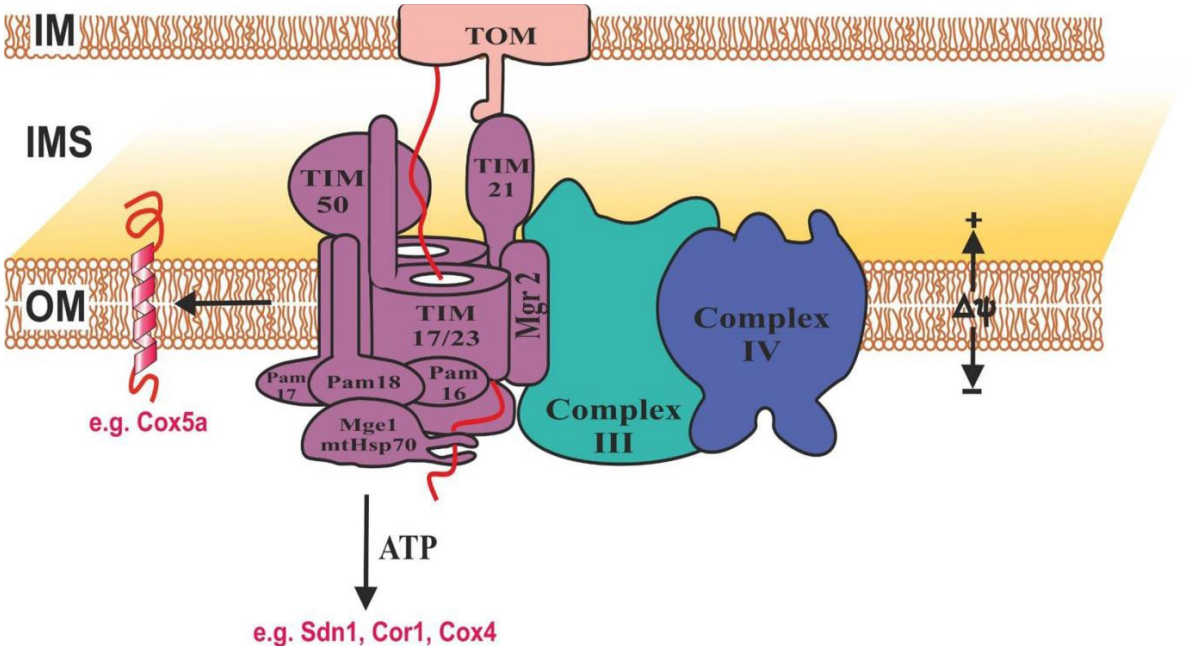

Figure 1.4: Association of inner membrane translocae TIM23 with respiratory super chain complex. *Precursor proteins are imported with help of outer membrane translocase (TOM) and handed to inner membrane membrane translocase to further import into matrix with help of ATP dependent Presequence translocase associated motor (PAM) complex. Association of TIM23 complex with respiratory chain supercomplex III+ IV (bc1-COX) supporting that membrane potential dependent translocation of precursor proteins across the inner membrane.(Adapted from BoguszKulawiak et al., 2013)*

1.4.1 MPP —peptidase cleaves the presequences of matrix precursors

Mitochondrial processing peptidase (MPP) in the matrix, immediately cleave the import precursor proteins at the N-terminal presequences which is essential for the further maturation and catalytic activity (Ito 1999, Gakh, Cavadini et al. 2002). Mas1 (Mif1, β-MPP) and Mas2 (Mif2, α-MPP) are two homologous subunits of MPP (Hawlitschek, Schneider et al. 1988, Witte, Jensen et al. 1988). Precursor proteins with extended conformation were cleaved N terminally by Mas1 (zinc-metalloprotease) during or immediately after import through the TIM23. MPP cleaves at specific site, with arginine at position minus 2 relative to the mature N-terminus (R-2motif: R-X↓X) (Vogtle, Wortelkamp et al. 2009). Further, matrix has another two aminopeptidases Icp55 and Oct1 to process the precursor proteins after MPP cleavage.

1.4.2 The mitochondrial processing peptidase (MPP) subunits are akin to the bc1-complex core subunits.

MPP subunits, Mas1 and Mas2 subunit are homologues to mitochondrial bc1-complex called Cor1 and Cor2. In *Neurospora crassa*, it was discovered that β-MPP (Mas1) and Cor1 are

indistinguishable proteins encoded by a single gene. Interestingly, in plants Mas1 and 2 subunits of MPP and substitute their activity and they integrate into the bc1-complex. More over *Oct1*Δ was shown to have respiratory defects in cells (Isaya, Miklos et al. 1994) (Figure 1.5).

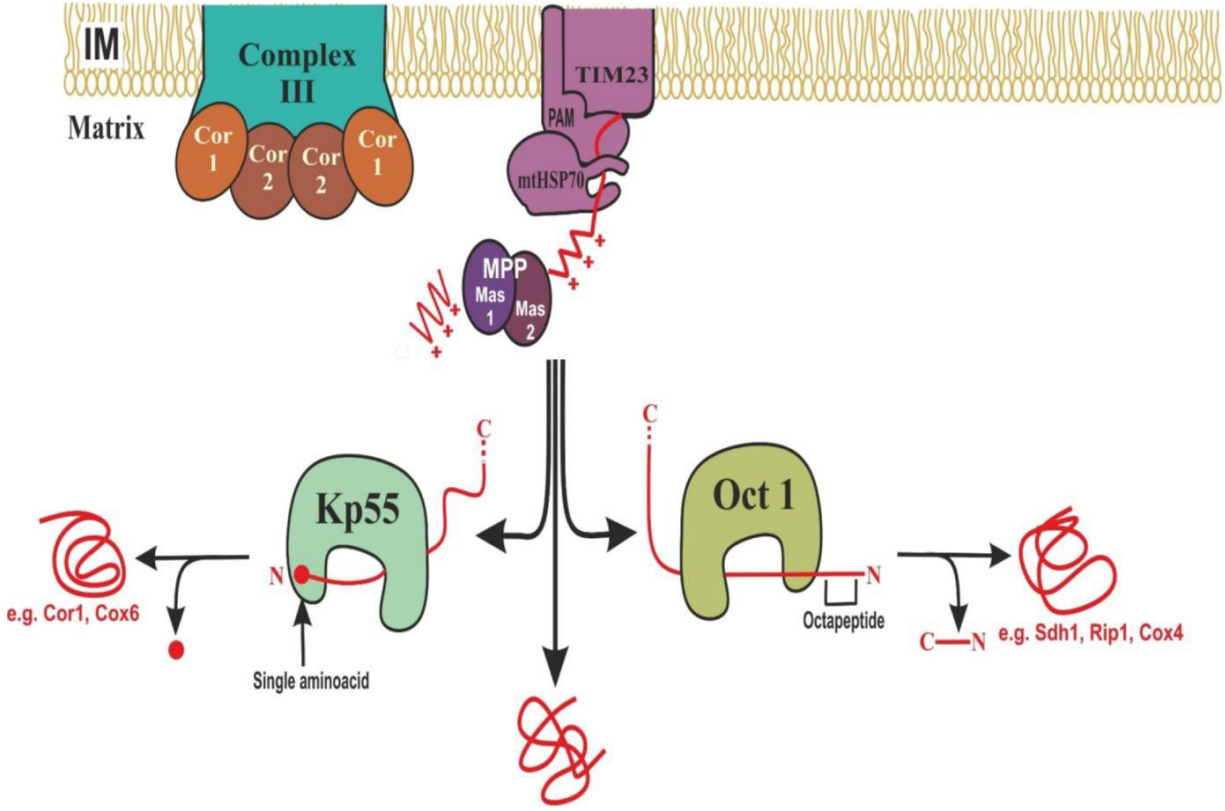

Figure 1.5: Subunits of mitochondrial processing proteases are homologues of respiratory chain complex core proteins. *Precursor proteins are imported to matrix through TIM23 complex and N terminus importing signal is cleaved by mitochondria processing proteases MPP. The subunits of MMP, Mas1 and Mas2 are homologues of core proteins Cor1 and Cor2 of the complex III. Intermediate cleavable peptidase Icp55 is involved in removal of single destablised N-terminal residue to stabilise the matrix protein. Oct1 is helping in cleavage of N-terminus octapeptide to generate stable matrix proteins. .(Adapted from BoguszKulawiak et al., 2013)*

1.5 Biogenesis of intermembrane space proteins

All of the assembly and processing machinery involved in biogenesis of inter membrane space proteins are related to respiratory biogenesis chain. There are several multiple pathways for parallel functions involved in biogenesis of IMS space proteins.

1.6 IMP — the mitochondrial inner membrane protease involves in releases of precursor proteins into the intermembrane space.

The release of specific soluble domains of innermembrane proteins were carried out by innermembrane protease complex (IMP). Imp1 and Imp2 are two inter membrane space

domains with different specificity and catalytically active (Schneider, Behrens et al. 1991). Som1 is another subunit which is catalytically inactive and interacts with Imp1 and helps in its activity (Jan, Esser et al. 2000). Inner membrane soluble proteins are substrates of TOM/TIM23 complex which are laterally inserted into inner membrane. These soluble inner membrane space proteins are released into membrane space after cleavage by IMP and MPP proteases act prior to C terminal soluble domain.

1.7 Cofactor insertion and complex formation in the intermembrane space proteins

Inner membrane space soluble proteins can be formed by cofactor insertion, which are imported through outermembrane TOM complex. TOM complex is involved in import of cytochrome c (apo-form) which then trapped in innermembrane space (Wiedemann, Kozjak et al. 2003). Heme lyases, catalyst present in the mitochondrial intermembrane space, help in the covalent attachment of heme group of c-type cytochromes through conserved cysteine residues (Mayer, Neupert et al. 1995). Other proteins like holo cytochrome c synthase, is imported through TOM complex and it can be trapped in inner membrane space by specific interactions. The mechanisms of trapping in inner membrane space could be explained by available inner membrane space domains of outer or inner membrane complexes which are hub for multiple interactions.

1.8 MIA — oxidative folding protein machinery

Small Tim chaperones are necessary for both import of hydrophobic outer membrane β-barrel precursors and inner membrane metabolite carriers (Wiedemann and Pfanner 2017)(ref). Cysteine motif containing intermembrane space precursors proteins are folded by using disulphide relay system in inter membrane space formed by both Mia40 and Erv1 which are essential for respiration and viability (Chacinska, Pfannschmidt et al. 2004) (Figure 1.6). Inner membrane space proteins imported through Mia 40 and Erv1 system having conserved sequence called intermembrane space sorting signal (MISS). And it is consists of two hydrophobic, single aromatic and a conserved cysteine which is acting docking site for initial disulphide bond formation with Mia40. Mia40 also acts as oxidoreductase enzymes, introduce intramolecular disulphide bonds to help in proper folding of the substrate proteins (Sideris, Petrakis et al. 2009). When a precursor protein imported or transferred from the TOM channel into the intermembrane space, Mia40 binds to its import signal. Mia40 dependent import into the intermembrane space is diminished in the absence of the MINOS subunit Fcj1. And it is also needed for the formation of contact sites between the inner and the outermembranes, Mia40 has chaperone activity which promotes the folding of substrates, which

usually contain two cysteine residues motif with either 3 or 9 amino acids between two cysteine residues (CX3C or CX9C)(Weckbecker, Longen et al. 2012). Three dimensional structures revealed that inter helical disulphide bonds are formed between Mia40 and substrates with CX3/9C in an antiparallel orientation. Erv1 reoxidizes the Mia40 to continue the folding cycle by forming ternary complex (Mia40-Erv1- substrates). Hot13, which is a zinc-binding protein,enhances the Erv1 dependent oxidation of Mia40 (Curran, Leuenberger et al. 2004). Further folding events are catalysed by small Tims after introducing the disulphide bonds.

1.9 Electrons are transferred to respiratory chain which are released during oxidative folding of imported intermembrane space proteins

Intially Erv2 was identified in endoplasmic reticulum before Erv1 was characterised in mitochondria, which donates electrons to molecular oxygen (Wang, Winther et al. 2007)(ref). Thus the flow of electrons in IMS captured the attention of many researchers. It has been shown that, electrons are transferred to cytochrome c which donates complex IV from mitochondrial intermembrane space proteins via Mia-Erv1 proteins (Allen, Balabanidou et al. 2005, Bihlmaier, Mesecke et al. 2007). Respiratory chain pump the protons across the inter membrane space before final transfer of electrons to molecular oxygen to maintain the membrane potential. Thus the respiratory chain and import complex are closely associated to conserve energy from the disulphide relay system. Remarkably, several studies have shown that IMS precursor substrate proteins transfer electrons directly to respiratory chain.

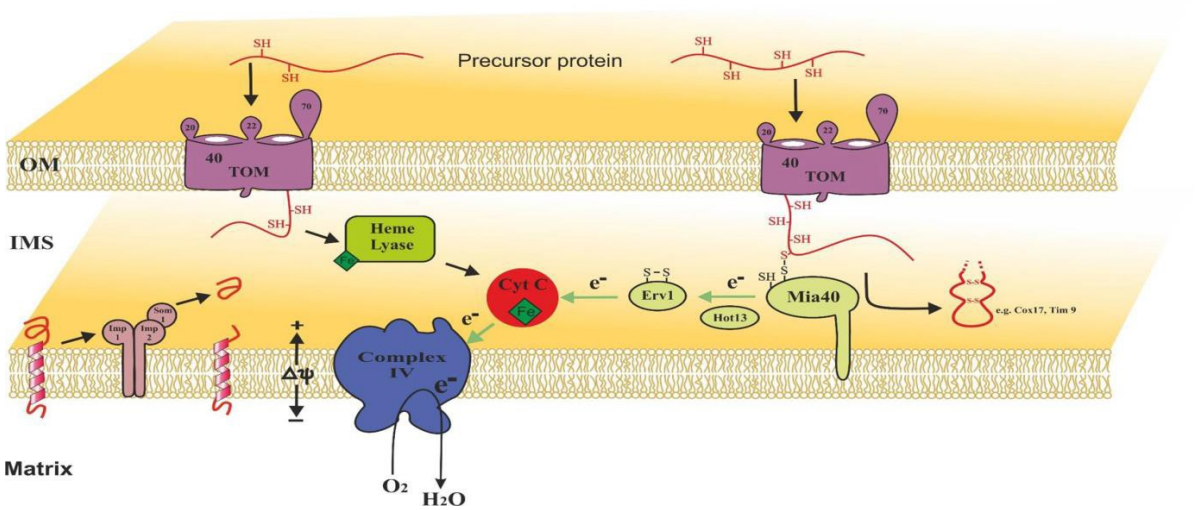

Figure 1.6: Transfer of electrons to respiratory chain from disulphide relay system.
Precursor proteins are imported through several import pathways and trapped inside by interacting with multiple domains facing towards IMS. Oxidative folding of IMS space proteins and cofactor insertion are catalysed by mitochondiral inner membrane space import and assembly machinery (MIA). Eletcrons released by disulphide formation of cystein containig precursor proteins during oxidative folding are donated to directly cytochrome c oxidase complex (IV) or via cytochrome c. (Adapted from BoguszKulawiak et al., 2013)

1.10 Carrier precursor proteins assembly and import

Unlike import of precursors with N-terminal pre-sequence, carrier proteins contain hydrophilic, hydrophobic, charged or uncharged sequence motifs as signal sequence which can be distributed throughout the whole polypeptide chain (Zara, Ferramosca et al. 2007). Import of carrier precursor proteins occur in sequential steps. After translation of proteins in cytosol, the hydrophobic carrier precursors are guided with help of cytosolic chaperones Hsp90 and Hsp70 to mitochondria outer membrane Tom70 receptors. Tom 22 membrane protein is involved in translocation through membrane via TOM complex. Small Tim9 and Tim10 chaperone complex bind to precursor proteins and help in preventing the protein from aggregation in inter membrane space aqueous space. Tim9–Tim10 complex promote the membrane insertion by guiding the carrier precursor to the TIM22 complex which is dependent on membrane potential. Finally the mature precursor proteins are released to IMS space (Figure 1.7).

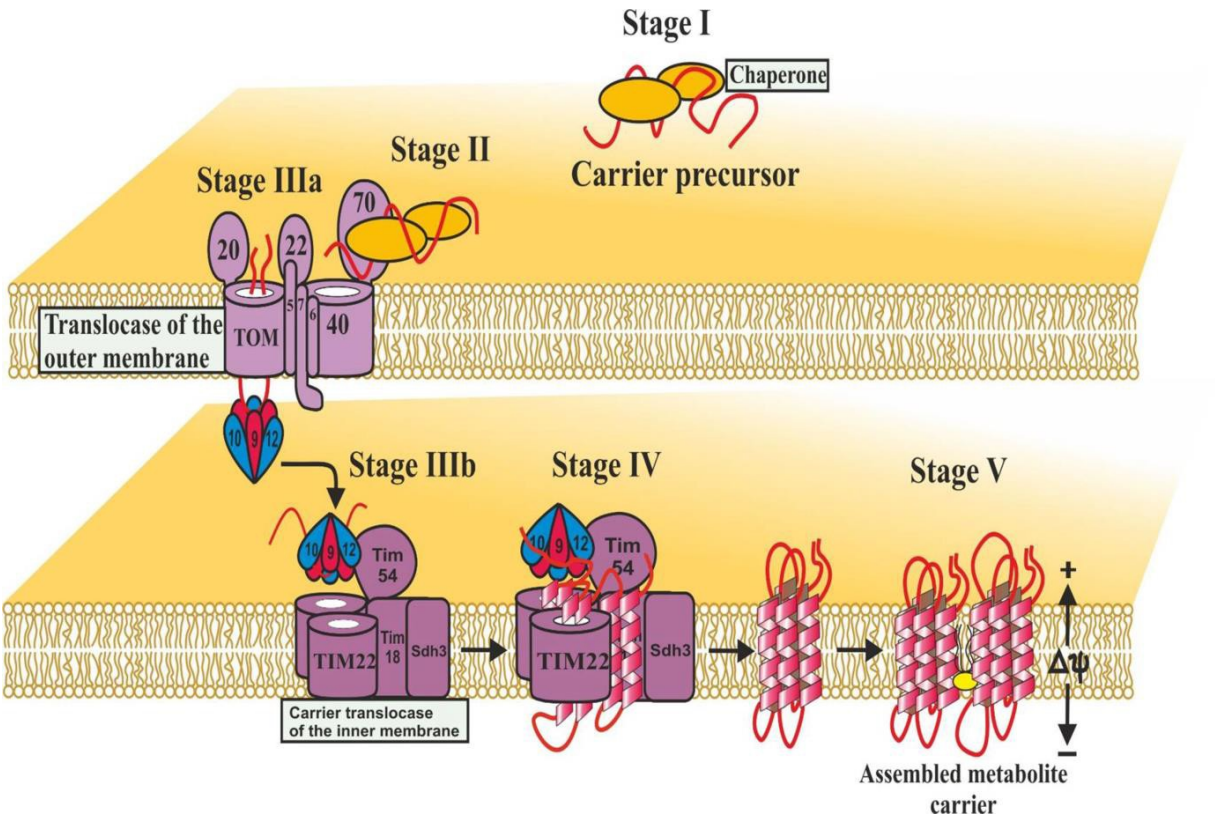

Figure legend 1.7: Metabolite carrier protein import pathway. *Metabolite carrier proteins are synthesised in cytosol and translocated through outer membrane translocase TOM 40 channel with help of cytosolic chaperones. After import into inner membrane space, precursors are bound to small TIMs chaperones and transferred to inner membrane translocase TIM22. Lateral insertion carrier proteins into inner membrane of mitochondria are depended on membrane potential. Finally carrier proteins dimerised and stablised with help of cardiolipids. (Adapted from* Boguszkulawiak *et al., 2013)*

1.11 TIM22 — innermembrane mitochondrial carrier translocase complex

TIM22 complex composed of Tim9, Tim10, Tim12, Tim18 and Tim54 subunits. It was identified in 1996 which is homologues with N-terminus translocase subunitsTim17 Carrier translocase exclusively insert all the metabolite carrier proteins into the inner membrane (Figure 1.8). Tim22 is capable of pore-forming core subunit of the complex hence the complex named as TIM22 complex (Kovermann, Truscott et al. 2002). TIM23 is the complex having Tim9 and Tim10 subunits, capable to form hexameric chaperone complex in IMS. Tim12 is an essential subunit of complex which is peripherally associated with TIM22 complex (Sirrenberg, Endres et al. 1998). The C terminus of Tim12 is associated with lipid of innermembrane, thus maintaining the sub-complex which is subsequently associated with other subunits to form TIM22 complex. TIM54 subunits have both N terminus sequence and larger C terminus inter membrane space domain (Kerscher, Holder et al. 1997). Deletion of Tim54 causes import defect of carrier proteins and growth defect Tim18 was discovered independently as multicopy suppressor of *tim54* mutant and was shown to co-precipitation with TIM22 complex (Kerscher, Sepuri et al. 2000). Tim18 has three transmembrane helical structures similar to sdh4 but their function in respiration remains to be explored, since it is not necessary in import of carrier proteins (Yankovskaya, Horsefield et al. 2003).

1.12 The respiratory chain subunit protein Sdh3 is a component of the carrier translocase

Defective growth of temperature sensitive mutants of tim22 is rescued by overexpression of Tim54 and Sdh3 (Figure 1.8)(Gebert, Gebert et al. 2011) (ref). Mutants of *S. cerevisiae* lacking mitochondrial DNA or having defect in respiratory chain complex form small colonies when grown on glucose and are called petites. On the other side, nuclear mutations in yeast strains are called petite negative which are are lethal in respiratory deficient cells. Nuclear encoded ADP/ATP carrier (AAC2) and of the β- subunit of the F_1F_0-ATP synthase (ATP2) deleted strains are not able to grow without mitochondrial DNA. These two proteins, involved in electrogenic exchange of cytosolic ATP for ADP, might be required in respiratory deficient yeast for maintaining the membrane potential. Deletion of TOM70 and TIM18 have shown petite-negative phenotype which is explained by the reason that they required for the import of the ADP/ATP carrier (Dunn, Lee et al. 2006). SDH3 is the lone subunit of complex II which shows petite-negative phenotype similar to tim18Δ. Deletion of sdh3 impairs the Tim22, Tim54 assembly as well as defect in metabolite carrier proteins. Antibody shift of the translocase and Quantitative mass spectrometry and have shown Sdh3 as stoichiometric subunit of the TIM22 complex. Existence of Sdh3 in both

respiratory and respiratory complexes reinforcement that the specific phenotype of its deletion (Gebert, Gebert et al. 2011).

1.13 The succinate dehydrogenase or complex II of the respiratory chain

The succinate dehydrogenase or complex II of the inner mitochondrial membrane have been studied well and it is play a role in both Krebs cycle and respiratory complex (Rutter, Winge et al. 2010) Succinate gets oxidised to fumarate by transferring the prosthetic FAD group (Yankovskaya, Horsefield et al. 2003). The SDH complex is involves in reduction of fumarate to succinate and it is structurally similar to the fumarate reductase. The SDH complex comprises of two subcomplexes, a catalytic soluble Sdh1 and Sdh2 and Sdh3 and Sdh4 innermembrane subunits which are hydrophobic in nature. Sdh1 is covalently bound to FAD. During oxidation, fumarate transfers the electrons to FAD and subsequently it is transferred to ubiquinone by the three iron–sulfur clusters localized in the Sdh1–Sdh2 subunits. Membrane embedded Sdh3 and Sdh4 bind to ubiquinone which is important for electron transfer as well as stability of complex II. Tertiary structural studies reveal that a b-type heme is present in the Sdh3–Sdh4 subunits however it does not involve in catalytic role of SDH complex. Deletion studies showed that Sdh3 and Sdh4 are important for recruiting catalytic Sdh1 and Sdh2 subunits and transfer electrons from Krebs cycle to respiratory chain (Nakamura, Yamaki et al. 1996, Lemire and Oyedotun 2002).

1.14 Sdh3, subunit of succinate dehydrogenase and its role in carrier translocase assembly

Sdh3 is a membrane protein, part of both SDH complex and carrier translocase (Gebert, Gebert et al. 2011)(ref). In both complexes, Sdh3 form hetrodimer with Sdh3 and Tim18 subunits respectively. Crystal structure analysis reveals that Tim18 is a close homologue of Sdh4; in addition, modelling based results suggested that Sdh3-Sdh4 is structurally similar to Sdh3-Tim18. Deletion studies have shown that SDH4 is important for maintaining the levels of Sdh3. Deletion of TIM18 slightly affects the Sdh3. In contrast, deletion of SDH3 significantly impairs the levels of both partner subunits proteins Tim18 and Sdh4. Based on these observations one can conclude that defective assembly in complex leads to degradation of subunits.

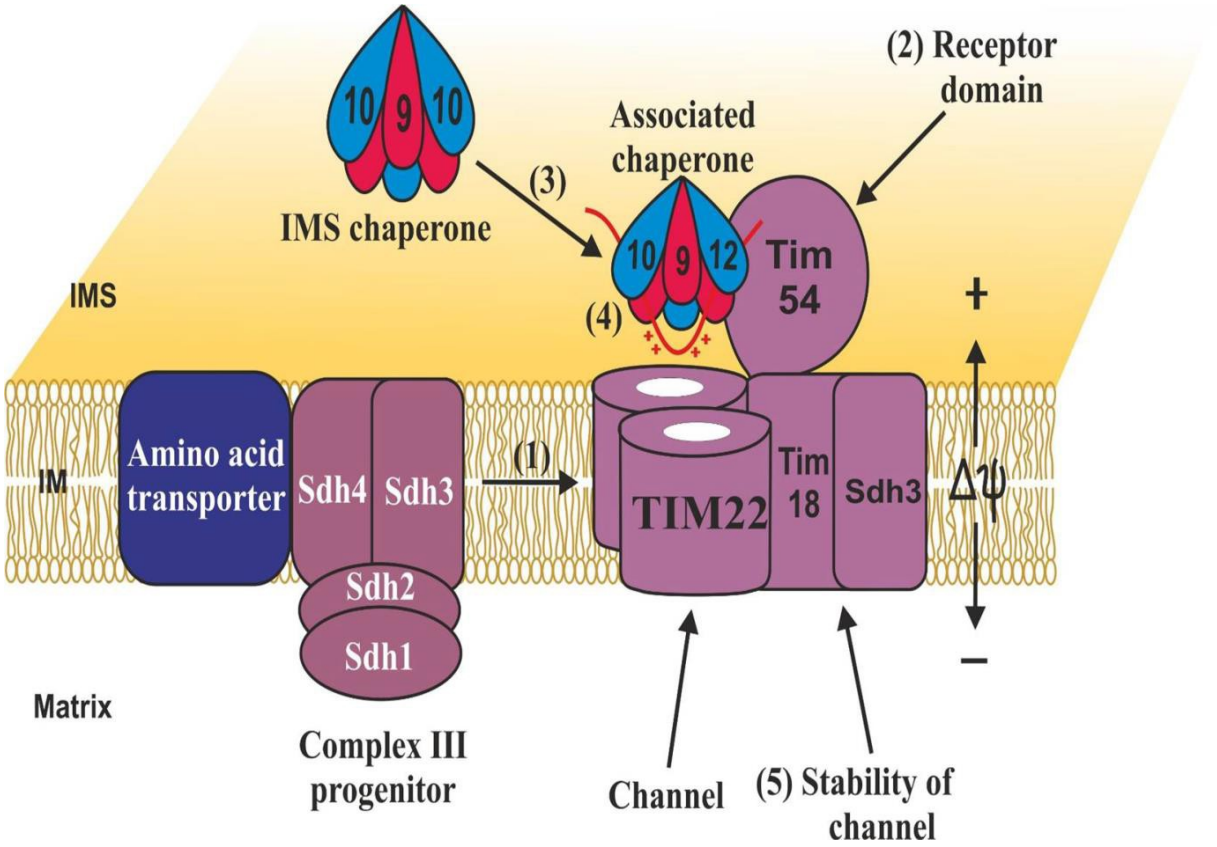

Figure 1.8: Hypothetical model for inner membrane translocase TIM22 evolution and function. (1) *Inner membrane mitochondrial translocase proteins Tim22, Tim18 and Sdh3 are derived from complex II progenitor with an assocaiton with aminoacid transporter. (2) Innermembrane translocase serve as intermembrane space receptor domain with evolution of Tim54.(3) Small TIMs Tim9-Tim10 hexameric chaperone complex are tethered to TIM22 complex due partial replacement of small Tim10 with translocase Tim12 subunit Tim54. (4) Positive charged matrix proteins are inserted into Tim22 channel is facilatated by proper orientation Tim54-Tim9-Tim12 small TIMS chapeorones in inner membrane space. (5) Tim22 channel which is flexible is stabilised by lateral Tim18-Sdh3 module. (Adapted from* BoguszKulawiak *et al., 2013)*

1.15 Assembly of the respiratory chain depends on many protein import and export pathways

1.15.1 Import of the nuclear-encoded mitochondrial subunits

The majority of mitochondria-targeted proteins enter the organelle through the outer membrane TOM complex. Further, insertion into mitochondrial inner membrane of proteins with N terminal presequence is explained by two conflicting models. First model is well established, 'conservative sorting' model suggesting that cytosol synthesised proteins are imported to matrix and subsequently exported to inner membrane through Oxa1 (Ott and Herrmann 2010). In contrast, inner membrane proteins containing are translocated through the TOM complex and

further released into the inner membrane with help of innermembrane mitochondrial TIM23 complex (Hell, Herrmann et al. 1998).

1.15.2 Synthesis and assembly of the mitochondrial-encoded subunits

Mitochondrial genome encodes 13 proteins in human and 8 in the yeast *S. cerevisiae* (Adams and Palmer 2003, Wallace 2007). Mitochondrial encoded proteins are synthesised by inner membrane bound ribosomes, subsequently embedded into membrane by Oxa1 which kinetically couples the translation and insertion due to cotranslation (Vogel, Bornhovd et al. 2006, Ott and Herrmann 2010). Most importantly, PAM import motor Hsp70 is also involved in cytochrome c oxidase biogenesis and interacts with ATPase synthase subunit 9 and var 1 (Herrmann, Stuart et al. 1994). For my thesis concern, I will focus more on cytochrome c oxidase. In yeast *S. cerevisiae* mature cytochrome *c* oxidase is composed of 11 subunits and it is targeted by new pathological aggregates like amyloid type and is also involved in providing protection from ROS (Tsukihara, Aoyama et al. 1996). Cytochrome c oxidase is composed of both nuclear encoded core subunits (Cox4, Cox5a/b, Cox6, Cox7, Cox8, Cox9, Cox12, and Cox13) (Dowhan, Bibus et al. 1985, Wright, Dircks et al. 1986, Aggeler and Capaldi 1990, Taanman and Capaldi 1993, Fontanesi, Soto et al. 2006) and mitochondria-encoded catalytic subunits (Cox1, Cox2, and Cox3) (Tsukihara, Aoyama et al. 1995, Riistama, Puustinen et al. 1996, Mills and Hosler 2005). Recent studies have discovered additional two factors; Rcf1 and Rcf2 (Chen, Young et al. 2012, Strogolova, Furness et al. 2012, Vukotic, Oeljeklaus et al. 2012). Cytochrome c oxidase has four redox centres (two copper centres and two iron centres) and many other metal centres whose functions are poorly studied (Tsukihara, Aoyama et al. 1995). Assembly of COX is explained by different modules involved in Cox1, Cox2 and Cox3 biogenesis (McStay, Su et al. 2013). Initially Cox1 (12 span membrane protein) is translated by recognising the 5' UTR region by activator proteins, Pet309, and Mss51. Cox1 forms a stable complex COA by associating with assembly activators Cox14 and Coa3 immediately after co-translational insertion of oxa1 (Decoster, Simon et al. 1990, Perez-Martinez, Broadley et al. 2003, Barrientos, Zambrano et al. 2004, Towpik 2005). COA assembly also poses a loop on Cox1 which is helpful for negative translation by Mss51 sequestration. Coa1 and Shy1 factors are recruited to COA followed by the release of Mss51 during the assembly progress (Barrientos, Zambrano et al. 2004, Mick, Wagner et al. 2007). First nuclear encoded subunits Cox5 and Cox6 form separate complex and assembled with Cox1 followed by hemes and metal cofactors insertion (Stiburek, Vesela et al. 2005). The intermediate Cox1-Cox5-Cox6 complex is assembled with mitochondrial subunits either with

Cox3 or Cox2 which are translated with help of regulatory proteins (Horan, Bourges et al. 2005). Assembly chaperones like Cox20 and Imp1 are involved in maturation of precursor Cox2. Cox2 protein is translated by binding with Pet111 (Herrmann, Bowler et al. 1995, Jia, Dienhart et al. 2003). Cox2 binds to the Cox1-Cox5a-Cox6 intermediate prior to, or directly after the addition of the Cox3 subunit (Su, McStay et al. 2014). Further assembly progression occurs by incorporating several intermediate complexes such as Cox5, Cox7 and Cox13 (Church, Goehring et al. 2005). Lastly, holoenzyme is formed by adding Cox12 and Cox13 components (Vukotic, Oeljeklaus et al. 2012).

1.15.3 Import is regulated by cytosolic precursor proteins.

This regulatory mechanism has been confined to small set of proteins which are closely related. Cytosolic precursors are mostly regulated at the extent of exposure to target sequence and several other factors like post-translational modifications, metabolic conditions, redox status of cells influencing the exposure of targeting sequence. Most of the precursor proteins undergo post-translational modifications and help in regulating the accessibility of the target motif. Recent studies emphasized more on dual targeting of mitochondrial proteins, regulated by several factors like alternative transcripts, dual starting translation site, isoforms coding for same genes, ambiguous targeting signals, two signals present in same protein along with reverse translocation and membrane permeabilization.

1.15.4 Precursor proteins import is regulated by binding with metabolite and partner proteins

Import of mitochondrial proteins, mostly metabolic enzymes, are regulated either positively or negatively by binding with metabolites or cofactors and depends on metabolic situations. Metabolites like heme, regulates the import of precursor proteins by impairing the sequestration towards TOM complex. The first step of heme biosynthesis is catalysed by 5-aminolevulinate synthase. The enzyme has a heme binding site which is regulated by negative feedback mechanism (Lathrop and Timko 1993, Dailey, Woodruff et al. 2005, Hamza and Dailey 2012). Partner protein regulates the localization of precursor proteins by masking the targeting sequence. DNA repairing enzyme Apn1 (apurinic/apyrimidinic endonuclease) has dual localization sequence containing protein having both nuclear and weak mitochondrial localization sites. Localisation of Apn1 was influenced by Pir1 (partner protein) (Vongsamphanh, Fortier et al. 2001) where C-terminal nuclear location motif of Apn1 was masked by Pir1 to allow the protein import into mitochondria.

1.15.4 Import Regulation by Covalent Modification or Cleavage of Precursor Proteins

Covalent modification like phosphorylation, myristoylation and fatty acid moieties are known to regulate the import of precursor proteins. Cytochrome P450 mono-oxygenase precursor proteins have both endoplasmic reticulum and mitochondrial targeting sequence and its fate is dependent on phosphorylation (Avadhani, Sangar et al. 2011). Protein kinases like A and C phosphorylates cytochrome P450 mono-oxygenases residues near mitochondria targeting sequence and favours its targeting into mitochondria. Phosphorylation affects ER and mitochondrial import machineries. It also increases the affinity for mitochondrial protein machineries like TOM, TIM 23 and Hsp70 (Robin, Anandatheerthavarada et al. 2002, Avadhani, Sangar et al. 2011). Myristolyation and phosphorylation of dual targeting precursor proteins decreases the affinity to SRP (signal recognition particle) and favours import into mitochondria. In addition to covalent modification, proteolytic cleavage also decides the import into mitochondria. For example, specific cytochrome P450 precursor gets cleaved at ER localisation site by proteases and helps in exposure of cryptic mitochondrial localisation signal (Avadhani, Sangar et al. 2011).

1.15.5 Regulation of Precursor Sorting by Protein Folding Before or During Import into Mitochondria

Proper protein folding can regulate both functions and destinations of proteins at dynamic rateand competes with mitochondrial import machinery (Strobel, Zollner et al. 2002). In yeast, adenylate kinase is mainly localised in the cytosol and small fraction is located in mitochondrial intermembrane space. Higher rate of folding of the enzyme prevents import into mitochondria by masking the mitochondrial targeting signal and makes the protein resides in cytosol. Another example is of fumarase enzyme which shuttles between cytosol and mitochondria and regulates metabolites by glyoxilate shunt (Sass, Karniely et al. 2003). Distribution of fumarase is also dependent on the folding rate (Regev-Rudzki, Battat et al. 2009). This enzyme is partially imported into mitochondria and presequence is cleaved off by MPP in the matrix. Retrograde translocation of more than half of the processed proteins into the cytosol is promoted by the rapid folding of fumarase, whereas the remaining proteins are fully imported into mitochondria.

1.15.6 Regulation of Mitochondrial Protein Entry Gate by Cytosolic Kinases

Mitochondrial import is regulated by cytosolic kinases which can phosphorylate not only the precursor proteins but also the proteins involved in import machinery. Several kinases have been found to regulate import machineries and are also involved in biogenesis of import components in both positive and negative ways. A well-studied kinase, protein kinase A is activated in

fermentable metabolism (glucose abundant condition), it phosphorylates the TOM40, channel forming protein in TOM complex. Phosphorylated TOM40 inhibits the early translocation step of precursor proteins (Rao, Schmidt et al. 2012). PKA also phosphorylates the TOM70, thus inhibits the receptor activity. TOM70 has both receptor site and chaperone binding site, therefore it recruits the chaperones like cytosolic Hsp70 and Hsp90 for folding of precursors during import. PKA selectively phosphorylates the serine residues of TOM70 near to chaperone binding site, thus inhibit the binding with chaperones. Hence, PKA delays the import of metabolite carrier proteins into mitochondria (Schmidt, Harbauer et al. 2011). Outer membrane MIM complex is involved in insertion of alpha helical proteins including precursor form of TOM2O and TOM70. Cytosolic kinase 2 phosphorylates the TOM22 and helps in import by promoting its binding with TOM20. Inhibition of phosphorylated TOM22 decreases the amount of TOM70 and TOM20 indicating the involvement of CK2 in biogenesis (Gerbeth, Schmidt et al. 2013).

Mitochondrial import regulation is closely associated with multiple stress adaptation of cell. It is also provides the ability to sense the different grades of stress (lower to higher levels) by unknown mechanisms and differentiate the degrees of stress. Import machinery, specifically TIM23 complex including Hsp70 and co-chaperones interacts with respiratory complexes (complex III and IV) (van der Laan, Wiedemann et al. 2006). Respiratory complex is responsible for ATP production and $\Delta\psi$ membrane potential maintenance of cell. Precursor proteins are translocated upto some extent due to membrane potential and further imported by ATP driven Hsp70 motor proteins. Several stress signalling pathways impair the energy production and respiratory complex of cell. In addition, stress induced aggregated proteins which are mostly engaged with Hsp70 chaperone, impair the import pathways.

Mitochondrial unfolded protein response is well studied by different groups (Pellegrino, Nargund et al. 2013, Jovaisaite, Mouchiroud et al. 2014). The response helps in communicating the signals from mitochondria to nucleus by retrograde pathway. Recent study has shown a connection between mitochondrial import proteins and mitochondrial stress in the *Caenorhabditis elegans* (Quiros, Prado et al. 2017). The activated transcription factor, associated with stress-1 (ATFS-1) has both nuclear and mitochondrial targeting signals (Nargund, Pellegrino et al. 2012). The normal healthy mitochondria can import ATFS-1 completely into matrix which gets degraded by Lon protease. In mild stress conditions, the mitochondrial import machinery (TOM40, TIM23, Hsp70 or membrane potential) is impaired which affects the import of ATFS-1 to mitochondria, which then gets localised to nucleus and activates the mitochondrial UPR.

The degraded peptides in the mitochondrial matrix alter the import machinery by several mechanisms. One of the known ways is that degraded peptides in matrix efflux from mitochondria into nucleus with help of HAF-1 porter and alter the import machinery. In higher stress conditions, import induces the specific autophagy (mitophagy) where damaged mitochondria undergo degradation. PINK1 (PTEN-induced putative kinase 1) and cytosolic ligase Parkin both are known to be involved in clearance of damaged mitochondria and are also closely associated with Parkinson's disease (Park, Hanekamp et al. 2006, Narendra and Youle 2011, Exner, Lutz et al. 2012). In healthy mitohcondria, PINK1 is partially imported into mitochondria by general import complex involving TOM, TIM23 complexes and membrane potential. Inner membrane rhomboid protease PARL (presenilin-associated rhomboid-like protein) cleaves the transmembrane segment of PINK1 leaving N-terminus part with destabilised residues that gets further degraded by ubiquitinylation. In damaged mitochondria, PINK1 cannot be translocated by impaired import machinery; it remains bound to TOM complex recruiting Parkin that results in ubiquitinylation of several mitochondrial proteins (Lazarou, Jin et al. 2012). PINK1 and Parkin along with the other proteins induce mitophagy in a stress dependent manner. Even though individual mechanisms involved in mild (ATFS-1) and strong (PINK1 and parkin) stress signalling are well studied, it is necessary to understand that how mitochondria senses the magnitude of stress since stress always occurs in gradient fashion. Import machinery is adopted from primordial prokaryotes 1.5 billion years ago which is integrated with several functions and systems. Import system cross-talks with several pathways both in physiological and pathological conditions and co-evolved parallelly with systems in cells. Thus import represents as ideal system involved in integrating cellular systems by sensing both cellular environment and stress conditions.

Hsp70 class of chaperones includes Ssc1, Ssq1 and Ecm1 having homology with bacterial Hsp70 Dnak. Among all three, Ssc1 is essential chaperone for cell surveillance and it is involved in multiple functions like protein import, protein folding and mitochondrial biogenesis. Ssc1 has two domains namely C-terminal peptide binding domain (PBD) and N-terminal nucleotide binding domain (NBD). Ssc1 exits in two functional states helping the opposing forms in chaperone cycle. Ssc1 bound to ATP state, the PBD forms an open conformation with high on and off rates of peptide binding. On the other hand, the PBD exists in closed conformation and has a high binding affinity for peptides when ssc1 is bound to ADP. Hsp70 has got huge attention in recent research and studies are showing that it is regulated by oxidative stress by undergoing glutathionylation and is also associated with pathogenesis of neurological disorders like Parkinson's, Huntington's and Alzheimer's. Several advanced structural studies revealed that

both domains of Hsp70 communicate by allosteric mechanism and it is influenced by both substrates and co-chaperons.

Two specific co-chaperons, Mdj1 and Mge1 are involved in regulation of chaperone cycle. Mdj1 is a J class, non-essential protein which helps in triggering the ATP hydrolysis and is also involved in mitochondrial respiration. GrpE family protein, Mge1 is an essential protein which helps in the exchange of nucleotides on Hsp70.

Hsp70 chaperone population is located in trans-membrane side of inner mitochondrial membrane and is assigned for the assembly of respiratory complex and translocation of pre proteins. Import and folding of proteins are dependent on two functions of Hsp70, ATPase activity and high affinity towards unfolded state of proteins. Initially, translocation of preproteins is aided by membrane potential ($\Delta\psi$) which mainly drives the positively charged presequence into matrix. Further translocation into matrix is driven by ATP hydrolysis of Hsp70. Power-stroke (pulling) and Brownian ratchet (trapping) models hypothesised the mechanism of import of pre proteins. Many evidences are available in support of Brownian model which explains the import of folded preproteins based on their ability to undergo a two way (reversible) unfolding because of thermal fluctuations. This thermal breathing allows the translocation of unfolded preproteins into the matrix through import channel with the help of Hsp70. According to power stroke model, sequential conformational change of Hsp70 generates the pulling forces on the polypeptide chain. This drives the unfolding of folded domain on the mitochondrial surface. From mutational analysis of Ssc1 and loosely folded preproteins import kinetics, import machinery follows distinct mechanisms based on the nature of individual preproteins. Another important function of Hsp70 is the folding of matrix proteins. Several disorders are associated with aggregated proteins. Hsp70 and co-chaperones Mge1 and Mdj1 are helps import and folding of proteins. Mdj1 is J class protein, increases the ATP hydrolysis, sequestration of aggregated proteins and transfer to Hsp70. In addition, Mdj1 plays essential role in mitochondrial respiration. Mge1 is essential for cell viability. It is a co-chaperone with multiple functions like iron cluster biosynthesis, protein import and protein folding. It exits as dimer, having N-terminus and C-terminus domains.

1.16 Mitochondrial respiration and ageing

Biological aging in a cell or organism is defined as progressive decline in its ability to resist stress, damage, or disease. Biological systems are permanently exposed to the effects of reactive oxygen species (ROS) which are generated as respiratory by-products as they rely mostly on oxidative

respiration for sustainability. According to the free-radical or mitochondrial theory of aging, free radicals damage mitochondrial DNA (mtDNA) along with many proteins and disturb aerobic respiration which leads to progressive decline in energy and eventually overwhelm stress resistance and self-repair systems, thus resulting in further functional decline and aging (Harman 1972, Burtner, Murakami et al. 2009, Kaeberlein 2010).

In support with the free radical/mitochondrial theory of aging, altered mitochondrial functions, especially respiration and ROS accumulation are common features in multiple aspects of aging. Despite the long-standing free radical theory of aging, evidences supporting and contradicting its postulates, collected from several studies on diverse model organisms continues to accumulate in the literature and make the relation between mitochondrial functions and aging complex (Longo and Fabrizio 2002, Bonawitz, Chatenay-Lapointe et al. 2007, Ristow and Schmeisser 2011). For instance, drosophila was shown to extend the life span under the overexpression of SOD. Correspondingly, overexpression of mitochondria targeted catalase in mice, not only showed increased life span, but also conferred reduction in ROS levels and oxidative damage (Warner 1994). Besides, deletion of the mitochondrial superoxide dismutase (SOD2) in Caenorhabditis elegans extended life span and increase in ROS generation (Cabreiro, Ackerman et al. 2011). In addition, recent studies proposed that threshold respiration at exponential phase and modulating the metabolic shift from fermentation to respiration at diauxic shift also extend the life span. Moreover, strains having respiratory capacity below the threshold show shorter life span that is independent of ROS accumulation (Ocampo, Liu et al. 2012). These observations further indicate that relation between ROS, respiration and life span is more complex. Growing evidences suggest that the extension of life span is affected by multiple factors like adaptive respiration, lipids and carbohydrates including trehalose and glycogen (Samokhvalov, Ignatov et al. 2004, Favre, Aguilar et al. 2008). In addition, deletion of the TOR1 gene could extend chronological life span in *S. cerevisiae* primarily by increasing mitochondrial mass, respiration and ROS production (Bonawitz, Chatenay-Lapointe et al. 2007).

Budding yeast, *Saccharomyces cerevisiae* serves as the best model for study of aging, contributing to the discovery of conserved longevity factors that modulate aging in mammals. It has been established that mitochondrial respiratory mutants severely affect the ability of yeast cells to accomplish a standard wild-type chronological life span (CLS). Mitochondrial functions play important roles in CLS extension mechanisms.

1.17 Mitochondrial quality control

Alteration in mitochondrial function is associated with a variety of diseases, including cancer, neurodegeneration and aging (Johannsen and Ravussin 2009). Autophagy is involved in the maintenance of the healthy proteome and organelle by degradation of misfolded and dysfunctional organelles. Mitochondrial has specialised quality control systems, protecting cells from dysfunctions arising due to aggregated proteins or respiratory defects (Karbowski and Youle 2011). Mistargeted or accumulated preproteins degraded by cytosolic proteases which acts as first line of defence (Livnat-Levanon and Glickman 2011). Mitochondrial matrix proteases, such as Lon and AAA+ family proteases are essential for regulating cellular functions by degrading the key functional proteins (Quiros, Langer et al. 2015). In addition to their conventional role in the degradation of oxidized and misfolded mitochondrial proteins, they also degrade non-assembled complex subunits. Mitochondria usually undergo dynamic opposing functions, fusion and fission to regulate both respiration and quality control (Chan 2012). The fusion and fission events are necessary for cell viability and helps in sorting of non-functional mitochondria from functional, facilitating their retention or removal from their mother cells (Vevea, Swayne et al. 2014). Fission of mitochondria is required for degrading the damaged mitochondria (Sathananthan and Trounson 2000). Fusion helps the mitochondria mixing to complement to pathogenic mtDNA mutations (Gilkerson, Schon et al. 2008). Fusion and fission events are dependent on membrane potential and functionality of mitochondria. Cells adapted specific autophagy (mitophagy) to remove the damaged mitochondria (Wei, Liu et al. 2015). During mitophagy, damaged mitochondria or fragmented mitochondria are sequestered into autophagosomal bodies with the help of receptors and are further transported to lysosomes for degradation. Lastly, cells undergo apoptosis when quality control is failed or cells are exposed to severe stress. Mitochondria are the key organelle involved in triggering the programmed cell death, release of pro apoptotic factors like cytochrome c into cytosol to activate the caspase cascades (Kerr, Wyllie et al. 1972). Research in the last decade arose two contradicting information, one hypothesis states that mitochondrial dysfunctions like reduced respiration, assembly defect in respiratory chain and iron sulphur cluster induce autophagy (Lopez de Figueroa, Lotz et al. 2015, Dong, Zhang et al. 2017). On the other hand, autophagy defective mutants leads to the mitochondrial dysfunctions like defective growth in non-fermentable carbon source, low respiratory capacity, low membrane potential (Tsukada and Ohsumi 1993). How defective mitochondrial respiration impairs the mitophagy under nitrogen starvation still remains unanswered. Two major nutrient signalling pathways, TORC1 and cyclic AMP activated PKA, negatively regulates autophagy by supressing the Atg1-Atg13 kinase complex of pre

autosomal structure (PAS) which is a protein assembly complex for autophagosome formation (Mizushima and Komatsu 2011). Recent studies suggest that inhibition of autophagy due to mitochondria dysfunction is independent of TORC1 (Jazwinski 2013). In contrast, respiration deficient cells show the active PKA and impaired Atg1-Atg13 complex (Graef and Nunnari 2011). Interestingly, in inactivated PKA cells lacking mtDNA, the autophagy flux is induced similar to wild type strains. The issues which remain indecipherable are how dysfunctional mitochondria impair autophagy induction under starvation, which seems to be independent of TORC1 and PKA and how mitochondria membrane potential regulates the PKA activity.

Aim of the study

Many neurological and metabolic disorders are mainly associated with failure of mitochondrial quality control and mitochondrial biogenesis. Among the various chaperone and proteases complexes implicated in pathogenesis of disorders, mitochondrial Hsp70 chaperone complex well studied quality control factors. Yeast mitochondrial Hsp70 chaperone help in cell survival under stress conditions by regulating the both mitochondria protein folding and import. . Mge1, a mitochondrial co-chaperone belongs to the most conserved cellular machineries throughout the tree of life. Among all components of Hsp70 complex Mge1 is lone co-chaperone showing changes its oligomeric state and helps in adaptation towards both thermal and oxidative stresses. It is necessary to explore structural details of Mge1, since it is lone co-chaperone sharing the functions with both Ssc1 and Ssq1 chaperones. Recently it was shown to form novel complex with Cox4 along with Hsp70 and it also has been localised in trans membrane space of inner membrane of mitochondria. In addition, Mge1 is also involved in resistance towards antifungal agents by regulating the ergosterol metabolism, iron cluster formation. But Mge1 is essential for growth even at absence of stress. However, the molecular mechanism underlying the essentiality nature of Mge1 has not been studied

All these observations tempt us to study the important role of Mge1 in detail. *Saccharomyces cerevisiae*, the budding yeast is useful model to study the various aspects of metabolic and neurological diseases like protein misfolding, oxidative stress, autophagy, mitophagy and mitochondrial respiratory complex assembly. Yeast has been shown to successful model for study the features of many neurological disorders like Parkinson's and Huntington's. In addition, yeast has been extensively used in industrial purpose. The basic cellular and molecular machinery for studying the functions like neuronal and metabolic functions are conserved in yeast making it an attractive unicellular, genitically and biochemically tractable model organism to study the pathways underlying the neurodegeneration.

The aim of the thesis was to characterize the close link between multiple stress adaption and mitochondrial functions. Because there were no changes in structures of other components Hsp70 chaperone complex under stress conditions that allowed to studying the structural details of Mge1. Moreover, Mge1 is one of the essential co chaperone of import motor indispensable for cell survival. We previously reporting that Mge1 undergoing lone methionine oxidation and get repaired by methionine sulfoxide reductase. In addition, our lab report identified key residue at hing region gain in thermal resistance and thermal stability. To understanding the importance of resides, genetic and biochemical experiments are carried out with variants lacking both them,

which could provide the important hint for allosteric signal. Moreover, I aimed to study the role of mitochondria in stress adaptation that might exhibit change in mitochondria biogenesis and respiration.

Attempts are made to decipher the importance of co evolution of import motor and cytochrome c oxidase and their role in adaptation to abiotic stresses. I also asses the stability of Mge1 in both *in-vivo* and *in-vitro* studies using genetic and biochemical techniques.

Chapter 2
Materials and Methods

Materials and methodology

2.1 Materials

2.2 Yeast stains construction

All yeast strains used in this study were congenic to BY4741 and listed in the table. Since *MGE1* is an essential gene, deleted diploid strain (*Mata/alpha;his⊿1/3his3⊿1;Leu2⊿0/leu2⊿0;lys2⊿0/LYS2;MET15/met15⊿0;ura3⊿0/ura3⊿0;OR232w::kanMX4/YOR232w*) is transformed with a 2µ plasmid containing MGE1 and it was purchased from EUROSCARF Germany. Wild type *MGE1* and mutants were cloned into 2µ *pTEF-LEU* plasmid. Clones were confirmed and transformed haploid strain of above mentioned strain. The URA3 plasmid was kick out by growing on 5FOA plates. Strains yNB67 (wild type), yNB69 (M155L), yNB70 (H167L), yNB103 (M155L, H167L) were generated from above strain by transforming plasmid pNB358 (pTEF-LEU wildtype *MGE1*), pNB361 (*pTEF-LEU* M155L), pNB353 (pTEF-LEU H167L) and pNB340 (pTEF-LEU M155L, H167L) respectively. For monitoring the autophagy and mitophagy, we transformed pRS423 *ATG:GFP* and pRS316 *DHFR-GFP* plasmids to above strains respectively.

Table 2.1 Yeast strains and their genotypes

strain	genotype	Source
YNB36	*Mata/alpha;his⊿1/3his3⊿1; Leu2⊿0/leu2⊿0;lys2⊿0/LYS2;MET15/met15⊿0; ura3⊿0/ura3⊿0;OR232w::kanMX4/YOR232w*	EUROSCRAF
YNB65	*Mat a, his⊿1, leu2⊿0, lys2⊿0, ura3 ⊿0, YOR232w::KANMX4*	This study
YNB66	*Mat a, his⊿1, leu2⊿0, lys2⊿0, ura3 ⊿0, YOR232w::KANMX4 pTEF-2µ- LEU*	This study
YNB67	*Mat a, his⊿1, leu2⊿0, lys2⊿0, ura3 ⊿0, YOR232w::KANMX4 pTEF-2µ-WT MGE1- LEU*	This study

YNB69	*Mat a, his⊿1, leu2⊿0, lys2⊿0, ura3 ⊿0, YOR232w::KANMX4 pTEF-2μ- M155L MGE1- LEU*	This study
YNB70	*Mat a, his⊿1, leu2⊿0, lys2⊿0, ura3 ⊿0, YOR232w::KANMX4 pTEF-2μ- H167L MGE1- LEU*	This study
YNB103	*Mat a, his⊿1, leu2⊿0, lys2⊿0, ura3 ⊿0, YOR232w::KANMX4 pTEF-2μ- M155L, H167L MGE1- LEU*	This study
YNB124	*Mat a, his⊿1, leu2⊿0, lys2⊿0, ura3 ⊿0, YCL033c::KANMX4 pTEF-2μ-URA MXR2-FLAG*	This study
YNB130	*Mat a, his⊿1, leu2⊿0, lys2⊿0, ura3 ⊿0, YCL033c::KANMX4 pTEF-2μ-LEU MGE1*	This study
YNB152	Strain YNB67 transformed with pRS423-*ATG8:GFP-HIS*	This study
YNB153	Strain YNB69 transformed with pRS423-*ATG8:GFP-HIS*	This study
YNB154	Strain YNB70 transformed with pRS423-*ATG8:GFP-HIS*	This study
YNB155	Strain YNB103 transformed with pRS423-*ATG8:GFP-HIS*	This study
YNB256	Strain YNB67 transformed with pRS 316 DHFR:*GFP-URA*	This study

YNB257	Strain YNB69 transformed with pRS 316 DHFR*:GFP-URA*	This study
YNB258	Strain YNB70 transformed with pRS 316 DHFR*:GFP-URA*	This study
YNB259	Strain YNB103 transformed with pRS 316 DHFR*:GFP-URA*	This study

Table 2.2 Plasmids list

Name	Description
pNB45	pTEF-MGE1, 2µ, URA
pNB358	pTEF-MGE1, 2µ, LEU
pNB361	pTEF-MGE1 M155L, 2µ, LEU
pNB353	pTEF-MGE1 H167L, 2µ, LEU
pNB340	pTEF-MGE1 M155l, H167L, 2µ, LEU
pNB475	pTEF MXR2-FLAG, 2µ, LEU
pNB61	pET28a+ MGE1
pNB351	pET28a+ M155L MGE1
pNB360	pET28a+ H167L MGE1
pNB447	pET28a+ M155L, H167L MGE1
pNB558	pET28a+ MDJ1
pNB671	pRSF Dual mt HSP70
pNB760	pRS423 ATG:GFP HIS
pNB506	pRS316 DHFR:GFP URA

Table 2.3 Yeast and E.coli growth media composition

YPD	1% yeast extract 2% peptone 2% Destrose
YPGal	1% yeast extract

	2% peptone 2% Galactose
YPG	1% yeast extract 2% peptone 3% Glycerol
Lactate media	3 g yeast extract, 1 g KH2PO4, 1 g NH4Cl, 0.5 g CaCl2, 0.5 g NaCl, 0.8 g $MgCl_2$, 1 g glucose. 100 ml 20% lactic acid, pH 5.5
YPL	1% yeast extract 2% peptone 2% Lactate pH 5.5
Synthetic complete (SC) medium	6,7 g/l yeast nitrogen base (YNB) with ammonium sulfate 1,5 g/l drop-out mix Carbon source: 2% (w/v) glucose* 2% (w/v) raffinose* 2% (w/v) galactose* Selection markers were added to sterilized media: adenine (40 µg/ml) histidine (20µg/ml) leucine (60 µg/ml) lysine (30 µg/ml) tryptophan (40µg/ml) uracil (20 µg/ml) 2% (w/v) glucose or 2% (w/v) galactose SC-agar plates-

	2% (w/v) Agar 0.7 g Aminoacid dropout mix 2% glucose
Bactoagar	Bactoagar was added to media and pH was adjusted before sterilization
LB or SOB media	1% (w/v) peptone 0,5% (w/v) yeast extract 1% (w/v) NaCl for LB-agar plates 1.5% (w/v) bactoagar for LB-ampicillin-medium 100 µg/ml ampicillin added to sterile LB-medium

Table 2.4 Primers list

PRIMER NUMER	SEQUENCE(5' …….3')	RESTRICTION SITES	INSERT
NB471	CGC GAATTC ATG GAG GAG CCG CAG TCA	EcoR1	P53 F PET 28
NB472	CGC CTC GAG TCA GTC TGA GTC AGG CCC	Xho1	P53 R PET28
NB435:	CGC CTC GAG ATG GAG GAG CCG CAG TCA	Xho1	P53 F PET28
NB436	CGC GAA TTC TCA GTC TGA GTC AGG CCC	Eco1	P53 R PET28
NB529	CCCA CCATG GAT GAA GCC AAA AGT GAA TCC	Nco1	YMGE1 WITH-OUT HIS TAG
NB540 A	GGG GTT AGA TGT ACA AGA GAT 3	SITE DIRECTED	F YMGE1 M155C
NB541 B	ATC TCT TGT ACA TCT AAC CCC 3		R YMGE1 M155C
NB579	AAA C AAG CTTTC ACC ATG GCT TTC CAA CAA GGT	HindIII	MDJ1F
NB560	CCCA CTC GAG TTA ATT TTT TTT GTC ACC	Xho1	MDJ1 R
NB561	CCC AGA ATT CAC CAT GTT GAG ATC ATC CGT T	EcoR1	HSP60 F
NB562	CCCA CTC GAG TTA CAT CAT ACC TGG CAT	Xho1	HSP60R
NB563	CCC AGA ATT CAC CAT GAA TAA TGC TGC AAA T	EcoR1	HSF1 F

NB564	CCCA CTC GAG CTA TTT CTT AGC TCG TTT	Xho1	HSF1 R
NB585	CCC AGA ATT CAC CAT GCT TGC TAA AAA C	EcoR1	SSC1 F
NB586	CCC ACT CGT GTT ACT GCT TAG TTT CAC C	Xho1	SSC1 R
NB589	AAA CAA GCT TTC ATG AAC GAA GCA TTC AAG GAC CCG TAC	HindIII	MDJ1 F(-MLS)
NB604	CCCA GAA TT C ACC ATG ATT CCG AGG ACT AGA	EcoR1	ZIM17
NB605	CCCA CTC GAG TCA TTT CTG GGA AGG GTG	Xho1	ZIM17

2.3 Methods used in the thesis

2.3.2 Cloning

Cloning was performed by digesting DNA using restriction enzymes (FERMENTAS). Usually plasmid DNA (200-400 ng) was digested for overnight in a total volume of 50 µl. Restricted digested plasmids and amplified PCR products were separated on 1% agarose gel electrophoresis and purified using nucleospin columns. Ligation was carried out by taking digested plasmid DNA and PCR product in 1:3 or 1:5 ratio and kept incubation at 22 °C for overnight along with T4 DNA ligase (FERMENTAS).

2.3.3 Preparation of chemically ultra-competent E.coli cells

E. coli cells were grown in 250 ml of bacterial LB medium (2% peptone, 0.5% yeast extract, 0.5% NaCl,) in a one litre volumes flask. The cultures were grown at 18 °C, orbital shaker maintained at 220 rpm speed until OD600 reached approximately 0.6 nm (about 20 hr). The culture was allowed to cool on ice for 10 mins and centrifuged at 2,500 g for 10 mins at 4 °C. The pellet was then resuspended in PIPES buffer (10 mM PIPES, 15 mM $CaCl_2$, 250 mMKCl; pH 6.7 adjusted with KOH). Cell suspension was kept on ice for 30 mins, later cells were spun at 4 °C with speed 2,400 g. And the pellet was then resuspended in 20 ml of PIPES buffer with 7% DMSO. Further, cells were kept on ice for 10 mins and aliquots were snap freeze with liquid N_2 before storage at -80 °C.

2.2.5 Plasmid DNA purification

DH5α E. coli strains were used to amplify the plasmid copy number. A single colony was inoculated into 10 ml LB medium containing with either Ampicillin (100 µg/ml) or Kanamycin (25 µg/ml) incubated for overnight at 37 °C with shaking 180 rpm speed. Cells were collected by spin at 13,000 rpm speed for 1 min on a tabletop centrifuge (Eppendorf, Germany). Plasmid DNA was purified by the QIAPrep Spin Miniprep Kit (QIAGEN, Germany).

2.2.6 Site directed mutagenesis (SDM)

For site-directed mutagenesis, high fidelity polymerase such as pfu or Phusion weas used to mutate codons. Primers listed in Table (2.4) were designed using standard procedure and PCR reaction conditions were followed as mentioned earlier. Reaction samples were cooled below 37ºC and 1 µl of Dpn I (FERMENTAS) was added and digestion mixture was kept in waterbath (37 ºC) for 45 mins to specifically digest the methylated (parental DNA) and hemi-methylated but not digest the amplified DNA. After Dpn1 digestion, the reaction mixture was transformed to DH5α E.coli strains and plasmid DNA was isolated as per methods described earlier. Mutations were confirmed by Sanger sequencing method.

2.2.7 Protocol for transformation of yeast strains

Yeast strains were transformed by following the standard procedure. Yeast cells were inoculated in YPD (10 ml) media and grown by keeping culture on shaker with speed 180 rpm at 30 °C and grown until OD reaches 0.6. The cells were centrifuged at 2,500 rpm for 5 mins, resuspended in 1 ml of 100 mM LiOAc (Lithium Acetate). 50-100 µl cells were taken from suspension and centrifuged at high speed for 30 secs and transformation mixture was prepared by adding 240 µl 50 % PEG, 36 µl 1 M LiOAc, 50 µl single standard DNA, 1 µg of plasmid DNA in sequential order and vortexed vigorously. The transformation mixture was later incubated in thermo mixture maintained at 30 °C with shaking (750 rpm) for 30 mins. Later yeast cells were subjected to heat shock by keeping the cells at 42 °C for 25 mins. Immediately after heat shock, cells were spun at high speed for 30 secs and resuspended in 500 µl of mill Q water and plated on drop out media and incubated at 30ºC for 2-3 days until colonies appeared.

2.2.8 Procedure for isolation of genomic DNA from yeast cells

Parental BY4741 yeast cells were inoculated into 10 ml of YPD media and grown for overnight at 30ºC in shaking incubator. Cells were then centrifuged at 5000 rpm followed by washing with water and resuspended in 0.5 ml H_2O. Again, the cell suspension was spin at high speed for 15 secs. The cell pellet was resuspended in 200 µl of breaking buffer (2% v/v Triton X 100, 1% v/v SDS, 100 mM NaCl, 10 mM Tris-Cl, pH8.0, 1 mM EDTA, pH 8.0) and cells were lysis by vortexing at high speed by adding 0.2 gm of 0.45 mm acid washed glass beads (Sigma). 200 µl of TE buffer (10 mM Tris-Cl pH7.5/8.0, 1 mM EDTA, pH 8.0) was added and the lysate was again vortexed for 20 secs and spin at high speed for 5 mins using Eppendorf table centrifuge. The aqueous layer was transferred to a autoclaved microfuge tube, equal volume of 100% ethanol was added and mixed gently by inversion. The Mixture was spin at 13,000 rpm for 3 mins at RT.

The supernatant was discarded and the pellet was kept for drying at room temperature and resuspended in 100 µl TE buffer. To remove RNA contaminants, 30 µl of 1 mg/ml RNase A was added and incubated for 1 hr at 37 °C and 10 µl of 4M NH_4COOCH_3 and 1 ml 100% ethanol was added and gently mixed. Mixture was spin at high speed for 3 mins at RT. The supernatant was discarded and the pellet (DNA) was kept for drying at room temperature. Finally, the pellet was resuspended in 100 µl of TE buffer. The concentration of DNA was quantified by Nanodrop (Thermo Scientific, USA) at a wavelength of 260 nm.

2.2.9 Yeast growth assays

Yeast cells were grown upto mid log phase at 30ºC. About 0.5 OD cells were suspended in sterile water and made serial dilutions by 10 folds. Each dilution (5-10 µl) were spotted on agar plates supplemented with selective media or glucose containing rich media, incubated for 2- 3 days at indicted temperatures.

2.2.10 Yeast cell lysates preparation for Western blotting

Yeast strains were grown for overnight in 10 ml appropriate selective medium. Cultures were centrifuged at 5,000 rpm for 5 mins (Eppendorf, Germany) at room temperature and cells were washed with sterilized water and resuspended in 50 µl buffer (50 mM Tris pH 7.5, 100 mM NaCl, 1 mM PMSF (phenylmethylsulfonyl fluoride)) along with 0.2 gm acid wash glass beads. This mixture was vortex vigorously and centrifuged (Eppendorf, Germany) at 13,000 rpm for 10 mins at 4ºC. The supernatant contains soluble proteins was estimated by Bradford protein assay kit (AMRESCO). 2XSDS sample buffer was added to 50 – 100 µg of protein and kept for boiling at 95 ºC for 5 mins. These samples were run on SDS_PAGE and western analysis or can be stored at -20 ºC.

2.2.11 Procedure of protein purification from E. coli cells

Mge1, Mdj1 and Mdj1 clones constructed into pET28a (+) vector were transformed to BL21 (DE3) bacterial competent cells. A single colony from transformed was inoculated into LB media and grown at 30ºC for 3-4 hrs by shaking at 220 rpm speed. Cultures were centrifuged at 8,000 rpm for 10 mins and resuspended in buffer (25 mM Tris-HCl pH 8.0, 100 mM NaCl, and 2 mM DTT) and stored at -80 ºC. Cell suspensions were thawed to 4 ºC and the suspension was lysed by extensive sonication for 20 cycles (15 sec ON and 45 sec OFF) at 30% amplitude. The bacterial lysates were cleared at high speed for 30 mins and the supernatant was loaded to Ni-NTA charged beads (Clontech, USA). Beads were washed with 3-5 volumes of buffer containing

20 mM imidazole. Finally, proteins were eluted with buffer containing 400 mM imidazole and dialyzed against buffer containing 10% glycerol without imidazole. Protein aliquots were subjected to snap freeze using liquid nitrogen and stored at -80ºC.

2.2.12 Purification of recombinant yeast mtHsp70 protein

The plasmid pRS Dual containing both Zim17 and Ssc1 genes (a kind gift from Patric Dsilva, IISc, Bangalore) was transformed by electroporation into E.coli (BL21 DE3) cells, grown in LB medium and protein was induced with 0.2 mM Isopropyl thiogalactoside (IPTG) at 25° C for 6 hrs. The cells were collected by centrifugation, suspended cells in 50ml of buffer B (50mM Tris-HCl pH 7.5 with 300 mM KCl, 5mM MgCl2 and 10% glycerol) containing 10mM imidazole. Cells were lysed with 0.1 mg/ml lysozyme, 1mM/ml PMSF and incubated at 4 °C for 60 mins followed by treatment with deoxycholate (0.2 %) for 15 mins. The cell suspension was sonicated for 5 cycles with 2 mins gap per every cycle. Protein lysate was centrifuged at high speed for 30 mins at 4 °C. The supernatant was loaded onto 1.5 ml of Ni-NTA column (Clone tech) pre-equilibrated with buffer B. Beads were washed with buffer B containing 1M KCl, 1 mM ATP, and 20 mM Imidazole. Finally, the proteins were eluted with buffer B with 400 mM Imidazole and dialyzed against buffer B without Imidazole. Proteins were snap freeze and stores at -80 °C till use.

2.2.13 Western blotting

Protein immuno-blotting was done by using yeast protein extract prepared by fallowing protocol. Equal amount of proteins were separated by 12% SDS PAGE (PolyAcrylamide Gel Electrophoresis) and transferred to nitrocellulose membrane using buffer (Towbin buffer) for overnight at 50 V. Transferred proteins were visualised by staining the membrane with Ponceau S stain (0.2% Ponceau S in 3% Acetic acid) followed by repeatedly washing with 1X TBST (0.1% Tween 20 in TBS: 25 mM Tris pH 7.4, 155 mM NaCl, with HCl). Blocking was done using 5% milk powder (non-fat) in 1X TBST for 1 hr at room temperature. The membrane was probed with the appropriate primary antibody or antisera by incubating on a shaker for overnight at 4ºC or 1 hour at room temperature. The membrane was further washed three times for every 15 mins with 1X TBST. Horse Radish Peroxidase (HRP) coupled rabbit anti-mouse or anti-rabbit IgG secondary antibodies were incubated with the membrane at room temperature for 1 hour followed by again washing for 3 times each 15 mins with 1X TBST. Finally, the membrane was developed by the Enhanced Chemiluminescence (ECL) reagent supplied by Bio-Rad or AMERSHAM.

2.2.14 Fluorescence microscopy analysis

Mid-log phase yeast cells, grown in selective media, cells were spin at 2000 rpm. Cells were suspended in sterile water, 10- 20 µl of cell suspension was spread on the glass slide and allowed to dry at RT. 5 µl of 50 % glycerol was added to avoid air bubbles and a coverslip was placed. Cells were viewed either with bright filed or GFP filter using a ZEISS microscope.

2.2.15 Yeast mitochondria isolation procedure

Yeast mitochondria were isolated using the standard procedure. Cells were grown in YPL or Semi-synthetic lactate media up to 1- 2 OD at 30ºC with shaking at 180 rpm speed. Cells were harvested by centrifuge (KUBOTA, Japan) at 5,000 rpm for 5 mins followed by washing with sterile water. The cells were resuspended in buffer containing 10 mM dithiothreitol (DTT) and 0.1 M Tris-SO4, pH 9.4 and incubated for 15 min with slow shaking. Again cells were harvested by centrifugation at 5000 rpm for 5 mins. Spheroplast was made lysing the cells by treating with Zymolyase (Lyticase Sigma) in 1.2 M sorbitol/20 mM phosphate buffer, pH 7.0 for 45 mins at 30ºC by slow shaking. Lysis was monitored by observing the OD of spheroplast 600 nm by UV-Visible spectrophotometer (HITACHI, Japan). After reaching the half the OD of without Zymolyase treated cells, spheroplast was gently washed with 1.2 M sorbitol two or three times at 3500 rpm in cold condition. Now spheroplast was resuspended in SEM buffer (250 mM sucrose, 1 mM EDTA, 10 mM 3-(N-morpholino) propanesulfonic acid [MOPS] and homogenized using Dounce homogenizer by giving 15 strokes. The homogenate was centrifuged at 3500 rpm for 5 mins. Repeat the homogenization step was repeated once more and the supernatant fraction was collected. The supernatant was spun at 10,000 rpm for 10 min (Eppendorf, Germany) and the pellet fraction was saved. The pellet was resuspended in SEM buffer and the supernatant was saved by centrifugation at 3500 rpm for 5 mins. Finally, the supernatant was centrifuged at 10,000 rpm for 10 mins and saved the pellet containing mitochondria and washed three times with SEM buffer by centrifugation at the same speed. The mitochondria were solubilized in SEM buffer (without BSA) and made into aliquots (10 mg/ml), snap freeze the samples and stored at -80 °C.

2.2.16 Ni-NTA pull-down assays

Wild type Mge1 with N terminal His Tag protein was denatured using urea as denaturant at different molar concentrations, loaded onto the Ni-NTA affinity beads and incubated for 1 hr at 4 °C. Mitochondria lysate was prepared by lysis in buffer (50 mM Tris-HCl, pH 8.0, 150 mM NaCl, 1% non-ionic detergent IGEPAL (Sigma), 0.5% deoxycholate) and to avoid non-specific

interactions, Ni-NTA beads were added. Pre-cleared lysates were incubated with Mge1-bound Ni beads for only 10 mins so as to minimise the renaturation of Ni-NTA bound urea treated Mge1. The beads were washed with the lysis buffer containing 20 mM Imidazole followed by eluting the bounded proteins with glycine buffer or 1XSDS sample buffer, further samples were separated using SDS-PAGE and analyzed by Western blot.

2.2.17 Cross-linking experiments

Mge1 and mt Hsp70 (Ssc1) proteins were mixed in a molar ratio of 1:3 in 200µl of cross-linking buffer (20 mM HEPES/KOH pH7.4, 80mM KCl, 5mM $MgCl_2$, 1mM PMSF). 2 µl of crosslinker (DSS) was added to protein mixture from a 12.5 mM stock and incubated at room temperature for 20 mins in dark. The crosslinking reaction was quenched by adding 40 mM Tris/HCl pH 7.5 for 15 mins. The cross-linked proteins were analyzed by SDS PAGE followed by CBB staining.

2.2.18 In-organello crosslinking assay

Isolated mitochondria were suspended in buffer (20 mM HEPES/KOH pH7.4, 80mM KCl, 5mM MgCl2, 1mM PMSF), incubated at indicated temperatures for 20 mins, followed by addition of the cross-linker disuccinimidyl suberate (DSS; Pierce) to final concentration 100 µM for another 20 mins at same temperatures. The reaction was quenched by addition of 40 mM Tris/HCl pH 7.5 at room temperature. The crosslinked proteins were either analyzed by western blot analysis or used for immunoprecipitation assay.

2.2.19 Far-UV CD spectroscopy

Mge1 proteins were taken in PBS (phosphate buffer saline) and CD spectra were obtained by using Jasco-810 spectropolarimeter (Japan) flushed with nitrogen gas. The spectra were recorded using a 0.1cm path length quartz cuvette with a scan rate 50 nm/mins. Average of three scans were presented in terms of Mean Residue Ellipticity (MRE) and plotted against wavelength in the range 260 to 200 nm. Thermal denaturation curves were obtained by continuous recording ellipticity at 218 nm from 25ºC to 90ºC with 1-degree rise per min. Data were analyzed using by fitting into two state equation using graph pad prism.

2.2.20 Oxygen consumption rate (OCR) measurement

Yeast cells were grown in YPD media at 30 ºC up to a mid-log phase and cellular respiration was measured by Clark type oxygen electrode (Hansatech Instruments, Norfolk, UK).

2.2.21 Reactive oxygen species (ROS) quantification

Yeast cells were grown at 30ºC in YPD media with shaking at 180 rpm speed. Cells (1-2 OD) were pellet down at 2000 rpm and resuspended in phosphate-buffered saline (PBS) containing 50 µM H2DCFDA dye and incubated at 30 °C for 20 mins. Cells were washed two times with PBS and finally resuspended in PBS. For mitochondria-specific ROS measurement, cells were incubated with 30 µm MITO-SOX (Invitrogen) dye in PBS buffer for 20 mins at room temperature. Becton-Dickinson FACS Calibur flow cytometer was used to measure the amount of ROS for 10,000 events. For H2DCFDA fluorescence, FL1 (green fluorescence-detecting) channel was used, for Mito-SOX dye, FL3 channel was used to quantify the ROS.

2.2.22 Measurement of mitochondrial membrane potential (Ψm)

Yeast mitochondria membrane potential Ψ was estimated using mitochondrial specific cationic fluorescent dye, DiOC6 (Invitrogen). 1 OD cells were suspended in PBS and incubated with 5 µM DiOC6 at room temperature for 30 mins. After incubation, cells were washed with 2 times of PBS by centrifugation at low speed for 2 mins. Immediately after cells resuspension in sheath fluid, membrane potential was measured using Becton Dickinson FACS Aria II flow cytometer (Becton Dickinson, USA). Excitation was performed using an FL1 filter, specifically excites the green fluorescence. For control purpose, cells were incubated with ionophore carbonyl cyanide m-chloro phenyl hydrazone (CCCP), which dissipates the membrane potential and mitochondria become hyperpolarized.

2.2.23 In vivo mitochondrial translation

Mitochondrial gene products were synthesized using mitochondrial ribosomal proteins and can be studied specifically using by inhibiting cytosolic translation. 250 µl of yeast cells from 3.0 OD/ ml were resuspended in 40 mM Kpi buffer with 2% galactose and incubated at 30ºC by adding 5 µl cycloheximide (7.5 mg/ml). The reaction was initiated by adding 2 µl of S35 (mCi/ml), incubated at 30 ºC for indicated time periods and reaction was terminated by adding chloramphenicol to a final concentration 0.5 mg/ml. For pulse-chase experiments, translation reaction was allowed for 15 mins, further reactions were incubated for indicated time intervals at 30 ºC. Equivalent amounts of total cellular components were separated by SDS-PAGE (17.5%), transferred to a nitrocellulose membrane, and the membrane was scanned using typhoon scanner.

2.2.24 In-vitro and In-vivo mitochondrial protein import assay

Mitochondria were isolated from yeast cells grown at 30 ºC as described earlier. Isolated mitochondria resuspended in buffer (Fat free bovine serum albumin, sucrose 80 mM, KCl 5 mM, MgCl2 5 mM, methionine 10 mM, 3-(N-morpholino) propanesulfonic acid(MOPS)/KOH pH 7.0, ATP 5 mM pH 7.0, and dithiothreitol (DTT) 1 mM) and incubated with Su9-DHFR (radiolabelled with S35) for indicated time periods at 30 ºC. Samples were treated with trypsin (5 µM) followed by treatment with trypsin inhibitor (25 µM) for protease protection assay and the proteins were separated using SDS PAGE and transferred to nitrocellulose membrane. Proteins were visualized by autoradiogram (GE healthcare). For in-vivo import assay, yeast cells were grown in YPD media up to mid-log phase at 25 ºC and cells were shifted to 37 ºC and grown for 4 hrs. Cells were harvested by centrifugation at high speed for 5 mins followed by washing with distilled water. Lysates were prepared using the acid wash glass beads method and resolved by SDS PAGE and analyzed by western analysis by probing with the anti-hsp60 antibody.

2.2.25 Preparation of H_2O_2 [1 M]

Hydrogen peroxide 30% purchased from Merck, chemicals. Molarity was estimated by taking absorbance at 240 nm using its extinction coefficient (E 240 nm=43.6 M^{-1} cm^{-1}). 1 M hydrogenperoxide was prepared by appropriate volume from 30% hydrogen peroxide and diluted to 1 ml with deionized water.

2.2.26 In vitro oxidation of Mge1 or mitochondria

Purified Mge1 was diluted to 1 mg/ml in PBS buffer and incubated with different concentration of hydrogen peroxide for 3-4 hrs in dark. Then proteins were dialyzed against PBS buffer to remove unreacted hydrogen peroxide. Isolated mitochondria were resuspended in buffer (250 mM sucrose, 10 mM MOPS, 80 mM KCl, 5 mM $MgCl_2$, 5 mM ATP, and 4 mM NADH) and treated with various concentrations of hydrogen peroxide for 1-2 hrs in dark.

2.2.27 Fluorescence quenching studies

Mge1 has a single tyrosine and 9 phenylalanine resides which will fluoresce with a low yield at 303 nm. The quenching studies were done by using static ionic quencher, potassium iodide (KI). 5 µM protein samples either native or oxidized were incubated with different molar concentrations of potassium iodide. Intrinsic fluorescence spectra were obtained by excitation at 275 nm and emission wavelength range of 290-370 nm. The Stern-Volmer constants were obtained from Stern-Volmer plots as described in [1].

2.2.28 Spectroscopic analysis

Intrinsic fluorescence spectra were recorded in the range of 300 to 400 nm using an excitation wavelength of 275 nm at room temperature by fluorescence spectrophotometer (FLUORO-MAX 3). The protein concentrations used were 10 μM, in phosphate buffer saline (pH 7.0). Three scans of each spectrum were averaged, and baselines of the buffer alone were subtracted. To monitor the surface hydrophobicity, fluorescence dye 4, 49-dianilino-1, 19- binaphthyl-5, 59-disulfonate (bis-ANS) was incubated with proteins. Spectra were recorded in the range of 400 to 600 nm, using an excitation wavelength of 390 nm with 2.5 nm excitation and emission slits. Amyloid-type fibrils were monitored by incubating proteins samples with probe thioflavin-T at room temperature. Spectra were recorded in the range of 470 to 570 nm, using an excitation wavelength of 444 nm with 10 nm excitation and emission slits. Recombinant wild type Mge1 protein purified from bacterial expression system, treated with 10 mM H_2O_2 for 12 hrs followed by dialysis. Congo Red, the spectra were recorded from 400 to 600 nm using UV-Visible spectrometer (HITACHI, Japan) for both the native protein and that oxidized proteins incubated with 20 μm dye. For turbidity assay, oxidized Mge1 proteins (10 μg/ml) in PBS (phosphate buffer saline) buffer were performed using FLURO-MAX-3. The scatter light was recorded using both excitation and emission at 600 nm, after 900 s of standing.

2.2.29 Atomic force microscopy (AFM) studies

Native and oxidized recombinant purified Mg1 protein (10 μg) was spread as thin layer on clean glass plate and dried by passing N_2 gas. Images were taken using NT-MDT (Japan) solver scanning probe microscopy equipment.

2.2.30 Protein-protein interaction studies

Interactions were studied by immunoprecipitation. Native and oxidized recombinant Mge1 protein (30μg), Hsp70 (30μg) and 30 μg of heat-denatured glutamate dehydrogenase (GDH) were incubated in PBS buffer and mixture were kept on ice for 2 hrs. To avoid non-specific interactions, mixtures were pre-cleared with protein A beads for 1 hour. Protein A Sepharose coupled Hsp70 antibody beads were added to mixture. Hsp70- bound proteins were eluted with glycine buffer and analysed by western blotting.

2.2.31 Molecular dynamics simulations studies and three dimensional structures of Mge1 and its mutants

The three-dimensional model structures of Mge1 and its mutant Msx of Saccharomyces cerevisiae (CAA99452.1) were built by Discovery Studio 2.5 as described in [2]. The 3D model of the mutant of Mge1, Msx155 was built in both chains of homodimer by changing Met155 to

its sulfoxide (Msx). The molecular dynamics simulations of wild-type and mutant Mge1 (Msx) homo-dimers were performed with 43a1 force fields using the GROMACS 4.5.5 package. And using the explicit solvent- SPC/E water model, Mge1 proteins were subjected to 50 ns MD simulations, under isothermal-isobaric conditions in a periodic triclinic box (15.56 x 9.362 x 8.0 nm). Negative charged Mge1 proteins were neutralized by supplementing with $2Na^+$ ions. The steepest-descent algorithm was used to find system local minimum energy for both 5000 steps and 1000 picoseconds (ps) position restrained dynamics to allot water molecules all over the system. The energy minimized modeled structures of both wild-type Mge1 and its mutants were used as the starting reference structures for more simulations. And we subjected the whole system to MD simulations for 50 ns, using 0.002 ps time step. For quantify the electrostatics, we employed the Particle Mesh Ewald (PME) summation method, with a real space cut-off of 10 Å, PME order of six and a relative tolerance between long- and short- range energies of 10-6. Short-range interactions were evaluated using a neighbor list of 10 Å updated every 10 steps, the Lennard-Jones (LJ) interactions and real space electrostatic interactions were truncated at 9 Å. To maintain the temperatures (25 ºC) and pressure (1 atm), we employed V-rescale thermostat and Parrinello-Rahman algorithm respectively. The LINCS algorithm was used to fix all bond parameters. The trajectory file was analyzed using visual dynamics or VMD which is obtained from MD. The Root Mean Square Deviations (RMSD) of both wild type Mge1 and mutant proteins backbone atoms were used analyze the both stability and equilibrium. The RMSD of Cα atoms is the average structure with respect to the reference structure, GROMACS program was used to fitting least-square. The g_rmsf was employed to calculate the Root Mean Square Fluctuations (RMSF) of protein Cα atoms to study the dynamic flexibility in various regions of the structure. And the g_energy was used to quantify the potential energy (PE) and kinetic energy (KE) of the model structures. The g_sas was used to calculate Solvent-accessible surface area (SASA) of proteins. Similar protocols were employed for the MD simulations and analyses of the Msx155.

2.2.32 RNA-Seq experiment and data analysis

Untagged yeast MGE1 wild type and its mutant strains were generated by transforming plasmids carrying MGE1 to genomic MGE1 deleted isogenic strains and duplicated cultures grown in YPD media up to mid-log phase at 30 ºC. Total RNA was isolated from cultures and RNA quality and concentration were assessed using the Agilent 2200 TapeStation system (Agilent Technologies, Santa Clara, USA) and NanoDrop 2000 Spectrophotometer (Thermo Fisher Scientific, Waltham, USA), respectively.

RNA-Seq was performed by Sandor Life Sciences., Ltd. Briefly, libraries for RNA-Seq were prepared using sample Prep Kit Sample Prep Kit (Illumina, USA) by following the manufacturer's protocol. The purified libraries were assessed using the Agilent 2200 TapeStation and Qubit® 2.0 (Life Technologies, USA), and subsequently sequenced on an Illumina HiSeq. Raw reads were trimmed for clean data and mapped using Tophat (v2.0.13) to the S288c genome. The gene expression abundance was normalized by FPKM (fragments per kilobase of exon per million fragments mapped) using Cufflinks (v2.2.1). Differentially expressed genes (DEGs) were identified, with the edge $|\log2 \text{ (Fold change)}| > 2$ and q-value < 0.05 as the criteria of significant gene expression difference.

Enrichment of GO terms and KEGG pathways was analyzed by using identified DEGs. Enrichment of functional categories among DEGs was performed with the MIPS Functional Catalogue (http://mips. helmholtz-muenchen.de/funcatDB/). Specific gene functions and biological pathways were annotated according to SGD (http://www.yeastgenome.org) and UniProt (http://www.uniprot.org/).

Chapter 3
Role of Mge1 in abiotic stresses adaptation

Introduction

Single cellular *Saccharomyces cerevisiae* serves as an ideal model system for studying highly conserved signaling pathways amongst eukaryotic organisms (Botstein, Chervitz et al. 1997). Given its versatility, it is also one of the preferred expression systems for industrial purposes (Steensels, Snoek et al. 2014). Yeast cells are hardy and can survive against abiotic stresses like fluctuations in temperature and pH, redox imbalances and osmotic shocks without gaining any deleterious effects. This endurance against abiotic stress is attributed to the several adaptive signaling pathways entwined in yeast that all converge on its mitochondria (Lahtvee, Kumar et al. 2016).

The network control centre for a variety of cellular pathways that includes ATP production, iron cluster biosynthesis, amino acid metabolism, fatty acid biosynthesis and apoptosis is the mitochondria (Friedman and Nunnari 2014). To coordinate and conduct its numerous functions, the mitochondrion is endowed with its own genetic and protein synthesis machinery. It is an essential organelle and any compromises on its functions can be manifested in neurodegenerative disorders, cancers and other myopathies (Mattson, Gleichmann et al. 2008).

Despite their own genome and protein synthesis machinery, mitochondria harbor a highly specialized and intricate protein import machinery to import proteins translated in the cytosol.. Mitochondrial protein import machinery and target proteins have been well elucidated and studied extensively, however, there is paucity of information on the regulation aspect. It has been shown that the import machinery works closely with the oxidative phosphorylation complexes that regulate respiration or are under its influence (Kulawiak, Hopker et al. 2013).

Despite the dependence of mitochondria on cytosolic proteins for carrying out their functions, mitochondria have the wherewithal to influence nuclear transcription. Perturbations in mitochondrial function are conveyed to the nucleus through apparently a well-regulated signaling process that is only being appreciated now. This back signaling of mitochondria to nucleus is known as mitochondrial retrograde signaling that is essential to conserve the cell's resources (Szczepanek, Lesnefsky et al. 2012).

The co-chaperone of mtHsp70 (Ssc1 and Ssq1 isoforms), Mge1, is a nucleotide exchange factor that has an unusual property. Mge1 alternates between a functional dimer and an inactive monomer, sometimes even aggregating under extreme oxidative duress. Structural changes in Mge1 are deep, invasive and affect both intra-molecular and inter-molecular interactions, the

latter has a rather swift effect on Mge1-Hsp70 (Moro and Muga 2006, Karri, Singh et al. 2018). It adapts to thermal and redox stresses by undergoing structural changes that impact motor function and folding of nascent peptides. Mge1 has also been implicated in anti-fungal resistance and sterol biosynthesis (Demuyser, Swinnen et al. 2017).

The current study implicates Mge1 as a hub for protecting against abiotic stresses. We find that its adaptation to stress extends beyond thermal and oxidative stresses. We have identified two single mutations (M155L; H167L) within Mge1 that can confer resistance to all abiotic stresses tested. Curiously, Mge1, harboring both these mutations (abbreviated as DM) is vulnerable to abiotic stress and has a poor growth phenotype. Most importantly, Mge1 DM strain exhibits slow growth on non-fermentable carbon medium and has reduced oxygen consumption rate (OCR). Gene ontology (GO) analysis from high throughput RNAseq study shows that Mge1 DM cells are defective in oxidative phosphorylation, respiration and amino acid metabolism. However, Mge1 DM is shown to induce several signaling pathways like mitophagy, autophagy, mitochondrial UPR (Unfolded Protein Response) ad mitochondrial retrograde signaling. Our biochemical studies show that Mge1 DM has reduced interaction with complex IV (cytochrome c oxidase) of ETC (Electron Transport Chain). Based on our genetic, biochemical and high throughput studies, we strongly believe that Mge1 acts as a nerve center for any kind of abiotic stress and has the potential to be a master regulator of mitochondrial functions be it respiration, protein import, protein folding, mitophagy, mitochondrial UPR or retrograde signaling.

Results

3.1 Mge1 responds to multiple abiotic stresses

Previous studies from our group have shown that Mge1 acts as a first line of defense against oxidative and thermal stresses. Dimeric Mge1 monomerizes when exposed to oxidative or thermal stress that impacts the mitochondrial Hsp70 chaperone cycle. They identified single point mutations in Mge1 which confer it resistance to oxidative (Mge1 M155L) and thermal (Mge1 H167L) stresses (Marada, Allu et al. 2013, Marada, Karri et al. 2016). We hypothesized that the presence of both the mutations within the same Mge1 molecule might confer it resistance to both oxidative and thermal stresses. To test this hypothesis, we generated a yeast strain expressing Mge1 M155L H167L (here onwards called as Mge1 DM) as described in the Methods section. We grew yeast strains expressing either wild type Mge1, Mge1 M155L, Mge1 H167L or Mge1 DM and exposed them to thermal stress (37^{o}C) or oxidative stress (2 mM H_2O_2). Contrary to our expectations, yeast strain harboring Mge1 DM is highly sensitive to both thermal and oxidative stress. Intriguingly, the Mge1 H167L mutant previously identified as a thermal resistant mutant is found to be resistant to oxidative stress as well. Inversely, Mge1 M155L, a oxidation resistant mutant is also a thermal resistant mutant. This result suggests that there might be an overlap in the adaptations that Mge1 undergoes towards thermal or oxidative stress. Interestingly, a recent report suggests that mitochondrion is a hub for all abiotic stresses (Lahtvee, Kumar et al. 2016).

However, there is paucity of information on the abiotic signaling components and the mechanism of action. The proposed pivotal role of mitochondria in abiotic stress, the versatility of Mge1 to sense and respond to oxidative and thermal stresses, its mitochondrial matrix location and the apparent lack of information on the abiotic signaling mechanism forced us to examine Mge1 in greater detail in connection with the whole repertoire of abiotic stresses and its response to abiotic stress. We repeated the above experiment, using a variety of abiotic stresses such as osmotic, salinity and detergents as shown (**Figure 3.1 A**). Consistent with the above result, we find that the Mge1 DM yeast strain is more vulnerable to every kind of abiotic stress compared to control strain carrying wild type Mge1. Remarkably, yeast strains carrying Mge1 M155L or Mge1 H167L are more robust as they are observed to be more resistant than the control strain to all the abiotic stresses that we tested.

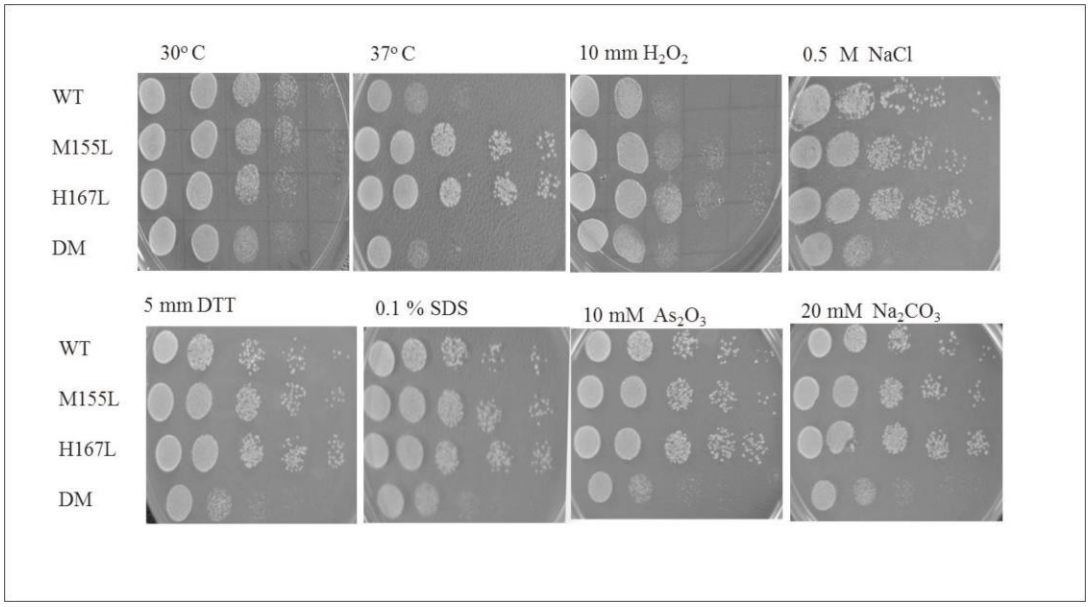

Figure 3.1 A Growth analyses of mutants of Mge1 in Yeast cells under multiple abiotic stresses. *Yeast cells transformed with pTEF 2μ plasmids containing wild type Mge1 and mutants Mge1 and their growth were compared. Yeast cells were grown upto mid log phase in YPD media and grown on SC-LEU plates supplemented with different stress agents*

To rule out the possibility of variable expression of Mge1 contributing to the observed result, we resolved whole cell extracts from all the above strains on SDS-PAGE, Western blotted and probed for Mge1 protein (**Figure 3.1 B**). Expression of Mge1 was uniform across all the strains except in Mge1 DM wherein we find relatively higher levels of Mge1, thus arguing against lowered expression for the hypersensitivity of the Mge1 DM strain. Taken together, the aforementioned results implicate Mge1 as a cellular sensor for abiotic stresses with an innate ability to adapt to the stress.

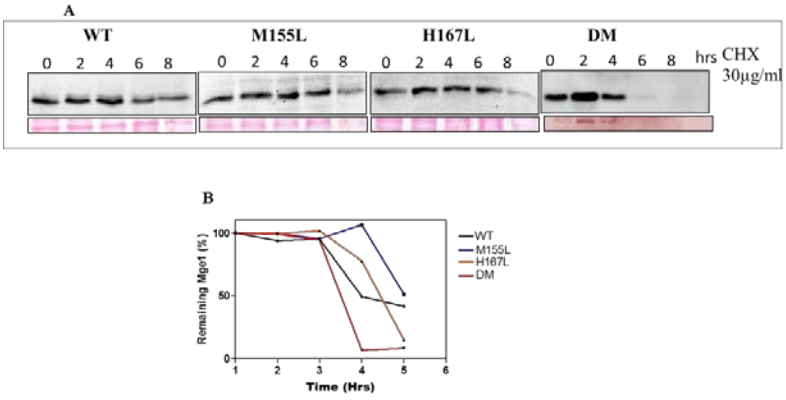

Figure 3.1 B. **The half-lives of Mge1 and its mutants.** *(A) Yeast cells expressing Mge1 and its mutants and treated with 65μg/ ml cycloheximide (CHX) in order to inhibit protein synthesis and cell growth for indicated time intervals. Cell lysates separated by SDS PAGE fallowed by western blot analysis with Mge1 antibody.*
(B) Represents quantified levels of remaining Mge1 after treatment with cycloheximide (CHX) using image J software

3.2 Double mutant Mge1 shows growth defect in non-fermentable carbon source

Mge1 is localized to the mitochondrial matrix and is close to the ETC (Voos, Gambill et al. 1994, Miao, Davis et al. 1997). We wanted to learn if there are any collateral physiological effects when Mge1 adapts to the abiotic stress as it has multiple functions. To do this, we initially wanted to understand the basic phenotype of the strains without any abiotic stress. We first tested the growth of wild type Mge1 and its mutant strains on non-fermentable carbon medium (**Figure 3.2**). Yeast strains carrying wild type Mge1 and the single mutants had comparable growth while Mge1 DM has a poor growth phenotype. Mge1 is a component of the import motor that is involved in the import of majority of mitochondrial matrix proteins through Tim23 complex.

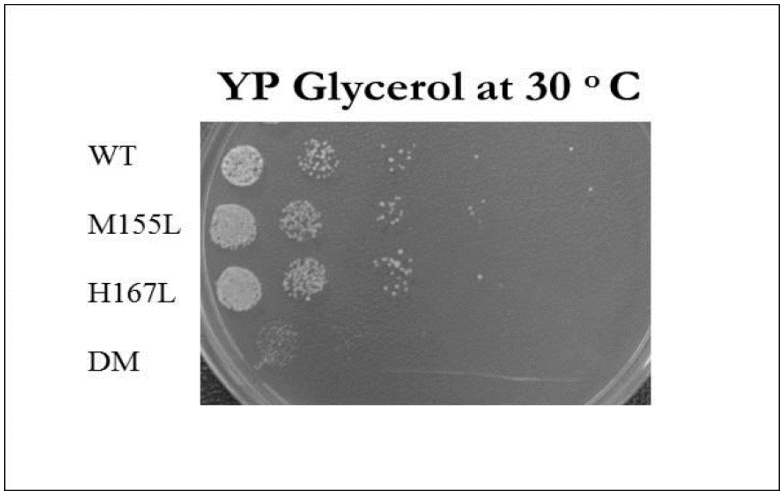

Figure 3.2 Double mutant of Mge1 shows defective growth in non-fermentable carbon source (glycerol). *Yeast cells expressing Mge1 and mutants were grown in Yeast extract-Peptone-Dextrose or YPD upto mid log phase and grown on yeast extract Glycerol plate with serial diluted cell suspension.*

3.3 Double mutant Mge1 shows import defect in both in vivo and in vitro studies

The lack of growth by Mge1 DM strain on non-fermentable carbon medium (YP Glycerol) and its increased sensitivity to abiotic stress may be attributed to compromised protein import, in particular import of ETC proteins. To prove if indeed this is the case, we monitored the temporal (0 to 8 min) *in vitro* import kinetics of radiolabeled subunit-Dihydrofolate reductase (Su-9 DHFR), a reporter protein in mitochondrial fractions isolated from wild type and mutant Mge1 strains as described in the Methods section. Although no significant defect in the processing nor protection of the protease fragment could be inferred from the quantification data, however, Mge1 DM strain had decreased import kinetics when compared to the wild type Mge1 strain (**Figure 3.3 A & B**). Further to confirm the in vitro import results, we did in vivo

import kinetic studies. Defective mitochondrial import motor complex is known to increase the cytosolic non processed precursor mitochondrial matrix proteins encoded by nuclear genome. Hsp60 protein import is sensitive to imbalance in ions and its assessment of cytosolic accumulated Hsp60 is well known method to detect compromised mitochondrial import (Kang, Ostermann et al. 1990). We had grown the yeast cells expressing mutants at 25 ^{o}C followed by 37 ^{o}C for 4 hrs. Cell lysates were prepared by the well-established acid-wash glass beads method, lysates were analysed by immunoblotting with anti Hsp60 antibody (**Figure 3.3.1**). We did not find defect in import at 25 ^{o}C or 37^{o}C in single mutants.The double mutant showed little or no defect in import at 25 ^{o}C, significant accumulation of Hsp60 in cytosol at 37 ^{o}C implying that double mutant cells impair in import at elevated temperatures.

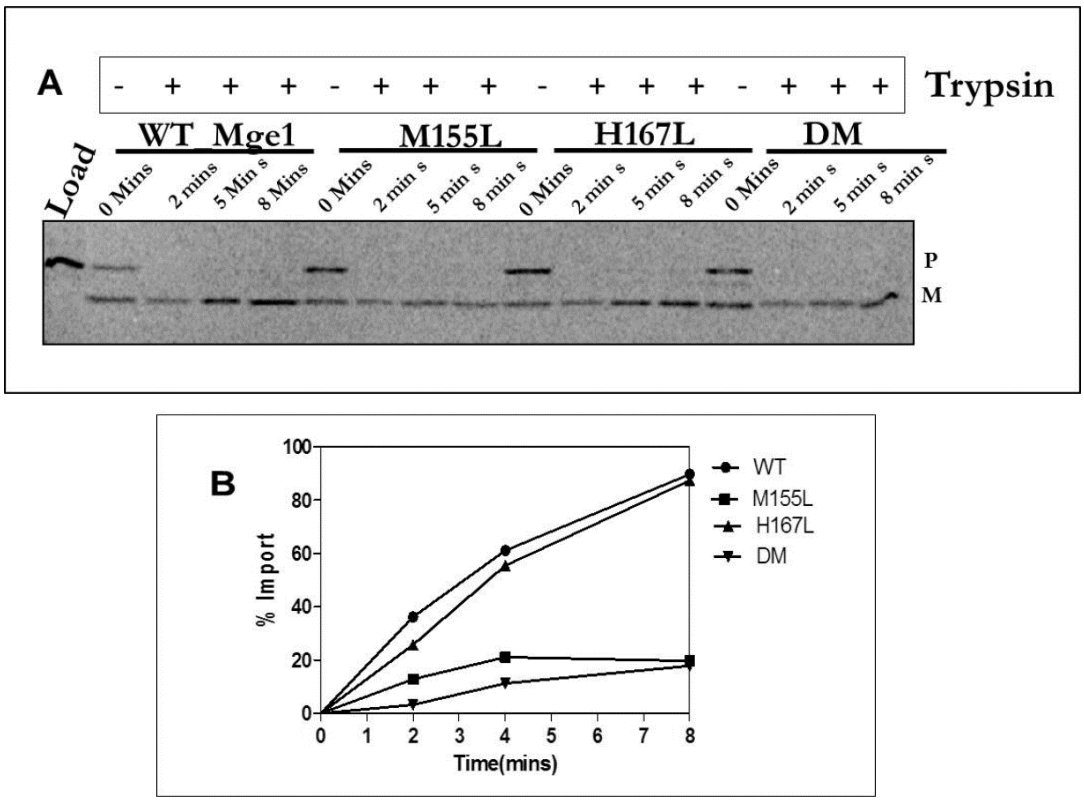

Figure 3.3 In vitro import analysis using radiolabelled SU9-DHFR, a reporter protein targeted to mitochondria matrix. (A) *Mitochondria were isolated from yeast cells expressing Mge1 and mutants and incubated with radiolabelled reporter protein for indicated time periods followed by trypsin digestion for 15 mins at cold temperature and analysed by autoradiograph.* **B** *Densitometry plots obtained from three independent experiments A using image J software. P-Precursor, M-Matured.*

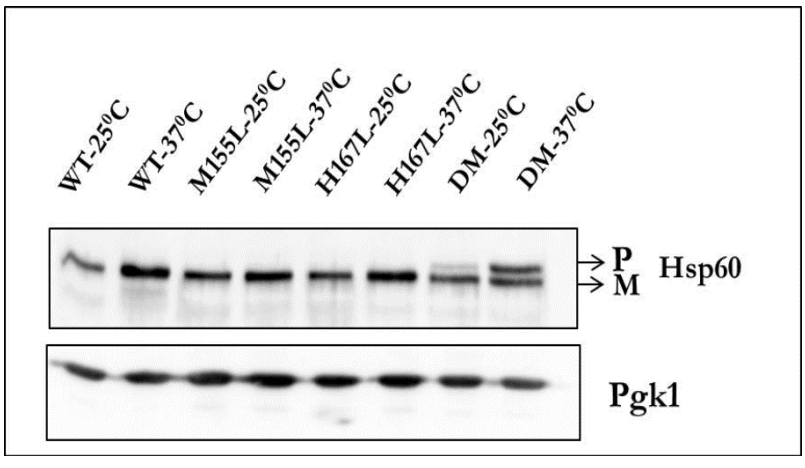

Figure 3.3.1 In vivo import analysis of yeast cells expressing Mge1 and its mutants by cytosolic accumulation of Hsp60. *Cells were grown at 25ºC upto mid log phase and shifted to 37º C for 4 hrs. Cell lysates were prepared and analysed Hsp60 accumulation by western blot analysis by probing Hsp60 and phosphoglycerate kinase (Pgk1) antibodies. P-Precursor, M-Matured.*

3.4 Double mutant Mge1 impairs mitochondrial membrane potential

Although no significant defect in the processing or protection of the protease fragment could be inferred from the quantification data, the Mge1 DM strain had decreased import kinetics when compared to the wild type Mge1 strain (Figure 2A). Hence, we measured the membrane potential using the cationic fluorescent dye DiO_6 that localizes in mitochondria in all the strains to check if the lower import kinetics in Mge1 DM strain could be explained by a decrease in membrane potential. However, there was no noticeable difference in membran potential between the single mutants and wild type strains, DM showing little defect in membrane potential as evident from quenching ability of DM mitochondria (**Figure 3.4**).

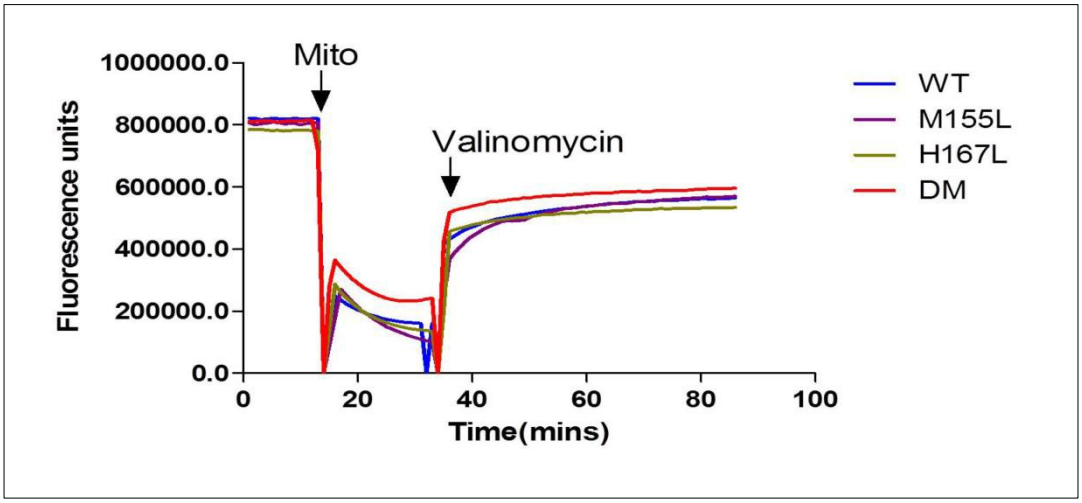

Figure 3.4 Double mutant Mge1 impairs membrane potential. *Comparison of mitochondria membrane potential of Mge1 mutants using potential dependent fluorescent dye, DiO6. The difference in fluorescence before and after the addition of valinomycin (Val.) represents an assessment of the magnitude of the difference ⊿ψ.*

3.5 Double mutant show reduced levels of cytochrome oxidase (Cox) proteins

As the moderate decrease in import kinetics in Mge1 DM cannot explain the severe growth defect on non-fermentable carbon source, we monitored the steady state levels of several mitochondrial proteins including respiratory chain proteins in the above strains. Mitochondria was isolated from the various strains from both permissive (30 ºC) and non-permissive temperatures (37ºC) proteins resolved on SDS-PAGE, western blotted and probed with mitochondrial protein specific antibodies (**Figure 3.5 A & B**). Wild type Mge1 and Mge1 single mutant strains had comparable protein levels in most cases. Compared to wild type Mge1 strain, Mge1 DM strain showed no change in major protein import receptors like Tim44, Tom40 and

Tim23. However, protein levels of cytochrome C oxidase Complex IV subunits like Cox4, Cox6 and Cox13 diminished while mitochondrial chaperones like Hsp70, Hsp60 and Pim1 increased in Mge1 DM strain (**Figure 3.5 A & B**). Incontrast to other mitochondrial protein levels, several subunits of complex IV including Cox4 were substantially decreased at 37 ºC in double mutant in comparision with wild type indicatating that under stringent conditions, the active complex IV inhibited in double mutant Mge1. Curiously, while Cox17 (Complex IV assembly factor?) decreased in the Mge1 single mutant strains, there was an increase in Cox12 (Complex IV subunit). An increase in Cox6 was observed in Mge1 H167L mutant strain. This result underscores the specificity in Mge1 action wherein there is selective depletion of Cox proteins while other structural and functional proteins involved in protein import are preserved.

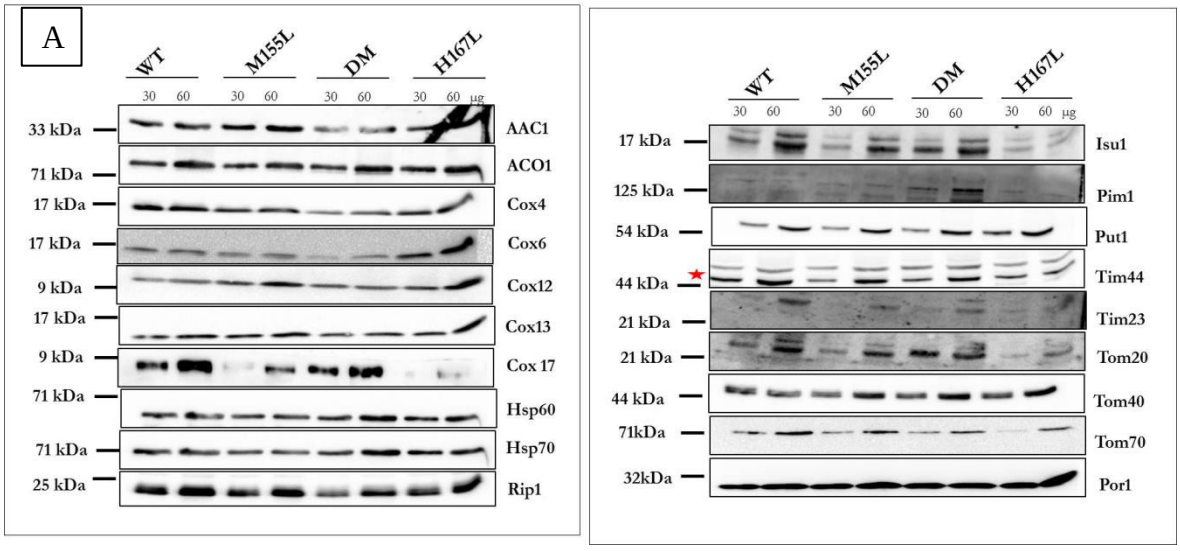

Figure 3.5 A Double mutant Mge1 shown respiration defect. *Steady state protein levels of mitochondria isolated from yeast cells expressing Mge1 and its mutants grown at 30º C, followed by western analysis.*

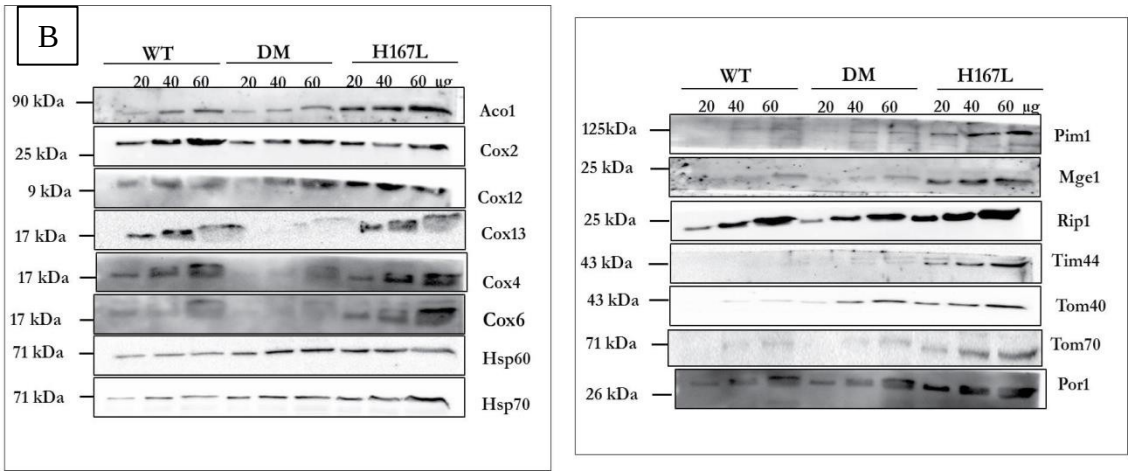

Figure 3.5 B Double mutant Mge1 shown respiration defect. *Steady state protein levels of mitochondria isolated from yeast cells expressing Mge1 and its mutants grown at 37º C, followed by western analysis*

3.6 Double mutant alters the mitochondrial functions

To gain insights into the ramifications of low levels of Cox protein subunits on the functional integrity of ETC, we assessed the activities of Complex III and IV and the overall Oxygen Consumption Rate (OCR) as described in the methods. To measure Complex III and IV activities, we isolated mitochondria from wild type and Mge1 mutant strains that were grown on semi-synthetic lactate (SS-Lac) medium as described in the methods. Between Complex III and Complex IV, the activity of the former in all the mutant Mge1 strains is comparable to that of wild type Mge1 strain. Complex IV activity is impaired in Mge1 DM strain relative to the wild type Mge1 strain (**Figure 3.6 A & B**). For measuring OCR in an Oxymeter, equal number of logarithmically growing yeast cells in YPD medium from wild type and mutant Mge1 strains were taken. We find 20-30% reduction in OCR in Mge1 DM strain when compared to wild type Mge1 strain and Mge1 single mutant strains (**Figure 3.6 C**). Mge1 DM strain is compromised for mitochondrial respiration. The above result clearly provides evidence that Mge1, an essential protein, is required for maintenance and functioning of ETC. This adds another dimension to the multifaceted Mge1 protein.

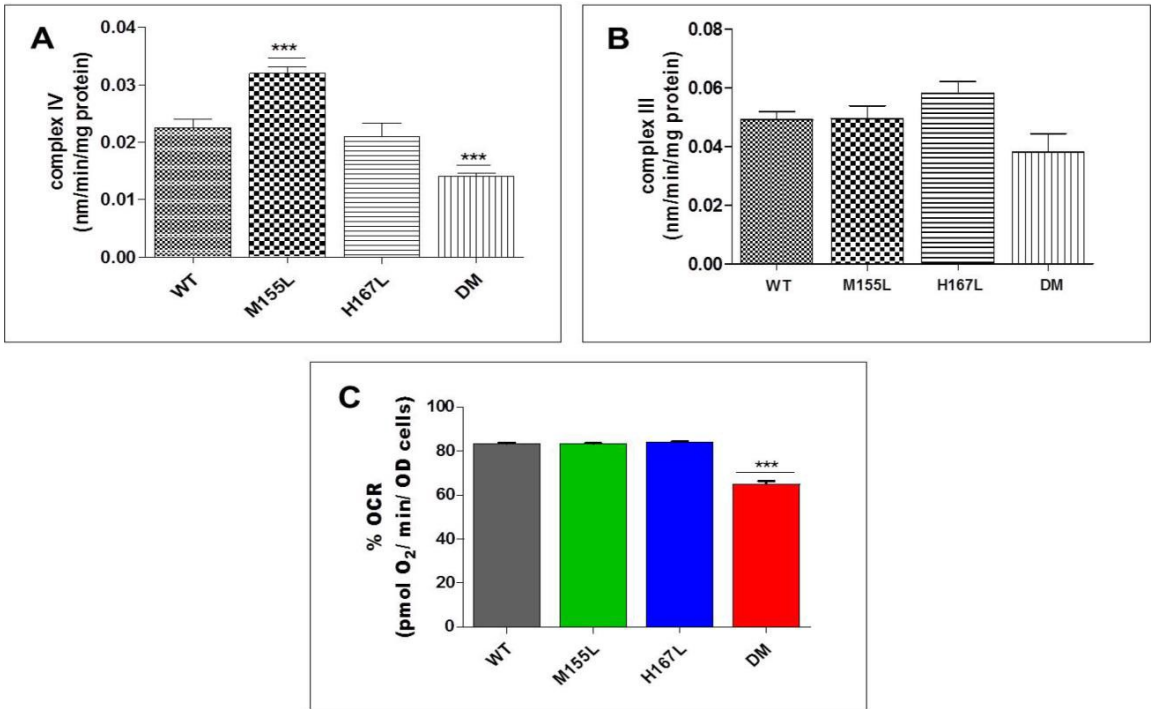

Figure 3.6 Double mutant Mge1 shows decreased complex activities and OCR. (A and B) *showing mitochondria respiratory complex IV and III activities, isolated from yeast cells expressing Mge1 and its mutants*. **C.** *Quantification of oxygen consumption rate in yeast cells grown in YPD media upto mid log phase using Oxymeter.*

3.7 Mge1 DM curtails respiratory super complexes during thermal stress

Although there is specific reduction in some Cox subunits of Complex IV and reduction both in Complex IV activity and in OCR in Mge1 DM strain, we could not detect any significant problem in the assembly or stability of its ETC complexes (**Figure 3.7**).

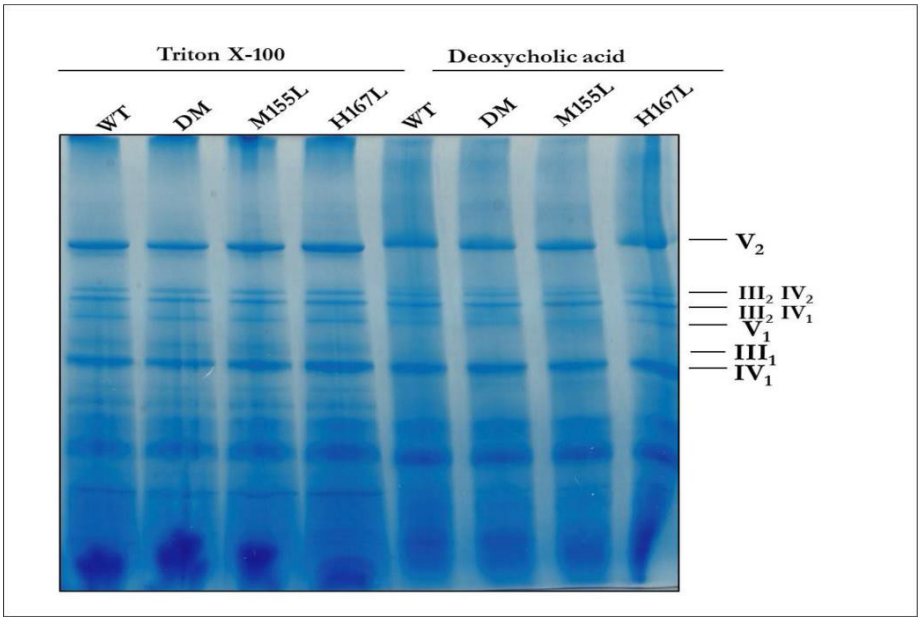

Figure 3.7 Blue-Native Page analyses of Mge1 mutants mitochondrial respiratory complexes. *Mitochondria isolated from Mge1 mutant strains, solubilized in Triton X-100 and Deoxycholic acid and separated by BN-PAGE.*

It has been reported that mitochondrial respiration can be directly correlated to the formation of supercomplexes (Complex III/III; Complex III/IV) (Cui, Conte et al. 2014). Critical amounts of Complex III or Complex IV are essential for Supercomplex formation and for mitochondrial respiration. Most importantly, Mge1 along with Cox4 and Hsp70 has been implicated in aiding in the formation of Super complex. Given the phenotype of Mge1 DM on non-fermentable carbon medium, its compromised Complex IV and OCR activities, its hypersensitivity to abiotic stress and role of Mge1 in Super complex formation, we suspected that Supercomplex formation will be defective in Mge1 DM strain when challenged with abiotic stress. To test if indeed this is true, we performed BN-PAGE on mitochondria isolated from wild type and mutant Mge1 strains that were grown in SS-Lac medium at 30 and 37°C as described in the methods. The gel was western transferred and probed with antibodies specific for Complex III and IV protein subunits as shown (**Figure 3.7.1**). We did not detect any difference in the Super complexes between the strains at 30°C. However, a severe reduction in Super complex III_2/IV is observed in Mge1 DM

strain as reflected by the decrease in Cox2 and Cox4 proteins. The level of Tom40 is comparable in all the strains and does not change with increase in temperature indicating the specific defect in Supercomplex formation.

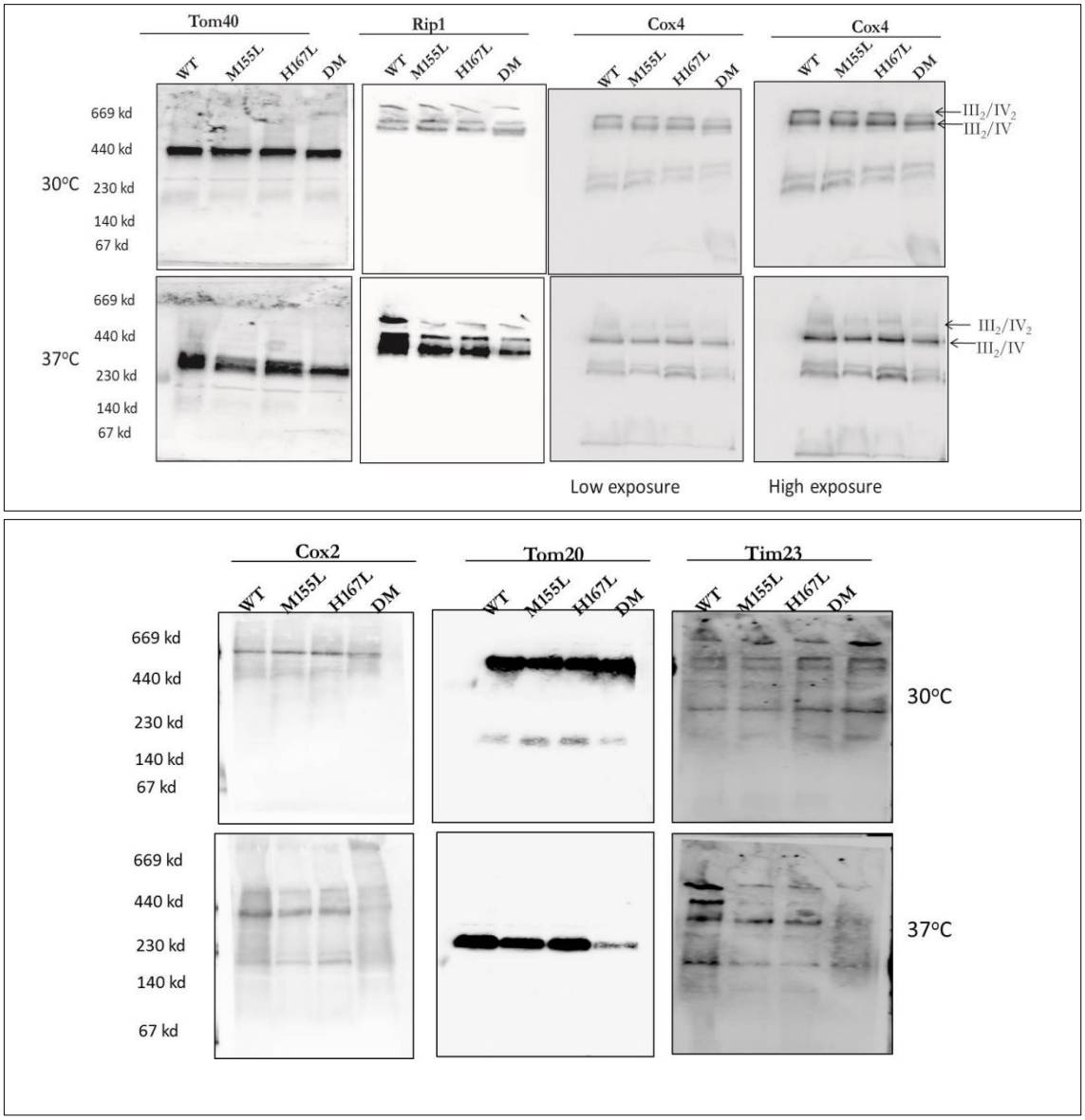

Figure 3.7.1 Respiratory chain super complexes are defective in the double mutant Mge1 strain. *Mitochondria were isolated from wild type and mutants of Mge1 under permissive conditions and were solubilised in digitonin followed by blue native PAGE. III, IV respiratory complex, TOM20, TIM23 and TOM40 import complexes were analysed by western blot analysis. Mge1 and mutants were grown in permissive conditions and shift to 37 ^{o}C for 32 hrs and mitochondria were isolated and analysed.*

3.8 DM Mge1 shows defect in Hsp70-Mge1-Cox4 complex.

To ascertain the effect of Mge1 DM in Hsp70-Mge1-Cox4 complex formation that serves as an intermediate in Complex III/IV formation, we carried out co-immuno-precipitation with Hsp70 antibody in mitochondrial extracts isolated from wild type Mge1 and Mge1 DM strains that were grown in 30ºC. The experiment was carried out either in presence of ADP or ATP so as to observe the specificity of Hsp70 binding as Hsp70 has greater affinity to ADP. The affinity of Hsp70 to Cox4 is greater in presence of ADP in wild type Mge1 strain. In case of Mge1 DM strain, Hsp70 is unable to bind to Cox4 even in the presence of ADP. Hsp70 interaction with Cox4 is highly specific as neither Cox13 nor Cox1 interact with it (Figure 3.8). This result corroborates the above result wherein we see a reduction in Super complex III/IV formation at an elevated temperature in the Mge1 DM strain as a Hsp70-Mge1-Cox4 acts as an intermediate. Mge1 appears to act as a glue between Hsp70 and Cox4. Mge1 DM is able to interact with Hsp70 but not with Cox4. Hsp70 does not directly interact with Cox4.

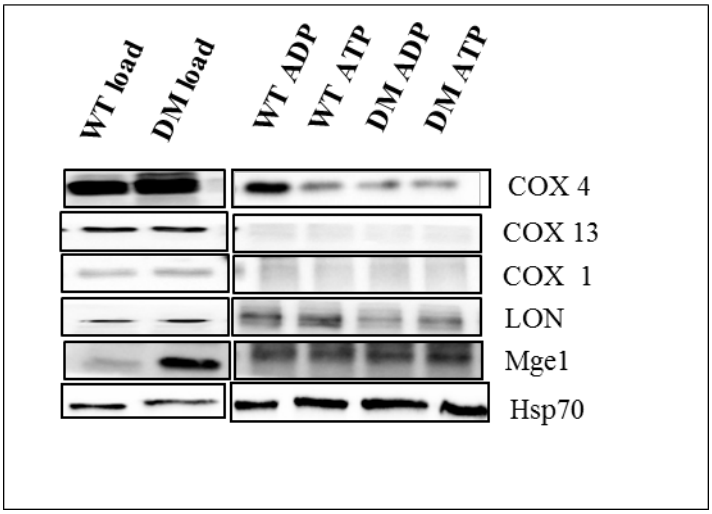

Figure 3.8 Double mutant Mge1 shown impaired Mge1-Hsp70-Cox4 complex. *Isolated mitochondria from WT and mutants Mge1 cells were lysed in digitonin and incubated with anti-mtHsp70 antibodies coupled to protein A–Sepharose. Bound proteins were eluted with glycine, pH 2.5, and analyzed by SDS–PAGE and Western blotting. Load, 3%; elution, 100%.*

3.9 Mitochondrial translation is not affected in Mge1-DM

Mitochondrial Hsp70 is shown to be involved in the regulation of translation of subunits of complex IV by interacting with the Mss51 which is atranslation activator (Fontanesi, Clemente et al. 2011). In addition, Cox4, a first nuclear encoded subunit associates with Cox1 and is involved in negative feedback regulation of the translation of other Cox proteins. Since a weak interaction is seen between Mge-Cox4-Hsp70 in Mge1-DM, we intended to determine whether any mitochondrial translation defect could be the reason for the reduced Complex IV subunits and super complex assembly. We performed *in-vivo* mitochondria translation using radioactive S^{35} methionine as described in the Methods section. We did not find any significant decrease in the translation rate in Mge1-DM when compared to WT (**Figure 3.9 A, B, C and D**). To test whether the decreased translation rate is due to increased turnover of translated products, pulse chase of mitochondrial translational products was carried out as described in the Methods section. We could find significant difference in turnover of mitochondrial translational products in Mge1-DM when compared to WT indicating that double mutant does not affect the mitochondrial translation machinery significantly (**Figure 3.9 e, F and G**).

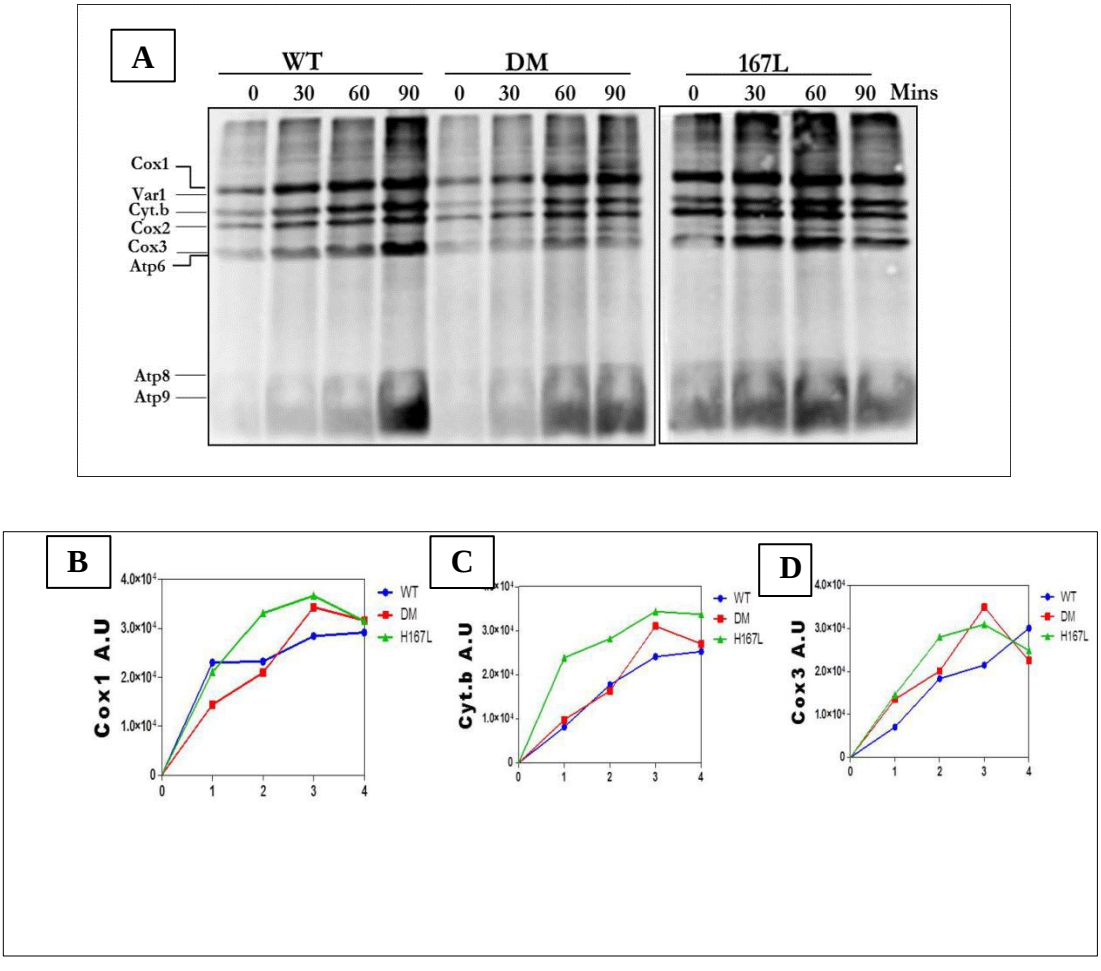

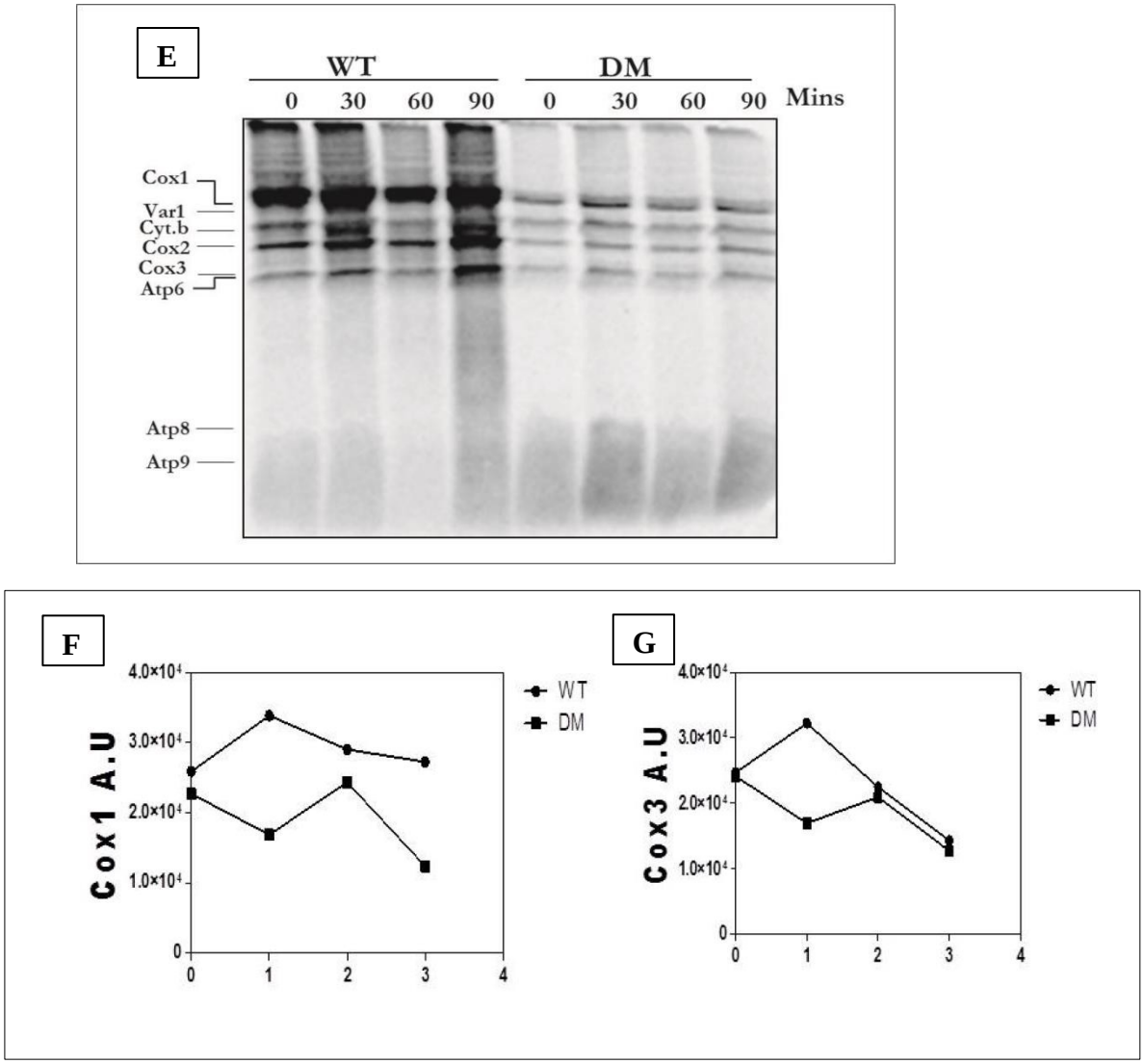

Figure 3.9 Double mutant Mge1 did not exhibit translation defect while the single mutant H167L display enhanced mitochondrial translation than wild type Mge1. (A*) In vivo labelling of mitochondrial translation products as described in methods. After pulse for indicated time intervals, cells were TCA precipitated, separated by SDS PAGE and subjected to auto-radiograph. Three independent experiments as in A were quantified using image J tool. (***B, C, and D***) line graphs plotted using quantified intensities of Cox1; Cytb1and Cox3 translated proteins from yeast cells expressing wild type Mge1, H167L and double mutant Mge1. (***E***) After 10 min pulse, translations were inhibited by addition of excess molar cold methionine and chloramphenicol. Samples were collected after 0, 30, 60 and 90 min chase and analysed as in A. (***F and G***) three independent experiments as in (B, C and D) were quantified and plotted for Cox1 and Cox3 proteins translated from wild type Mge1 and double mutant.*

3.10 Mge1 single mutants show enhanced chronological life span

Chronological life span (CLS) or the longevity of yeast cells is defined as the time duration of cells that remain viable after the commencement of the stationary phase. High cellular respiration and enrichment of anti-oxidant systems directly correlates to longer CLS(Bratic and Larsson 2013). Our results show that Mge1 plays an important role in respiration and in Supercomplex formation. As an extension to this observation, we wanted to determine the relationship between Mge1 and CLS. To this end, we studied CLS in wild Mge1 and Mge1 mutant strains as described in the Methods section. Cells from wild type Mge1 and mutant strains were monitored for colony forming ability once in five days over a period of 30 days. Cells were diluted, spread on YPD plates (in triplicate), incubated for 1-2 days and numbers of colonies were counted. Mge1 DM strain exhibits shortened CLS compared to wild type Mge1 strain while the Mge1 single mutants have extended CLS (**Figure 3.10 A**).

Recently, it has been shown that adaptive ROS signal during exponential phase extends CLS in yeast cells most probably through TORC1 (Pan, Schroeder et al. 2011). To understand the effect of ROS in the observed differences in CLS amongst the Mge1 mutant strains, we used 2' 7' Dichloro fluorescin dye to measure total cellular ROS in exponentially growing cells as described in the Methods section. The results show that all the Mge1 mutants have ROS levels that are lower than wild type Mge1, with Mge1 DM having the lowest (**Figure 3.10 B & C**). Most importantly, there is no apparent correlation of total cellular ROS levels to CLS. Despite this result, we checked if there is any correlation between mitochondrial ROS and CLS if not total ROS. Towards this end, we measured mitochondrial superoxide levels that are typifies mitochondrial ROS levels using MitoSox fluorescent dye. The results were similar to that obtained for total cellular ROS underscoring the apparent disconnect between ROS and CLS.

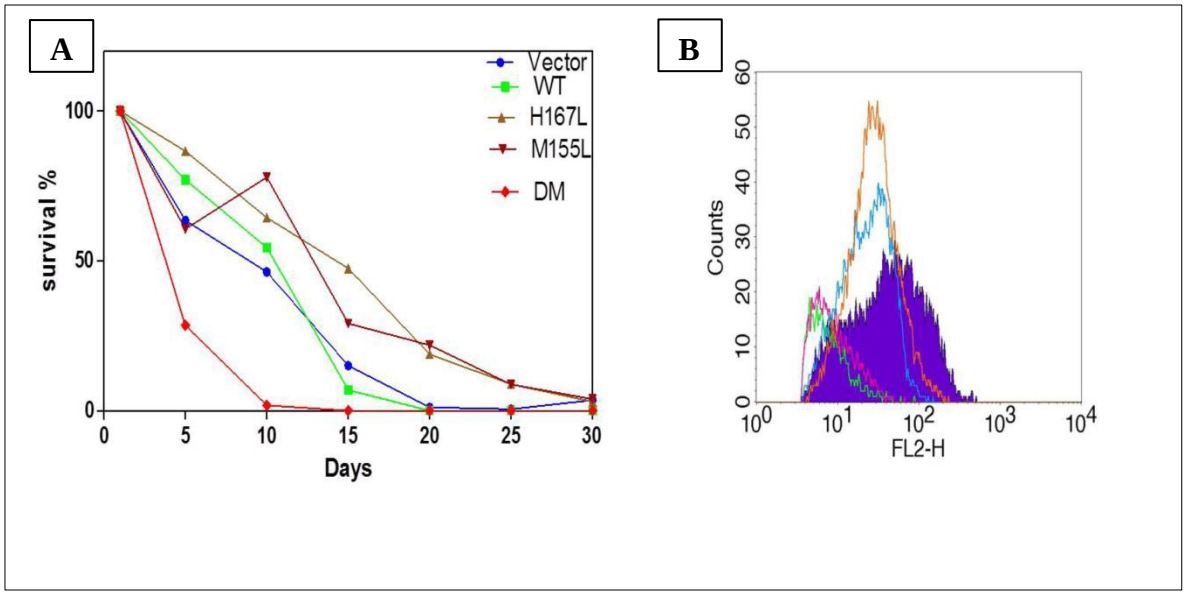

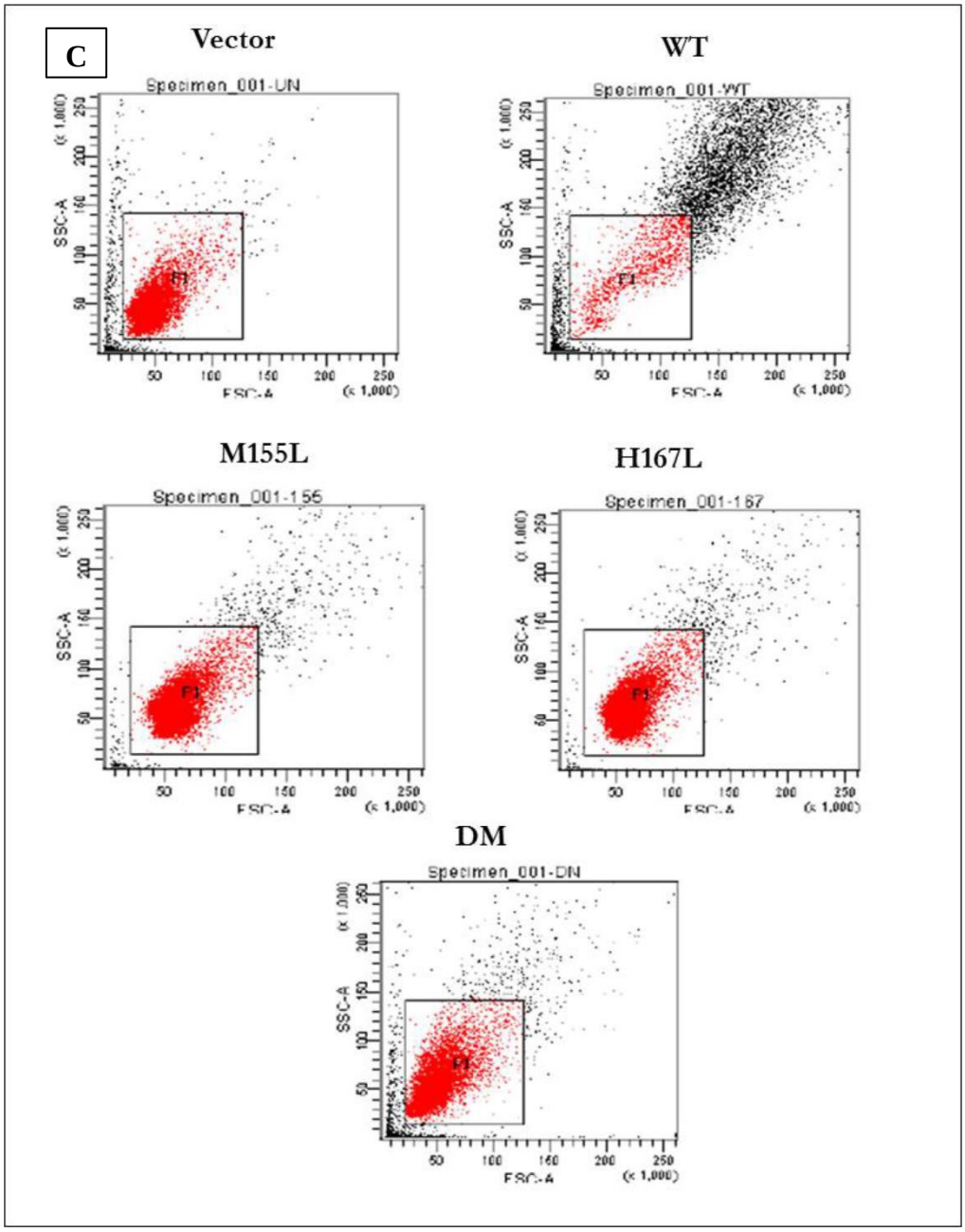

Figure 3.10 both the single mutants M155L and H167L extends life span, double mutant Mge1 shown severe defect in the extension of CLS. (A). *CLS of wild type Mge1 and its mutants under nitrogen starvation media compared with wild BY4741 strain. (***B & C)***. Quantification of both cellular and mitochondrial ROS content of yeast strains was done by FACS as described in the Methods section.*

3.11 Mge1 DM induces adaptive stress response for survival by altering various cellular pathways

Mitophagy is a process to remove and maintain healthy mitochondrial population for cell survival and growth (Diot, Morten et al. 2016). During mitophagy, mitochondria fuse with vacuoles and the mitochondrial components are recycled. Mitophagy can be induced either by amino acid starvation or nitrogen starvation. However, respiratory deficient cells show a delay mitophagy indicating that active respiring cells are more agile in responding to stress. Mitophagy can be monitored by following the life cycle of Su9-DHFR-GFP. Su9 pre-sequence targets DHFR-GFP to the mitochondrial matrix. Upon mitophagy, free GFP is released while DHFR gets degraded. The level of free GFP can be used as measure of the rate of mitophagy. Hence, to examine if the observed altered respiration in Mge1 mutants affects mitophagy, we transformed all the Mge1 strains with pRS416 plasmid carrying Su9-DHFR-GFP as described in the methods. Transformants were positive for targeting of Su9-DHFR-GFP to mitochondria by immunofluorescence (**Figure 3.11**).

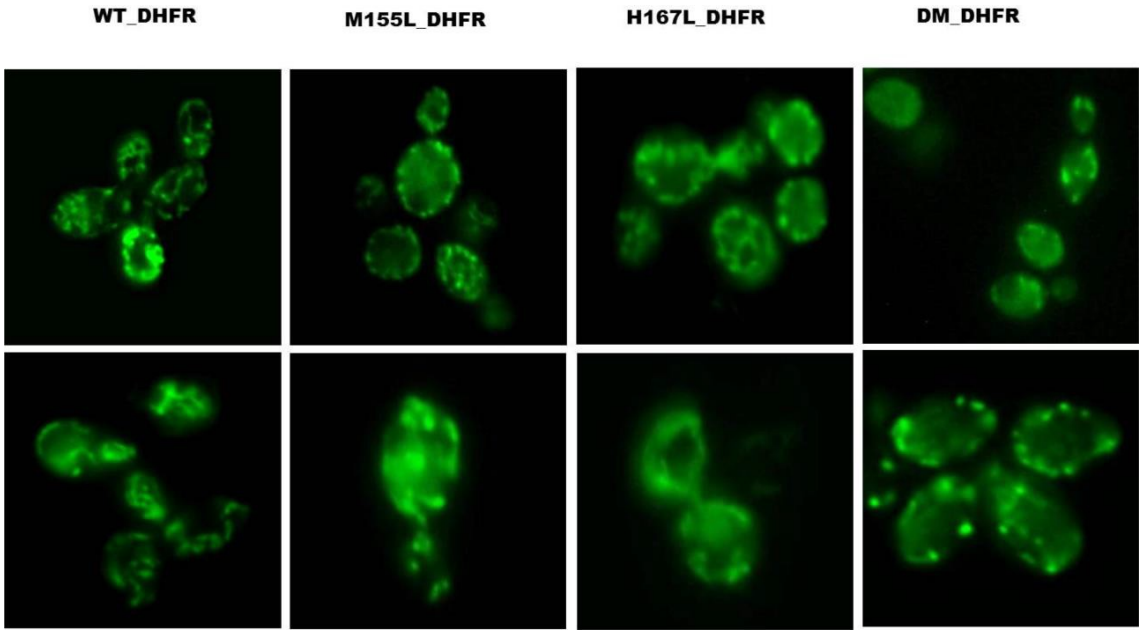

Figure 3.11 Wild type Mge1 and single mutants of Mge1 exhibits network kind of mitochondrial morphology, DM shown punctate morphology. *Yeast cells were transformed with Su9-DHFR-GFP and grown for overnight at 30° C and images were obtained by fluorescence microscopy.*

Overnight cultures of the positive transformants grown in semi-synthetic lactate (SSLac) medium were washed and exposed to nitrogen starvation in order to induce mitophagy. Cells were collected at 0, 2, 4 and 6 hrs, lysed and resolved on SDS-PAGE. Western blotting was carried out and the blots probed with antibody specific to GFP. Consistent with the theory that active respiration is important for induction of mitophagy during stress, we find that Mge1 single mutants exhibit significantly higher levels of free GFP compared to Mge1 wild type strain at all time points. In contrast, DM Mge1 is defective in mitophagy as free GFP is not detected at any time point despite the GFP-DHFR levels decreasing at 4 and 6 hours (**Figure 3.11.1 A & B**). In order to rule out the observed defective mitophagy in double mutant Mge1 due to impairment in general autophagy, we compared the autophagy induction in wild type and double mutant Mge1 by transforming ATG8-GFP into yeast strains. We observed release of free Gfp at 25 kd indicating that DM did not impair the autophagy.Our results provide a new narrative on the relationship between abiotic stress, respiration, CLS and mitophagy, with Mge1 playing a pivotal role that impinges on each of these functions.

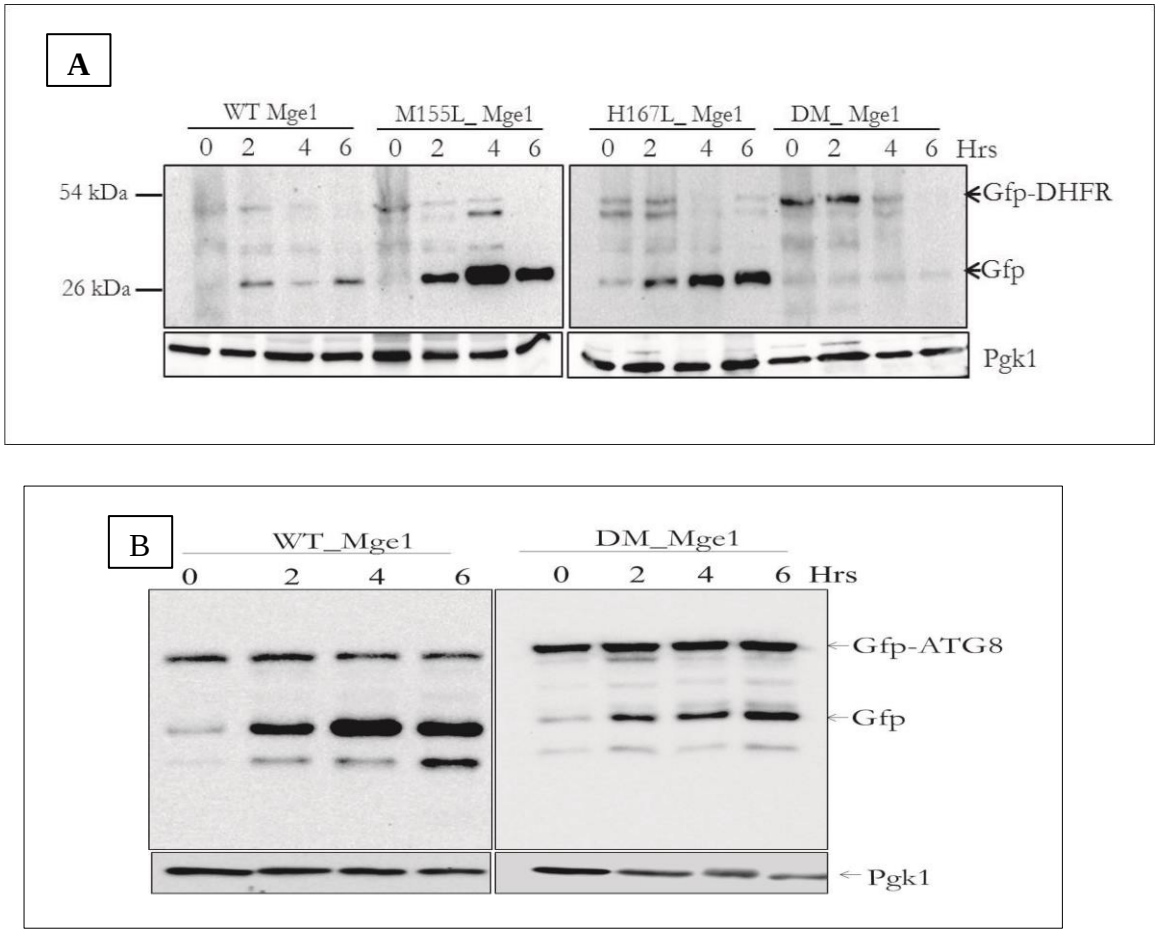

Figure 3.11.1 Double mutant Mge1 causes mitophagy induction defect but not autophagy. (A) *Yeast strains transformed with an expressing plasmid expressing SU9-DHFR were grown in YPL media upto 16 hrs. Then cells were washed and replaced with nitrogen starvation media and mitophagy induced for indicated time periods. Cell lysates were prepared from yeast strains and analysed by western blot using anti-GFP antibody. (***B)** *Autophagy analysis using transform GFP-ATG8 to yeast strains. Cell lysates were analysed by SDS PAGE followed by western blot using anti-GFP antibody.*

3.12 A global view of RNA-seq transcriptome profile of wild type Mge1 and its double mutant.

A total of 6546 open reading frames (ORFs) were quantified for FPKM (fragemnets per kilobase pair of ttranscript per million mapped reads) in the RNA seq data. When we compared with the glaobal transcriptome data of wild type and double mutant Mge1, we observed large number of significantly differentially expressed loci with 499 upreglated, and 288 down regulated transcripts whereas 5819 transcripts remains neutral (**Figure 3.12 and Table 3.1**). These results suggest that the transcriptome profile of the double mutant Mge1 differs from that of wild type strain. Cells carrying single mutant M155L had similar abiotic stresses resistance to H167L mutant, whereas cells carrying double mutant cause severe growth defect compared to the wild type strains. Since the double mutant shows defective growth in glycerol, it prompted us to further investigation.

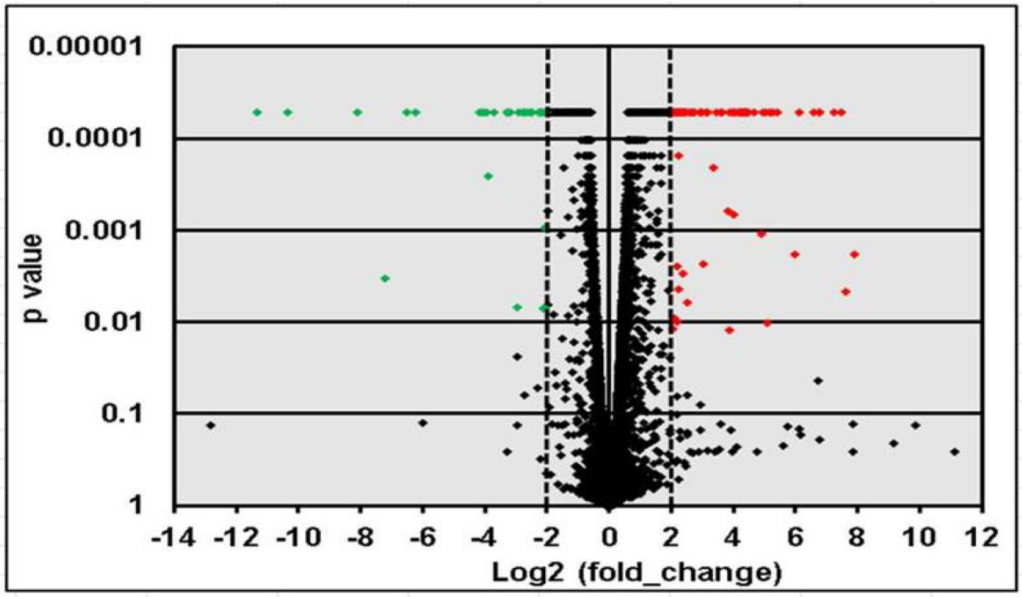

Figure 3.12 Total RNA SEQ analyses both wild type and double mutant Mge1 strains. *Scatter plots showing linear regressions of the average log$_2$ changes of mRNA experiments.*

Table 3.1 Summary table of total RNA levels which are altered and which neutral.

Statistics:				
Category	Total	UP	DOWN	NEUTRAL
Both_WT_&_DM	6546	499	228	5819
Only_WT	4	NA	NA	NA
Only_DM	42	NA	NA	NA
Significant_Both_WT_&_DM	133	93	40	NA
Significant_Only_DM	26	NA	NA	NA

Yeast cells stress sensitivity is linked to both poor respiration and growth on non-fermentable carbon source. In order to metabolise these types of carbon sources, yeast cells shift from fermentation to respiration in the mitochondria. To understand the how the double mutant Mge1 changes the expression levels of genes that adapt for stresses, mRNA levels were compared between yeast cells with wild type and double mutant Mge1 (**Table 3.2**). In the double mutant, genes encoding sub set of ETC components (COX (cytochrome c oxidase) family proteins) and ATPase were significantly down regulated as compared with wild type, with a Z-score of log2(fold) change in expression. Direct comparision between transcriptome and proteins levels between wild type and double mutant Mge1 yeast have consistently found decreased expression of double mutant mRNA encoding genes involved in respiration.

This line of evidence indicates that the double mutant Mge1 is directly involved in down-regulating the expression of respiratory genes regardless of metabolic state when cells are grown in dextrose media. Yeast cells with double mutant Mge1 grow poorly in glycerol media and have less electron gradients across the mitochondria membrane than the wild type. During anaerobic growth condition Cox5b is expressed as compared to its paralog Cox5a which is expressed in aerobic growth condition. The Cox5b expression was upregulated in double mutant Mge1 yeast cells than wild type. Most of the 288 genes which are downregulated in double mutant Mge1 cells are involved in ribosomes biogenesis, structural ribosomes proteins and translation. Ribosomal mRNA decreased the most in yeast expressing double mutant Mge1 which grow poorly in glycerol media. Yeast cells which are growth defective, reduces the ribosomal biogenesis which is costly process.

Table 3.2 GO enrichment and KEGG pathway analysis. *The top five GO terms enriched in wild type Mge1 vs DM (double mutant) DEGs, determined based on the lowest p values, were analyzed by REVIGO.*

Pathway	p.geomean	stat.mean	p.val	q.val	set.size
sce01100 Metabolic pathways	1.89827E-05	-4.206004954	1.89827E-05	0.001006081	110
sce01110 Biosynthesis of secondary metabolites	0.005396134	-2.599073666	0.005396134	0.057199024	50
sce01130 Biosynthesis of antibiotics	0.000918571	-3.21760073	0.000918571	0.016228084	43
sce01230 Biosynthesis of amino acids	0.003804698	-2.772264909	0.003804698	0.050412252	29
sce00190 Oxidative phosphorylation	4.79206E-05	-4.378962122	4.79206E-05	0.001269895	27

3.13 Mge1 regulates the other aspects of mitochondrial metabolism

Since Mge1 resides in mitochondria, we assessed the mitochondria function of both wild type and double mutant Mge1 strains. In addition, Mge1 is shown to be involved in iron cluster biosynthesis. Moreover, we observed less respiration in double mutant Mge1 yeast cells. Taken togather, yeast cells harboring Mge1 DM appear to possess less oxidative phosphorylation and consequently less respiration than wild type. The mitochondrial DNA content of these cells is the same, as is evident from the translation results. Of the global metabolic pathway, we identified aminoacid metabolism, lipid metabolism and nucleic acid metabolism to be significantly down regulated in the double mutant Mge1(**Table 3.1 & Figure 3.13**). Among all the down regulated pathways, almost all of the genes involved in amino acid metabolism were down regulated suggesting that the biosynthesis of aminoacids was supressed in the double mutant Mge1.

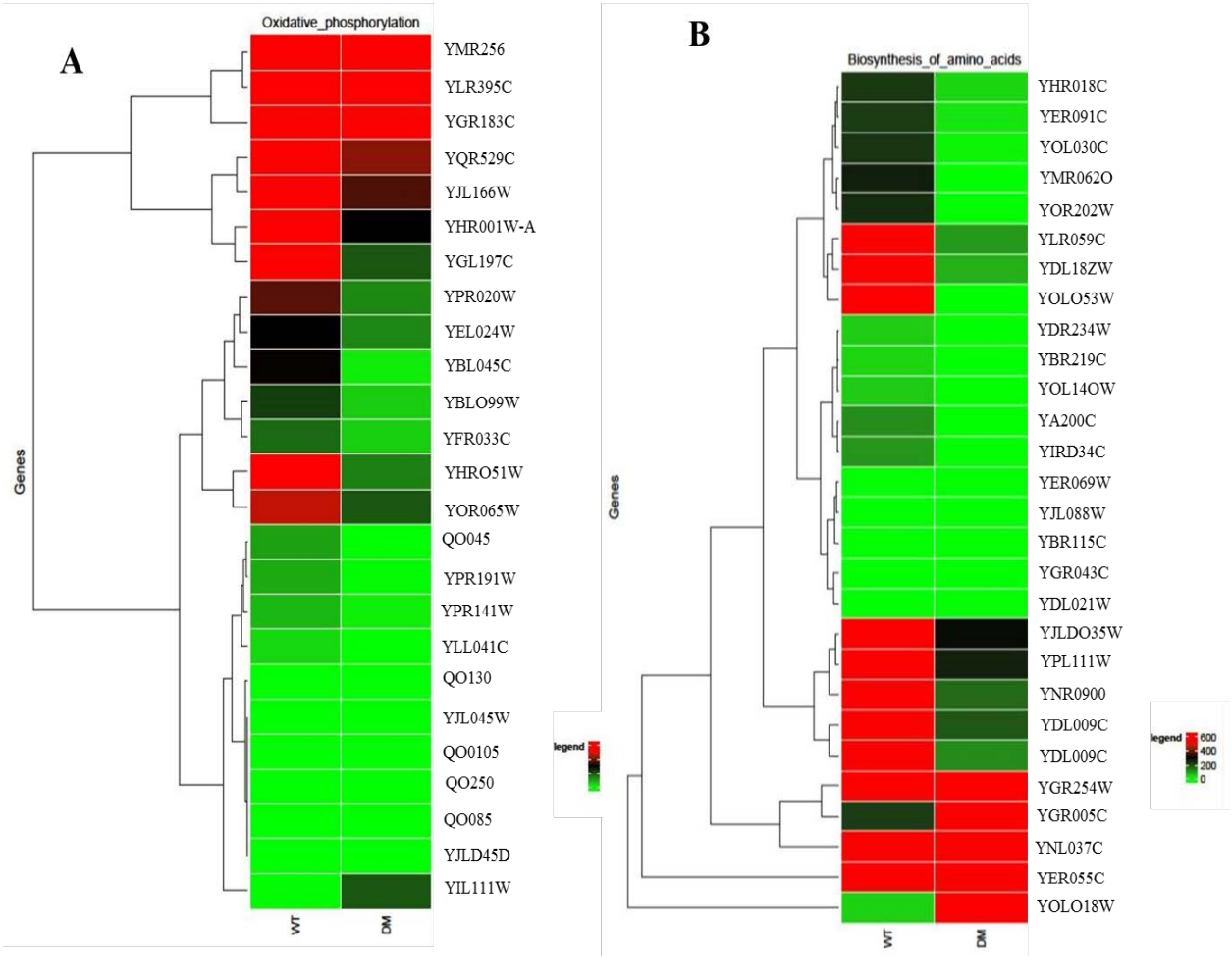

Figure 3.13 Double mutant Mge1 show a down regulated set of the key metabolic pathways.(A & B) *Heatmaps showing expression for OXPHOS and aminoacids metabolism. Bright red coloration indicates strong up-regulation of expression and bright green indicates strong down-regulation.*

3.14 Discussion

To understand whether the decreased levels of Cox proteins is because of lowered import kinetics, we measured the import kinetics at 37ºC and also looked at their steady state levels. We noticed a spike in the import kinetics in the Mge1 DM strain over the wild type Mge1 strain; nonetheless, the Cox proteins were still low. As most of the Cox proteins are imported from the cytosol, we wonder whether that cytoplasmic synthesis is affected or degradation.

Mitochondrial protein import is sensitive to multiple stresses like osmotic, thermal, oxidation and saline stresses. Any defect in the import machinery and its functions are finely tuned to the metabolic rate of mitochondrial respiration (Harbauer, Zahedi et al. 2014). TIM23 is one of the inner membrane complexes, extensively studied in terms of assembly of individual components and import mechanisms. Although the Hsp70 import motor is the main component for translocation of majority of mitochondrial matrix proteins and is also directly involved in the assembly of respiratory complex, which other regulatory proteins which are involved in sensing the stress remains unexplored (Fontanesi, Soto et al. 2010). Earlier, Mge1 has been known to responds to both thermal and oxidative stress by changing its oligomer state to monomer state and it is known to detach from the Hsp70 chaperone (Moro and Muga 2006, Marada, Allu et al. 2013). Recently, we also reported that Mge1 is oxidised by hydrogen peroxide levels and get repaired by methionine sulfoxide reductase (Allu, Marada et al. 2015). Here, we show, based on mutational and growth assays suggest that Mge1 is responding to multiple abiotic stresses. Mge1 is the lone co-chaperone involved in many functions like iron cluster biosynthesis, antifungal resistance and cytochrome oxidase assembly. Using molecular docking and simulation studies, we observed structural alterations in the two single mutants Mge1 M155L (Karri, Singh et al. 2018) and Mge1 H167L mutant. Based on these results, we assume that missense mutations in Mge1 are probably responsible for structural adaptations leading to gain in function phenotype in the presence of various abiotic stresses. Further, Mge1-DM could be structurally and functionally different from WT and single mutants. Based on these pleotropic functions of Mge1, we believe that mutants it alter the Mge1 biophysical structure, which leads to altered mitochondrial functions, altered cellular functions and stress responses. Electron transport chain defects are associated with many physiological and pathological disorders. In particular, mitochondrial respiration has a dynamic role in regulating cellular metabolism, growth, development and adaption to multiple stress conditions.

In our mutational analysis, both single mutants M155L and H167L show resistance towards multiple stress, whereas the double mutant shows severe growth defect and is sensitive towards

environmental stresses. This observation is suggests that structural alterations of Mge1 may be necessary for adaptation. Further detailed biophysical structural studies are necessary to understand how mutants are behaving differently to stresses. In addition, the behavior of the double mutant particularly in growth defect in non-fermentable source strongly supports the idea that the mport machinery is involved in the regulation of mitochondrial respiration. From mitochondrial steady state protein analysis, we find that the double mutant specifically shows decreased Cox protein levels without much change in import machinery proteins and significant decrease in oxygen consumption rate. These results strongly suggest that Mge1 has a role in regulating mitochondrial respiration. Coimmuno-precipitation analysis supports that the idea that the double mutant Mge1 affects in forming the complex Hsp70-Mge1-Cox4 and showing significant decrease in complex IV activity with little or no defect in complex III activity. In conclusion, our data strongly supporting that Mge1 is involved in the assembly of cytochrome oxidase, which will affects the mitochondrial respiration.

Reduction of mitochondrial respiration in the Mge1 double mutant, indicates that Mge1 is necessary for proper function of complex IV. Cytochrome oxidase is a respiratory complex embedded in inner membrane of mitochondria, encoded by both nuclear and mitochondrial genes and can also form super complex with complex III. Several import machinery proteins are involved in the assembly of cytochrome c oxidase. In support with previous reports, Mge1 is involved in forming complex with Hsp70 and Cox4 and it also helps in assembly cytochrome c oxidase. Mitochondrial respiration is well known function involving in cellular metabolism, development, stress response, and adaptation to extreme environmental stresses. However so far no sensory protein has been reported that in complex biogenesis. Here we strongly believe that Mge1 is sensory protein important for respiratory complex biogenesis.

Although Mge1 is majorly involved in import of mitochondrial matrix proteins, we could not found significant alteration in major matrix imported proteins and import machinery proteins in double mutant. Instead double mutant selectively impair the Hsp60 import at permissive temperature but at elevated temperatures it shows severe defect in Hsp60 import. This specific defect may be explained two reasons. 1) Import of Hsp60 protein specifically regulated by membrane ionic balance 2) Dual localisation of Hsp60 is implicated in proteastasis. Further studies are necessary for role of regulation of import of individual proteins.

Mitochondria with reduced respiration in double mutant may be inducing the permanent stress adaptation condition by activating stress signal like ROS for activating defence mechanisms (Shadel and Horvath 2015). We failed to correlate the changes in ROS and membrane potential with sensitivity to multiple stresses. Mostly, dysfunction in complex activities markedly

susceptible to exogenous stress involving in autophagy. Double mutant of Mge1 showing significant amount of processing of ATG8 GFP. Based on our results indicate that cells are undergo specific mode of cellular response when complex IV impaired. Based on ability of cells auto clearing of dysfunctional organelle and aggregated proteins by autophagy, dysfunctional cytochrome c oxidase may trigger the elimination of dysfunctional mitochondria by specialised process called mitophagy.

Most importantly we identified novel mutants in Mge1 growing rapidly and resistance to multiple stresses. Based on our results we do not think that dysfunction in cytochrome c oxidase alone responsible for sensitive to multiple stresses. As Mge1 is pleotropic protein regulates the multiple functions, double mutant might have defect in the multiple signalling pathways responsible for slow growth phenotype. Transcripotme analysis, we identified few key regulatory pathways impaired which are associated with mitochondrial functions. Cellular metabolism, amino acid metabolism and OXPHOS metabolism are common pathways reported known to down regulated when cells are multiple abiotic stresses. All these pathways regulates and maintain the multiple defence mechanisms like antioxidant, membrane integrity, ionic balance, protein turnover, replication, translation and respiration shift to anaerobic. Further in support with transcriptome data we found double Mge1 inducing mitochondrial UPR where Hsp60, Hsp70 and protease like Lon which are can take care of aggregated proteins in mitochondria. We also believe that double mutant might have ionic imbalance which causes cytosolic accumulation of Hsp60 specifically.

In conclusion, we have shown Mge1 is novel sensory protein of import machinery and capable to regulate the multiple converged pathways activated when cells are exposed to multiple abiotic stresses. It is the first report which connects closely multiple stress and regulation of mitochondrial import machinery. This study will also help in understanding and development of yeast strains useful in industrial purpose.

3.15 Summary

Earlier studies on single point mutants, M155L and H167L of Mge1 show minor changes in structure, yet do not affect the reaction to abiotic stress very different from the wild type. With this in mind we have studied the properties of the double mutant (M155L, H167L) DM Mge1 in this chapter. We find that growth is decreased in DM at abiotic stress, in contrast to that in WT, M155L and H67L as shown in Figure 3.1.

We next found that DM shows both respiratory defective growth (Figure 3.2) and respiratory supercomplexes assembly at the non- permissive temperature, 37ºC, as Figure 3.7.1 reveals.

From transcriptional analysis, double mutant shown specifically down regulate the amino acid and OXPHOS and sterol metabolisms (Figure 3.13) and increased in levels of chaperones and proteases which are prime target for many abiotic stresses as Figure 3.5 reveals.

We also found that DM cause significant defect in aging extension as shown figure 3.10 and also defect in mitophagy induction in starvation media when compared to wild type and single mutants as Figure 3.11.1 reveals.

Chapter 4

Biophysical and Biochemical properties of Mge1

Introduction

Mge1 is a conserved protein from lower prokaryotes to higher eukaryotes (Westermann, Prip-Buus et al. 1995). Its *E.coli* analogue GrpE exists as a dimer in solution showing (Harrison, HayerHartl et al. 1997) unordered structure in N terminus and C terminus with four helical structure followed by beta sheets involving in distinct functions. Recent studies have shown that N-terminus of GrpE mimics as a substrate for Hsp70 thereby affecting the substrate binding activity (Kityk, Vogel et al. 2015, Melero, Moro et al. 2015). Mge1 shows adaptation to oxidative stress, thermal stress and osmotic stress and so does its mutant H167L (Moro and Muga 2006, Marada, Karri et al. 2016). It also shows an involvement in resistance to antifungal, agent Flucanozole (Demuyser, Swinnen et al. 2017). In previous chapter, we identified two novel single mutants in Mge1 which show resistance to multiple abiotic stresses in yeast cells (Marada, Allu et al. 2013, Marada, Karri et al. 2016). Interestingly, we inserted both mutations in the molecule as Mge1 DM (see chapter 1) and observed sever defect in growth against multiple stresses with defective respiration. Although mapping these mutations on available *E.coli* three dimensional co crystal structures can provide the location and predicting thier effect on interactions with DnaK, the exact impact of these industrial useful missense mutations of Mge1 on the folding pathways remains to be elucidated experimentally. To better understand the mechanisms of Mge1's role in adaptation in abiotic stress, evaluating the two single mutants M155L and H167L which are conferring resistance to stresses, and the double mutant which is showing sensitivity to same conditions. These mutants are highly conserved and previous studies have reported that these two mutants represent two extreme possibilities, but both lead to a highly resistant phenotype to abiotic stresses. The earlier one, M155L is located at a surface exposed area which gets oxidized by hydrogen peroxide (Allu, Marada et al. 2015). The presence of this mutation is expected to have role in folding and aggregation of proteins. The second mutation H167L is located at the hing region between four alpha helices and beta turns (Marada, Karri et al. 2016).

Overall this indicates that two distinct structural single mutants of Mge1 interact with Hsp70complex and later contributes resistance to multiple abiotic stresses. The structural studies regarding binding of residues in Hsp70 and Mge1 is poorly understood. This present chapter describes the conformational analysis of and additive functional properties, so as to gain a new insight of interactions in the Mge1-Hsp70 complex.

Results

4.1 Mutants of Mge1 show increased helical content

Based on our previous chapter cellular assays, published studies, and mutational analysis of *E.coli* GrpE and data obtained from allosteric regulation of Hsp70 allowed us to study selective Mge1 residues that contribute significantly in interaction with Hsp70. To examine the effect of inserted mutation on Mge1 folding, thermal denaturation and fluorescence quenching studies were analysed in detail. Towards this, we cloned, expressed, isolated, purified and studied the biophysical properties of WT Mge1, and its M155L mutant, H167L mutant and the double mutant DM Mge1 (containing both M155L and H167L mutation in the same molecule). The purified proteins are shown to be pure as revealed (**Figure 4.1**).

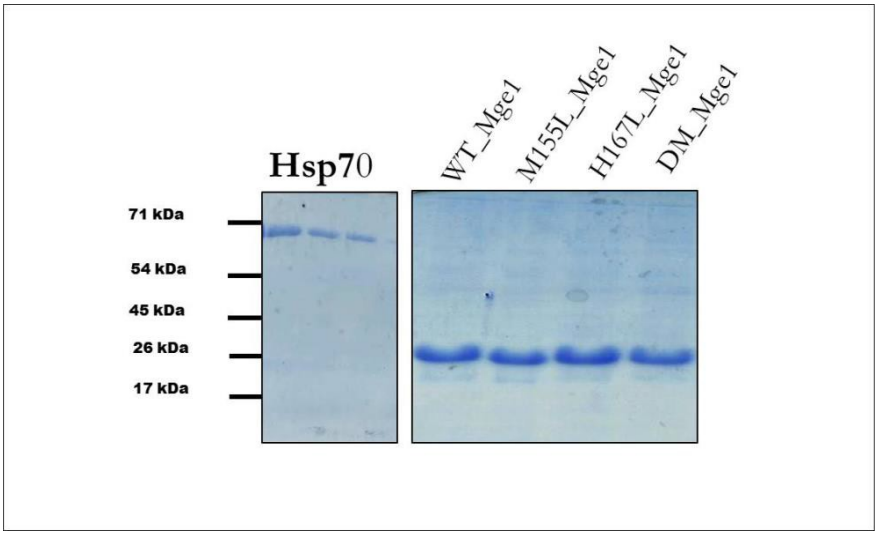

Figure 4.1: Single step purification of His tagged wild type Mge1, mutants of Mge1 and Hsp70 proteins using Ni-NTA agarose column. *SDS PAGE of Nickel tagged proteins were expressed in E.coli cells and purified using gravity based Ni-NTA coloumns.*

First, we analyzed the secondary structure content of Mgel proteins by deconvoluting the spectra obtained from CD spectrophotometer using the CDNN2.1 tool (**Figure 4.1.1 and Table 4.1**). Wild type Mge1 and M155L as estimated to have (69%) alpha helical content whereas H167L (89.5%) and DM (75.9%) showing increased amount of alpha helical content. These results further supported that structural changes in mutants of Mge1 are influencing factor for distinct phenotype exhibited by cells expressing Mge1 mutants.

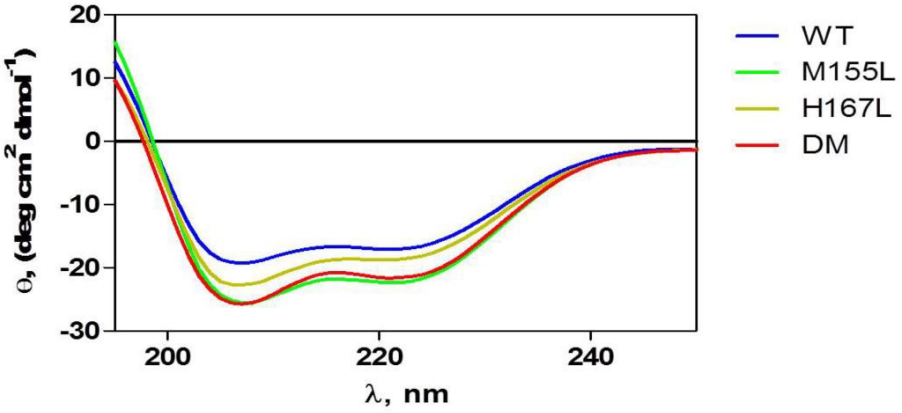

Figure 4.1.1 Secondary structure spectra of Mge1 and its mutants obtained in the UV region (260-190 nm), using a CD spectrophotometer. *100 μg/ml of Mge1 wild type and its mutants proteins were used for recording spectra.*

-

Table 4.1 Percent levels of secondary structure in Mge1 and its mutants

Protein	% α-helix	% β- sheet	% Turns	% Unordered
Wild type Mge1	69.6	11.9	7.5	11
M155L	69.8	11.7	7.9	10.6
H167L	89.5	2.5	4.5	3.5
DM	75.9	11.1	5.0	8.0

4.2 H167L and DM Mge1 are folded compactly

To further evaluate the changes in Mge1 structure, we compared the intrinsic fluorescence intensities and employed quenching studies using Potassium Iodide as a static water soluble quencher. Higher levels of quenching of the aromatic (trp, tyr, phe) in spectra of tyrosine of both single mutants of Mge1 and opposite phenomenon where low yield in emission spectra in double mutant mge1 when compared to wild type Mge1 support that mutants are somewhat different in their tertiary structure than wild type Mge1(**Figure 4.2**).

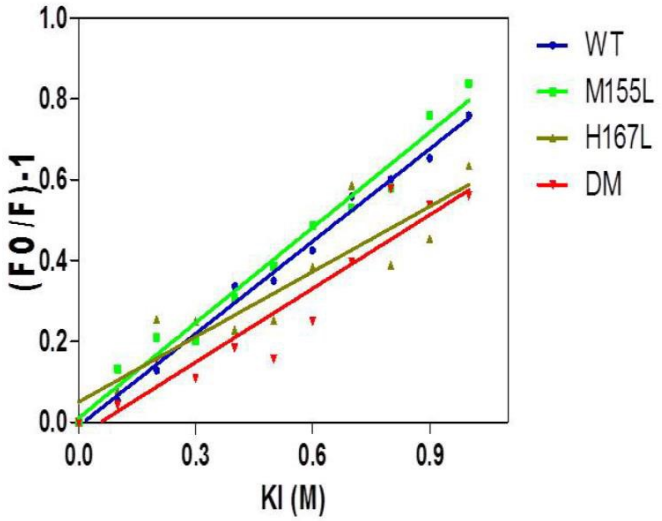

Figure 4.2: Quenching of tyrosine residues of Mge1 and mutants with ionic quencher, potassium iodide. *Proteins (100μg/ml) of Mge1 and its mutants were incubated with different molar concentrations of potassium iodide, intrinsic fluroscence was measured followed by plotting intensity against PI molar concentration.*

Ksv values obtained from Stern-Volmer plot, both wild type and M155L quench equally by KI where Ksv values are nearly equal (wild type Ksv value of 0.99±0.14, M155L Ksv value of 1.01±0.11), H167L having Ksv value of 0.95±0.14, whereas double mutant display significant decrease in Ksv value of 0.52±0.09 suggesting that H167L folded compactly than wild type as mentioned earlier (Marada, Karri et al. 2016), and the double mutant Mge1 is significantly more compact and altered its structure.

4.3 Both single mutants and double mutant of Mge1 show better thermal stabilty

We had reported that the double mutant Mge1 shown impaired growth at elevated temperatures. Hence we monitored the thermal stability of mutants of Mge1 by far-UV CD spectrophotometer. From **table 4.2**, both single mutants M155L and H167L gains thermal stability by ~5ºC (i.e. structurally somewhat more stable) when compared to wild type protein. Conceivably, double mutant shows a thermal stability by ~10ºC almost the additive of individual single mutants. It thus appears that the two mutants in DM have better protection from thermal denaturation.

Table 4.2 Thermal transitions of Mge1 and its mutants

Mge1 and mutants	Tm (°C)
WT_Mge1	37
M155L_Mge1	41
H167L_Mge1	41
DM_Mge1	45

Next we have tried to correlate the compactness and thermal stability of Mge1 proteins. To investigate the conformational changes in Mge1 mutant proteins; we used the limited proteolysis on in vitro purified Mge1 proteins using the procedure published previously (Marada, Karri et al. 2016). These proteins were subjected to trypsin digestion for various time intervals and the accessibility to protease were analysed (**Figure 4.3).** Intrestingly, we found an increase in trypsin digestion in mutants of Mge1 espescially in H167L and DM in oppose to quenching results, suggesting that mutant proteins showing greater flexibility. Eventhough we observed greater increase in atability in DM we did observe in much change in typing digestion kinetics, indicating that may be trypsing digestion sites eaqually asccesble in both H167L and DM. It is necessary to employ advanced methods to understand structural details in greater manner. These results again support that the two single mutants are show an additive effect in the double mutant.

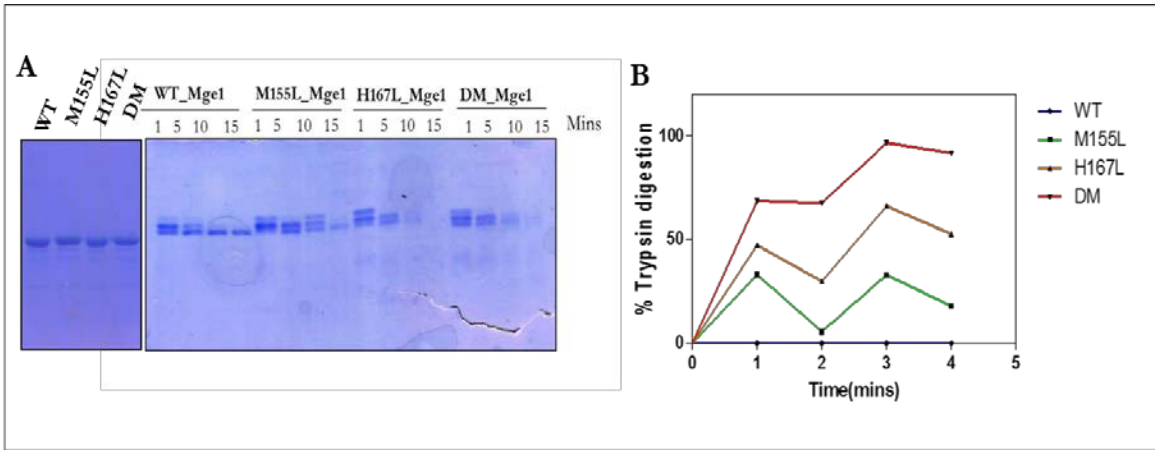

Figure 4.3 Limited proteolysis assay, *(A) incubating Mge1 proteins with trypsin at a 100: 1 ratio at 25°C for various time points and analyzed by SDS PAGE. (B) Represents the quantified levels of proteins remaining after trypsin digestion using image J software.*

4.4 Both H167L and DM exhibit lower binding affinity to Hsp70 than wild type Mge1, M155L is almost similar to WT.

Since Mge1 preferentially binds to Hsp70 and enhance its enhance the ATPase activity, we wondered whether the tooMge1 mutants could form strong interaction with Hsp70. To test thisidea, we incubated the purified proteins with Hsp70 to analyse the interaction studies using the immune-precipitations assay and enzyme linked immunosorbent (ELISA) methods **(Figure 4.4).** In support of our earlier report, H167L exhibited lower affinity for Hsp70 chaperone when compared to wild type Mge1(Marada, Karri et al. 2016). Remarkably, double mutant Mge1 shows the lowest affinity, and distinct a saturation curve suggesting that higher molar concentration of Mge1 is needed to saturate the Hsp70, whereas M155L mutant did not show difference in affinity for Hsp70 when compared to wild type Mge1.Mge1 is a co-chaperone exchanging the nucleotides to continue chaperone cycle by transient interaction with Hsp70. These results support the suggestion that transient interactions are enough for nucleotide exchange activity of Mge1.

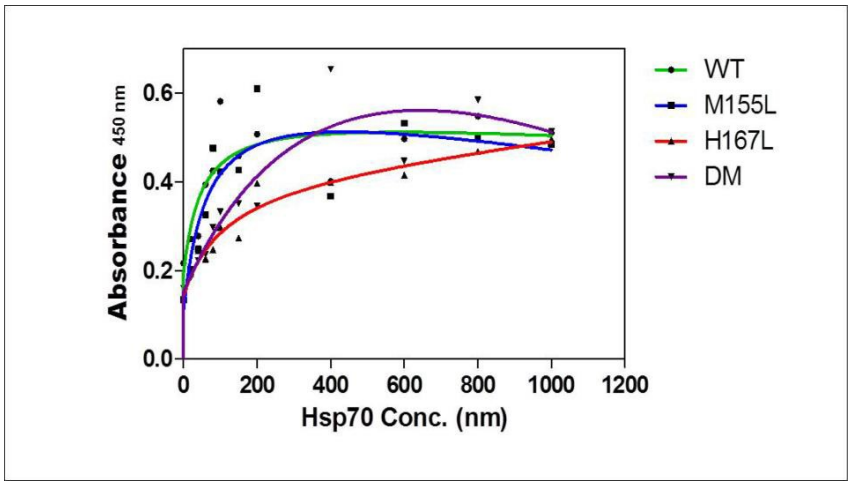

Figure 4.4 Analysis of Mge1 proteins interactions with Hsp70 using ELISA. *1 μg of Mge1 and its mutant proteins were incubated with increasing concentrations of Hsp70 (Ssc1) for 1 hour at room temperature in buffer containing Mg $(OAc)_2$ 10 mM, AMP-PNP (1mM). Antiserum against mt Hsp70, followed by horse peroxidase tagged secondary antiobody was used to detect the bound Hsp70, using TMB/H_2O_2 subrtate based reagent. Reactions were terminated using 2N H_2SO_4 and absorbance was measured at 450 nm.*

4.5 Mutants of Mge1 have show higher ATPase and Chaperone activity

For ATPase assay, we co expressed Hsp70 with co chaperone Zim17 (which helps in Hsp70 folding) and purified Hsp70 from bacterial cells. We observed a remarkable increase in ATP hydrolysis in both single mutants and the double mutant. Single mutants show 2 fold increase in ATP hydrolysis whereas the double mutant shows nearly 4 fold increase in ATP hydrolysis (**Figure 4.5**).

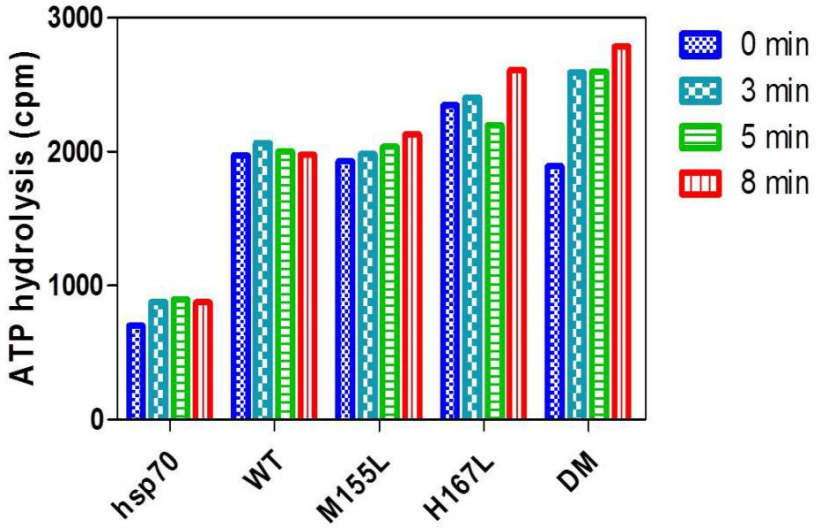

Figure 4.5 Effect of Mge1 proteins on the ATPase activity of Hsp70. *Hsp70 bound radio-labelled γATP was inbated with Mge1 and its mutants in buffer containg 3 ATP, $MgCl_2$ and 1% BSA, ATP hydrolysis was monitored under single turn over conditions at different time intervals and the percentage of ATP-to-Pi conversion.*

To further validate the kinetics we did G6PDH (glucose 6 phosphate dehydrogenase) refolding kinetics, we followed well established method to quantify the refolding ability of Hsp70 using chemical denatured G6PDH substrate (Kumar, Reddy et al. 2005). The single mutant H167L showed 20% higher refolding kinetics and the double mutant show 40% higher refolding, whereas in single mutant M155L just a little change in the refolding ability is observed when compared to wild type (Figure 4.5.1 A). Further we also checked the "preventive aggregation property" of Hsp70 in the presence of Mge1 mutants. We incubated the chemically denatured Rhodanase (Sigma) enzyme with Hsp70 and Mge1 mutants, and monitored the percentage of aggregation. Hsp70 with both wild type Mge1 and M155L were showing 20% reduction in aggregation of Rhodanase, whereas H167L and double mutant displayed significant protection against Rhodanse aggregates (**Figure 4.5.1 B**).

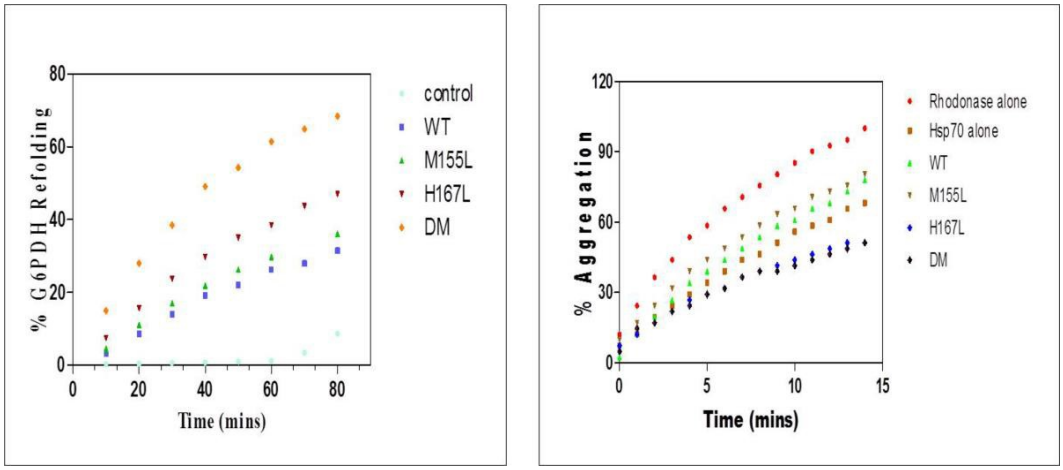

Figure 4.5.1 Effect of Mge1 mutant proteins on the chaperone activities of Hsp70. *(A) Refoliding activity of Hsp70, chemically denaturation of G6PDH (glucose 6 phosphate dehydrogenase) using guanidium hydrochloride was refolded in the presence of wild type Hsp70 (Ssc1) and Mge1 mutant proteins. Chemical denatured G6PDH incubated with alone Hsp70 used as control. (B) Prevention of rhodanese aggregation. Denatured rhodanese (0.46 mM) was added to mtHsp70 protein (4.6 mM) alone, and a preformed complex of 1.15 mM of mtHsp70. BSA was used as a negative control for chaperoning activity. The aggregation of rhodanese was measured at a wavelength of 320 nm and the normalized values were plotted setting the aggregation pattern of rhodanese alone as 100%. WT-wild type Mge1, M155L, H167L and DM(double mutant) are mutants of Mge1.*

4.6 Discussion

Even though Mge1 is involved in many mitochondrial functions, studies regarding the structural and conformational properties of Mge1 were very low. Therefore, we introduced and identified mutations with distinct phenotypes in yeast cells expressing Mge1 and studied structural changes, enabling us to address the possible mechanisms by which disruption or enhanced Hsp70 functions leads to change in cellular functions in yeast.

Our previous findings have suggested that both M155L and H167L mutants of Mge1 show enhanced resistance to multiple abiotic stresses and respiration. Remarkably, when we introduce both the mutants, in the same chian as a double mutant, we found both respiration defect and growth defect in yeast cells. This led us to check the conformational changes using CD and fluorescence spectroscopy. Both M155L and H167L along with double mutant Mge1 show increase in the alpha helical content and in their compactness as evident from quenching studies. Thermal stability analysis suggests that M155L and H167L mutants show Tm value of 42 ºC whereas the double mutant shows 47 ºC suggesting that mutants are thermally a bit more stable than wild type (Tm 37ºC). Interactions studies revealed that both single mutants and double mutant show similar level of interaction with Hsp70 when compared to wild type Mge1, but single mutants display significant decrease in their interaction with Hsp70, in the presence of ATP indicating that mutants enhance the nucleotide exchange activity than wild type Mge1. To further confirm this, we compared their biochemical activities. M155L only slightly enhances ATP hydrolysis whereas H167L and double mutant enhanced ATPase activity of Hsp70 by 2 and 4 folds respectively. Both G6PDH refolding kinetics and Rhodonase aggregation assays supported the idea that both H167L and double mutants enhance the chaperone cycle as observed in ATPase assay, but M155L show similar kinetics with wild type Mge1. More strikingly, the double mutant showed enhanced in vitro ATPase and folding activities which are in contradiction to in vivo results where the double mutant impairs the import kinetics and accumulation of aggregated proteins in isolated mitochondria.

For cell survival, the ratio between and GrpE and DnaK should be maintained properly. At higher temperatures, Hsp70 is tightly bound with nascent peptides where Mge1 is no longer bind with Hsp70 because of changes in its structure. Although Hsp70 independently bind to substrates in the ATP bound state, Mge1 influences its the import, chaperone and folding activity by its nucleotide exchange activity. Retrospectively thermally stable double mutant Mge1 with enhanced ATPase activity may impair the imbalance between the ATP bound and ADP bound state of Hsp70 particularly at higher temperatures, thus directly influencing the overall

folding and import kinetics in *in-vivo* conditions. Consequently, the double mutant would cause the imbalance in quality control in mitochondria matrix and in trans membrane space of inner mitochondria membrane leading to mitochondrial dysfunctions. Importantly, Mge1 has been shown to form ATP sensitive trait complex Hsp70-Cox4-Mge1. In this previous chapter, we found that the double mutant Mge1 impairs the complex. In addition, double Mge1 showed severe defect in growth at elevated temperatures. Therefore, we predict that the double mutant Mge1 displays a dynamic interaction with Hsp70 and this defect could cause the impairment in the import and respiratory assembly, resulting in defect in respiration.

Although single mutants and double mutant Mge1 display secondary structure content and enhanced thermal stability, remarkably, in vivo half-life of the double mutant is greatly reduced when compared to wild type Mge1. Limited proteolysis assay shows that the double mutant has a greater susceptibility, similar to in vivo results. The double mutant appear to be more accessible to proteases present in the matrix or increased levels of proteases (mtUPR) due to mitochondria dysfunctions induced by impairment in both folding and import. This is evident from in vivo results. Based on our results, it is reasonable to believe that the mitochondria dysfunctions and defects in growth in the double mutant Mge1 is attributed to overall reduced half-life associated with high degree of conformation plasticity. More importantly, the mutants of Mge1 are found to be present in highly conserved region of protein, affirming the possibility of distinct phenotypes associated with the change in topology to a similar extent across species.

Chapter 5
Importance of Mge1 methionine oxidation

Introduction

Reactive Oxygen Species (ROS) is a double-edged sword with its paradoxical effects (Alfadda and Sallam 2012). It is well established that ROS regulates several cellular signaling pathways (Schieber and Chandel 2014). The mechanism of reversible covalent modification for ROS has been clearly elucidated (Allu, Marada et al. 2015). Elevated levels of ROS induce structural damage besides altering protein activities (Rodrigues, Reddy et al. 2008). Free radicals enriched in oxygen react with proteins to form various protein entities that include oxidized degradable forms and high molecular weight aggregates that frequently exhibit toxic effects (Herczenik and Gebbink 2008). Protein aggregates have been implicated as one of the key factors in the etiology of diseases like Alzheimer's, Huntington and Parkinson (Markesbery and Carney 1999). Oxidized proteins have been cited as one of the causes for the progression of several pathologies (Young, Crotty et al. 2010).

The Post Translational Modifications (PTMs) of proteins like methylation, phosphorylation, acetylation and ubiquitinylation dramatically increase the repertoire of protein functions and their versatility (Deribe, Pawson et al. 2010). Oxidation-reduction, one of the PTMs has been known to frequently occur as a consequence of fluctuations in cellular redox levels. A multitude of amino acids that include cysteine, methionine, tyrosine, tryptophan, and histidine within proteins have been shown to be vulnerable to oxidation (Stadtman, Van Remmen et al. 2005) (Bourdon and Blache 2001). In particular, derivatives of methionine oxidation, methionine sulfoxide, and sulfone modulate the host protein's function, conformation, and stability (Vogt 1995). Even a single oxidized amino acid residue with in protein is sufficient to have marked effects on inter and intra protein interactions besides protein-solvent interactions (Jahn and Radford 2005).

Mge1, an essential mitochondrial matrix protein, is ubiquitous in its prevalence (Feder and Hofmann 1999). It is a functional homolog of bacterial GrpE and human Mge1 (GRPEL1) with representative candidates in archaea, eubacteria and in eukaryotic related organelles such as chloroplasts and mitochondria. Mge1 is highly conserved functionally and is a member of the Nucleotide Exchange Factor (NEF) family. Given the convergence of sequence, function and location, Mge1 fulfils its expected role as a co-chaperone of mitochondrial Hsp70 and SSQ1 that have a direct effect on mitochondrial protein import, protein translocation, Fe-S cluster formation, folding of proteins to attain their native tertiary structures during normal growth conditions and stabilization of partially folded proteins during heat shock conditions(Ellis 1993, Georgopoulos and Welch 1993, Welch 1993, Schmidt, Strub et al. 2001, Dutkiewicz, Marszalek et al. 2006, Gomez, Perez-Gallardo et al. 2014, Murari, Thiriveedi et al. 2015). It augments and

intensifies the exchange of ATP for ADP in the Hsp70 functional cycle. Functional Mge1 is a homodimer harbouring N- terminal long α- helix, four helical bundles and a C- terminal compact β- sheet domain. The crystal structure of asymmetric DnaK-GrpE complex reveals that N-terminal α- helix and the four helical bundles are responsible for dimerization, while the compact C-terminal β- sheet is involved in its binding to DnaK (Wu, Naveen et al. 2012).

Mge1 is the conserved functional homolog in *Saccharomyces cerevisiae*, archaea, eubacteria and chloroplasts as well. Previously, our lab has reported that Mge1 undergoes oxidative modification through oxidation of its lone methionine residues in position 155 (Met155), leading the formation of methionine sulfoxide (or sulfone) (Allu, Marada et al. 2015). It was known that both thermal and oxidative stress inactivate the dimeric Mge1 and affect the Hsp70 chaperone cycle. In general cells or organisms are exposed to multiple stresses in a continuous gradient manner, but Mge1 has been shown to adaptation stress by changing its oligomeric state (Moro and Muga 2006). Interestingly dimeric stable mutant R40C was shown to derail the chaperone activity of Hsp70 (Siegenthaler and Christen 2005). We believe that gaining insight into the structure of Mge1 is of value in understanding the underlying mechanism behind the adaptation of Mge1 to oxidative stress and its interaction with Hsp70, and Mxr2.

Oxidized Mge1 is reduced by a mitochondrial localized enzyme Methionine Sulfoxide Reductase called Mxr2, both *in vitro* and *in vivo*. We have also shown that Mxr2 preferentially binds to oxidized Mge1 underscoring the physiological and functional importance of this binding. Studies from our lab and others have shown that thermal or oxidative stress converts the active dimeric form of Mge1/GrpE to an inactive monomeric form that slows down the Hsp70 chaperone cycle (Moro and Muga 2006, Marada, Allu et al. 2013). Curiously, a single point mutation of arginine to cysteine at position 40 creates a stable dimeric form of *E. coli* GrpE that also derails the Hsp70 chaperone cycle (Grimshaw, Jelesarov et al. 2003). Hence, we believe that gaining insights into the structure of Mge1 is crucial to understand the underlining mechanism in the adaptation of Mge1 to oxidative stress and interaction with Hsp70 and Mxr2.

In this study, we investigate the effect of low and high levels of oxidative stress on Mge1 structure. We employ biophysical and biochemical methods that include circular dichroism (CD), fluorescence spectroscopy, molecular dynamics (MD) simulations, atomic microscopy (AFM) and co-immunoprecipitation experiments to comprehend the Mge1 structural alterations that direct and regulate its binding to Mxr2 or Hsp70. Oxidation induced selective and local structural adaptations are probably necessary to detach Mge1 from Hsp70 prior to dissociation into monomer. In addition, we show that sequestration of Mxr2 by oxidized Mge1 or *vice versa*

preclude the formation of repeated Mge1 monomeric aggregates so as to maintain the chaperone cycle of Hsp70.

5.1 Results

5.2 Mge1 oxidation leads to a more open conformation

We purified recombinant Mge1 protein and treated the proteins with hydrogen peroxide which is widely used for oxidation, used in the range from 10 to 100 mM concentrations. Change in the structural content of Mge1 was monitored using CD. **Table 5.1 and Figure 5.1** reveals that as H_2O_2 concentration increases, there is a decrease in the α- helical content, with an almost three-fold increase in the content of β- sheet, and a slight increase in the percentage of turns.

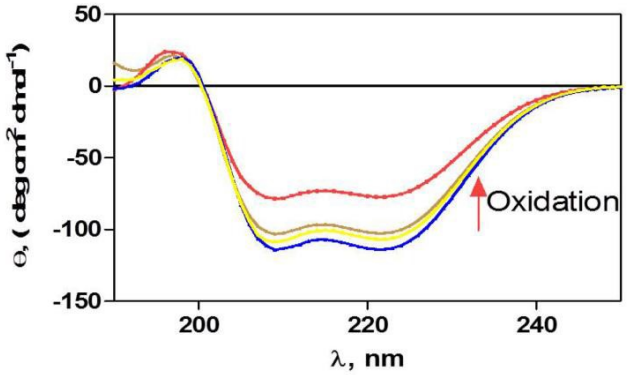

Figure 5.1 Oxidation of Mge1 causes a change in thein secondary structure content. *Recombinant Mge1 purified protein was treated with hydrogen peroxide for 8 hrs, dialysed agianst PBS buffer and CD spectra obtained at between 260-190. Black line-0 mM, Blue-5mM, Yellow-10mM, Brown-50mM, Red-100mM H_2O_2 concentrations*

Table 5.1 Percent levels of secondary structure in native and oxidized Mge1 proteins

$[H_2O_2]$	% α-helix	% β- sheet	% Turns	% Unordered
0 mM	44.6	10.5	18.9	25
5 mM	44	12.8	18.9	26.3
10 mM	34.1	18.3	20.1	30.1
50 mM	29.3	21.6	20.9	28.2
100 mM	25.8	26.8	21.8	25.7

Based on this study, we hypothesized that oxidation of Met155 in Mge1 impacts the stability of the conformation of Mge1. We quantified the thermodynamic stability of Mge1 protein under mild (10 mM H_2O_2) and severe (100 mM H_2O_2) oxidizing conditions, using native protein as a control, as described in the Methods section. Thermal unfolding curves were recorded by heating both oxidized and un-oxidized native proteins in the range of 20-80 ºC. The data were fitted into a homo-dimer two state equations using Graph Pad software. A transition from native to

unfolded state is observed in all the samples albeit to a varying degree. The transition between native and unfolded state was less pronounced in 10 mM H_2O_2 concentration, essentially cooperative and two-state, just as in the control (**Figure 5.2**). Treatment with 100 mM H_2O_2 has a more drastic effect on the unfolding. The transition is more rapid and less cooperative. The above results demonstrate that severe oxidation unfolds Mge1 and lowers the melting temperature by 5°C.

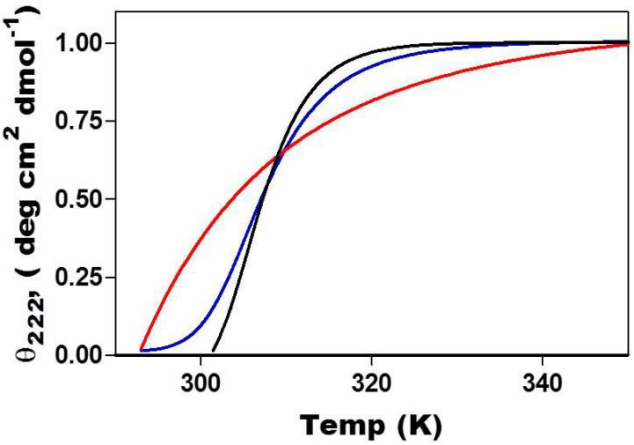

Figure 5.2 Thermal stability of native and oxidized Mge1. *CD spectra of Mge1 protein treated with varying concentrations of H_2O_2 were carried out and processed as described in the methods. The processed CD spectra are shown here. Native wild type Mge1 is represented in black. Mge1 treated with 10mM and 100mM H_2O_2 are represented in blue and red respectively.*

To delve into the implied conformational changes in oxidized Mge1 proteins and their effect on Mge1-Hsp70 interactions, we employed MD simulations studies. Our previous work (Marada, Karri et al. 2016), showed that the modeled Mge1 (60 amino acids onwards that align with a solved crystal structure of E.coli GrpE) homo-dimer comprises a long N-terminal α- helical region, a central region and a C-terminal β-sheet run. The long and short α-helices of the homo-dimer form a central four-helical bundle from which the compact β- sheet domain harboring a hydrophobic core is extended on either side. In each monomer of Mge1, Met155 residue is solvent exposed and is located in the four-helical bundle close to the region that connects to the β- sheet domain.

In the template structure (PDB_ID: 1DKG), Phe86 (in proximal GrpE) is proposed to be involved in positioning of Arg183 side chain from the β-sheet domain. Arg183 forms an intermolecular hydrogen bond with Glu28 of DnaK. Corresponding residues in the A chain of

Mge1 model are Phe112 and Arg213, which are stabilized by cation-π interactions (3.56 Å) and form hydrogen bonding interactions with its neighboring adjacent residues (Gln107 with Phe112, and Leu210, Asn211, Ile215 with Arg213) in the wild type protein. In case of oxidized Mge1 methionine sulphoxide (Msx155), these two residues (Phe112 and Arg213) move far apart (14.3 Å) thereby disrupting the nonbonding interactions present in the same monomer. This leads to a more extended or open structural conformation in oxidized Mge1 (**Figure 5.3**).

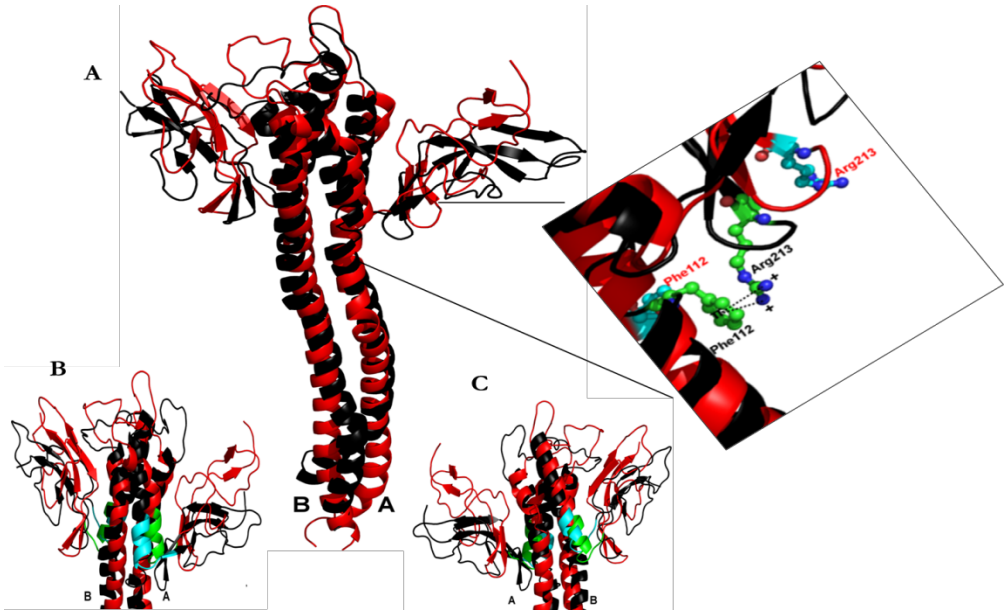

Figure 2. Secondary and tertiary structural changes upon oxidation.
(A) *Superimposition of initial (Black) and average structures (Red) from MD simulations of yeast oxidized Mge1. The model displays the movement of the β-sheet domain towards the four helical bundles in the oxidized Mge1 (red). Insert showing cation-π interaction between Arg213 and Phe112 in the initial structure is marked in black, the average structure are marked in red.* ***(B) and (C)*** *A closer anterior (B) and posterior (C) views of the four helical bundle from the superimposed Figure 2A. Figures 2B and 2C show the loss in helicity in case of the oxidized Mge1 (red).*

On superimposition of the average structures of wild type and oxidized Mge1 (abbreviated as Msx155), Figure 5.3 shows the movement of β-sheet domain towards the four helical bundle in case of Mge1 Msx155. To validate this observation, we calculated the hydrogen bond distances using the Molbridge program (Kumar, Kailasam et al. 2014). Residues of Mge1 Msx155 A chain, Val203, Gln204, Leu206, and Arg216 are seem to make stable intra-molecular hydrogen bonds throughout MD simulations. These stable hydrogen bonds between the four-helix bundle and β- sheets are absent in the wild type Mge1. In MD simulations, the wild type Mge1was seen to

equilibrate at a root mean square distance or RMSD of 5.5 Å and Mge1 Msx155 equilibrated with an RMSD of 5.3 Å. The potential energies during the MD were estimatedto be -1.395 x 10^{-5} kJ mol^{-1} for wild type and -1.39 x 10^{-5} kJ mol^{-1} for oxidized Mge1, signifying almost equal stability of both the structures (**Figure 5.4 A**). We next simulated the structural fluctuations of the molecules.

The root mean square fluctuations or RMSF values of all Cα atoms for wild type and oxidized Mge1 are shown (**Figure 5.4 B**). Oxidized Mge1 follows similar fluctuation patterns as wild type Mge1, however, slightly larger fluctuations are observed in the regions 92-114, and 123-129 with reference to Mge1 (see the peaks in Figure 5.4B). Understandably, the C-terminal region of chain A and N-terminal region of chain B also display higher fluctuations. The 92-114 amino acid sequence comprises a long helical region just preceding the helical bundle. The region comprising 123-129 amino acids of Mge1 forms four helical bundle in the A chain of wild type Mge1 while in oxidized Mge1, this region displays loss of helicity during the course of MD simulations. Further, the β-sheet region of both chains of Mge1 exhibit greater fluctuations in oxidized Mge1 compared to wild type that can be attributed to the movement of this region towards the four helix bundle. We also observe loss of helicity in Mge1 Msx155 between amino acids Asp120 and Leu132, whereas the corresponding region in wild type Mge1 remains intact during the MD simulation. This observation indicates a change in the secondary structure in oxidized Mge1. MD simulations results appear to show that methionine oxidation destabilizes nearby residues leading to loss in intra-molecular interactions and thus loss in secondary structure. MD simulations and CD studies suggest that the stretch of amino acids in between 120 and 132 in Mge1 are probably important in switching from alpha helical to unordered region.

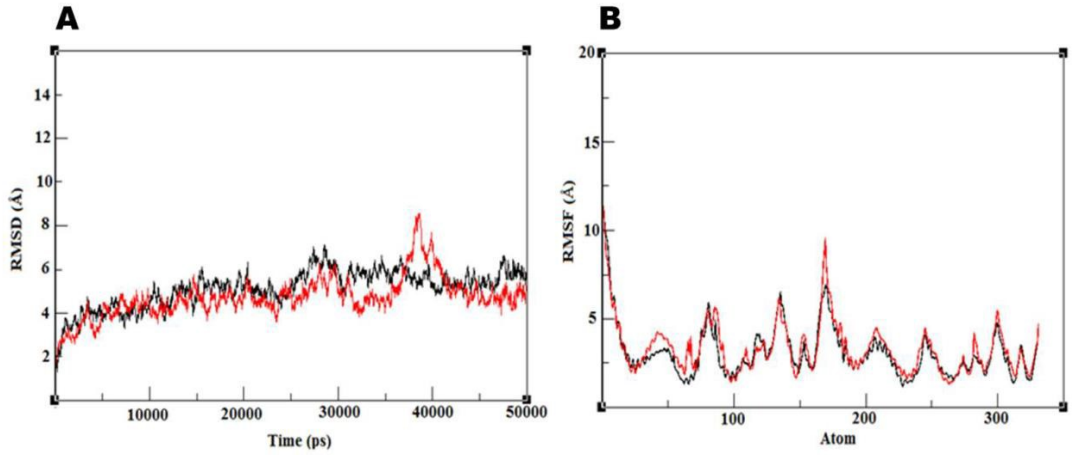

Figure 5.4 Back bone root mean square deviations and fluctuations as function of time. **(A)** *RMSD plots of Ca atoms in wild type Mge1 (black) and oxidized Mge1 (red).* **(B)** *RMSF plots of Ca atoms in wild type Mge1 (black) and oxidized Mge1 (red).*

Solvation effect is known to play a significant role in maintaining the protein folding and stability. Changes in solvation effect are accompanied by changes in protein-protein interactions and protein structure modifications. Accordingly, using MD, we attempted to estimation the extent of opening up the molecule upon oxidation, *i.e*; the solvent-accessible surface area or SASA of the molecule upon oxidation. SASA was calculated for both native and oxidized Mge1 (**Figure 5.5**). The native and oxidized Mge1 proteins have total accessible surface of 200 and 213 nm^2 respectively. Hydrophobic and hydrophilic accessible surface of native Mge1 was found to be 109 and 88 nm^2 whereas for oxidized protein it was found to be 120 and 98 nm^2 respectively. These results suggest that oxidized Mge1 protein has a higher SASA (or more open). These differences in SASA of native and oxidized protein may indicate the redistribution of some amino acid residues from the buried region of globular structure to the surface or vice versa. The increase in hydrophobic and hydrophilic surface areas in oxidized Mge1 is probably responsible for its exposed structure and reduced affinity towards Hsp70.

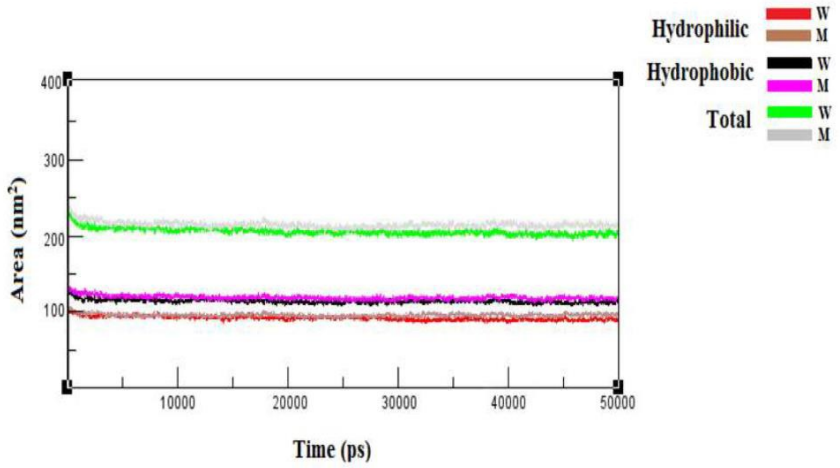

Figure 5.5 Oxidation of methionine increases the exposed surface area of Mge1. *A plot of Solvent Accessible Surface Area (SASA) of wild type (W) and oxidized (M) Mge1 against MD simulation time is shown. Total SASA, hydrophobic and hydrophilic values for wild type (W) and oxidized (M) Mge1 are indicated.*

To confirm that indeed oxidation of Mge1 has increased solvation concomitant with change in structure; we carried out aromatic residue quenching studies. Potassium Iodide (KI) was used as a water soluble static quencher as described under the Methods section. Using Stern-Volmer plot, we compared the Stern-Volmer constants (Ksv) of wild type Mge1 under normal and oxidative stress (10 mM H_2O_2) conditions. Consistent with our previous reported values, wild

type Mge1 displays a Ksv value of 0.82 ± 0.15 whereas oxidized Mge1 shows a Ksv value 6.63 ± 1.63 (**Figure 5.6**).

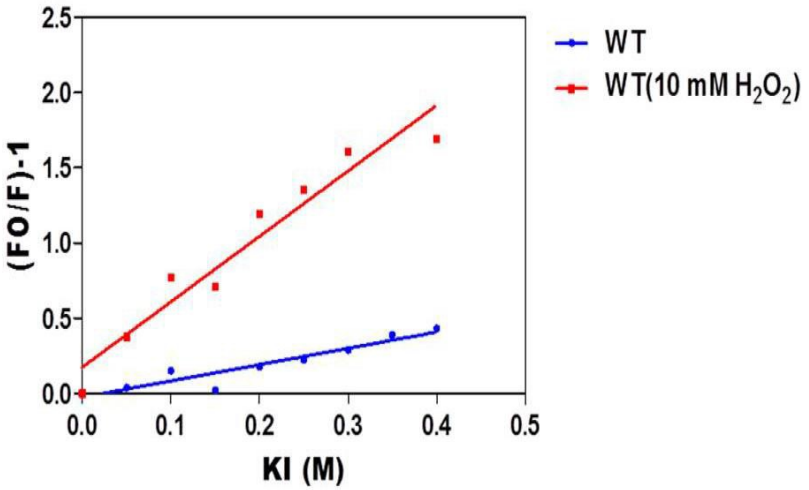

Figure 5.6 Oxidation of methionine of Mge1 makes less compactness. *Intrinsic spectra of native and oxidized Mge1 proteins were obtained using 100 μg/ml Mge1 proteins were used to recorded using fluroscence spectrophotometer and plotted Stern-Volmer to obtian KSV values.*

The aforementioned studies reveal that oxidation of Mge1 affects its secondary structure in vitro, or a more open conformation, with a greater solvation and aromatic exposure..

5.2 Oxidation of Mge1 leads to its aggregation

The Mge1 monomers that are formed as a result of oxidative stress can regain their normal function once the duress is removed. However, it is possible that the monomers might aggregate precluding it from being a substrate to Mxr2 when there is severe oxidative stress and the aggregated monomers might not be functional anymore. To investigate if there is indeed monomer aggregation during persistent or severe oxidative stress, we used theturbidity induced light scattering assay to observe the formation of Mge1 aggregates, if any. Recombinant Mge1 protein was treated with or without H_2O_2 (100 mM) and the formation of aggregates was monitored using light scattering spectroscopy as described in the Methods section. A significant increase in scattering of light is observed in presence of the 100 mM H_2O_2 that increases with time while no light scattering is observed in case of un-oxidized Mge1 (**Figure 5.7**). The temporal increase in scattering of light with persistent oxidation stress suggests that protein aggregates are being formed.

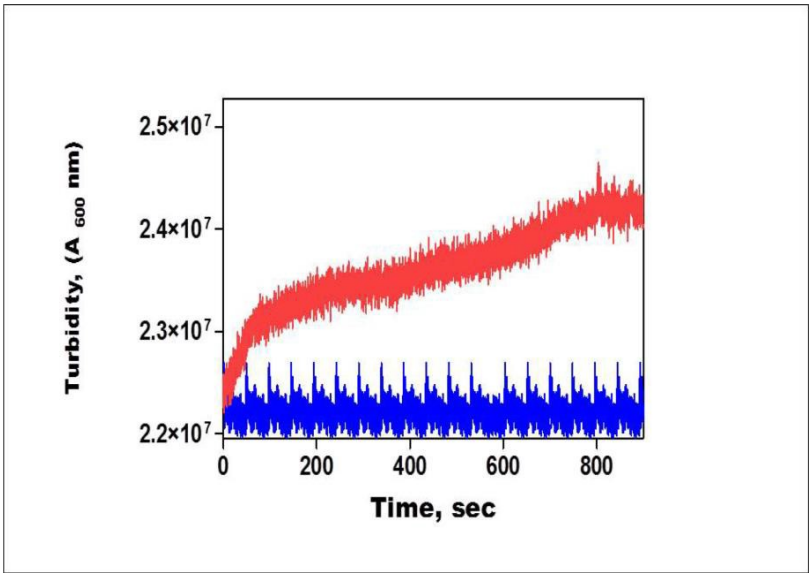

Figure 5.7 Mge1 oxidation induces aggregation. *Time course based light scattering assay was done at 600 nm for 900 sec by measuring light scattering units from a fluorescence spectrophotometer using native Mge1 (blue) and 10 mM H_2O_2 treated Mge1 (orange). The concentration of Mge1 was 10 μg/ml.*

Oxidation of methionine renders the amino acid polar. Paradoxically, oxidation leads to aggregation that is usually marked by an increase in surface hydrophobicity. To probe if indeed there is an increase in surface hydrophobicity in the aggregates despite methionine oxidation, we resorted to monitor binding of fluorescent probes to exposed hydrophobic patches on Mge1 aggregates (Rosen and Weber 1969). We employed ANS or Bis-ANS fluorescent probes as they have been widely used to study exposure of hydrophobic patches of misfolded or partial folded proteins. A significant increase in fluorescence was observed temporally in presence of both ANS and Bis-ANS binding assays suggesting that oxidation of Mge1 indeed increases the total hydrophobic surface area(Vogt 1995) albeit oxidized methionine becoming polar (**Figure 5.8**).

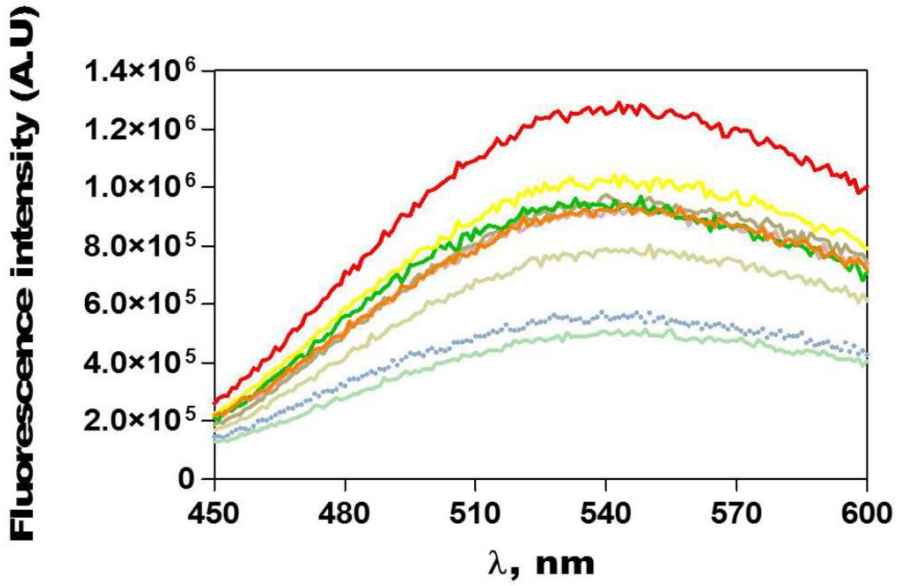

Figure 5.8 Mge1 oxidation increases surface hydrophobicity as monitored by fluorescence. *Surface hydrophobic residues were monitored by Bis-ANS extrinsic fluorescent dyes using Fluoro-MAX-3 fluorescence spectrophotometer. Mge1 protein was incubated with 10 mM H_2O_2 and spectra were obtained by adding 20 μM Bis-ANS at every one hour up to 24 hrs at room temperature using an excitation wavelength of 390 nm and emission spectra were scanned from 400 to 600 nm at 3 nm slit.*

Protein aggregation plays an adverse role in the pathogenesis of many human diseases especially neurodegenerative diseases. Reasoning that mitochondrial dysfunction is mostly correlated with neurodegenerative diseases that are hallmarked by amyloid kind of aggregates, we monitored whether Mge1 aggregates fits into the amyloid type. We followed the binding kinetics of fluorescence dyes, thioflavin T and Congo Red to oxidized Mge1 (**Figure 5.9 A and B**). These dyes are known to bind to amyloid fibrils. Consistent with known results with amyloid fibrils, we observe a significant increase in the fluorescence in presence of thioflavin T with time suggesting that Mge1 aggregates may be of the amyloid type. A red shift in Congo Red absorbance spectra was also noted that correlates with the formation of amyloid type aggregates.

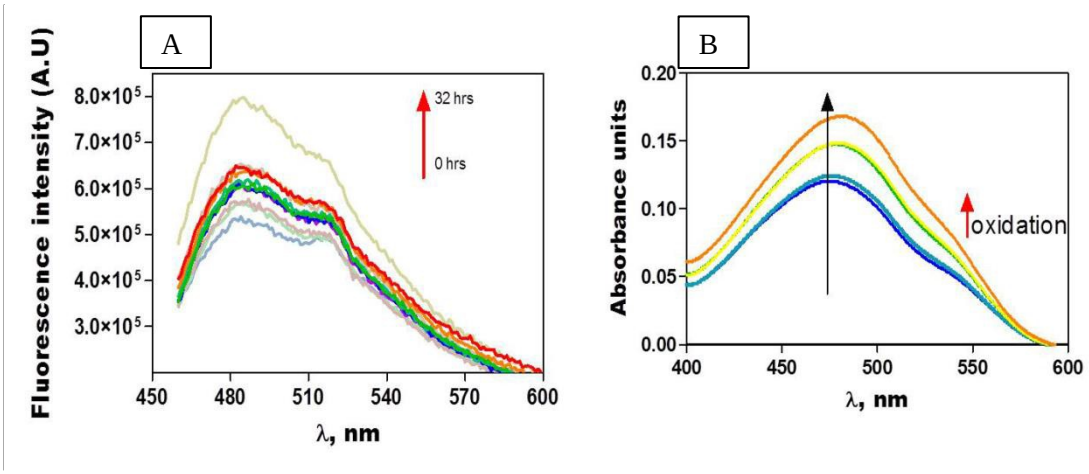

Figure 5.9 Oxidized Mge1 forms amyloid type aggregates. *Aggregation of oxidized Mge1 was monitored using Thioflavin-T (A) and Congo Red (B). In case of (A), recombinant Mge1 protein was treated with 10 mM H_2O_2 prior to addition of Thioflavin-T as described in the Methods section. Spectra were obtained every hour using an excitation wavelength of 444 nm and emission spectra were noted from 450 nm to 600 nm. For (B), recombinant Mge1 was treated with various concentrations of H_2O_2: 0 (blue), 1 mM (light blue), 2 mM (Green), 5 mM (yellow) and 10 mM (red) along with 10 μM Congo Red for 30 min at room temperature. Spectra were collected from 400-600 nm using UV-visible spectrophotometer.*

This increase in β- sheet was also predicted from our CD spectroscopic studies. To further confirm on the type of aggregate formation by oxidized Mge1, we resorted to Atomic Force Microscopy (AFM). Recombinant Mge1 was treated with 10 mM or 100 mM H_2O_2 for three hours and subjected to AFM. Oxidized Mge1 displays a monomeric repetitive structure type of aggregation and its intensity increases with increase in H_2O_2 (Figure 5.10).

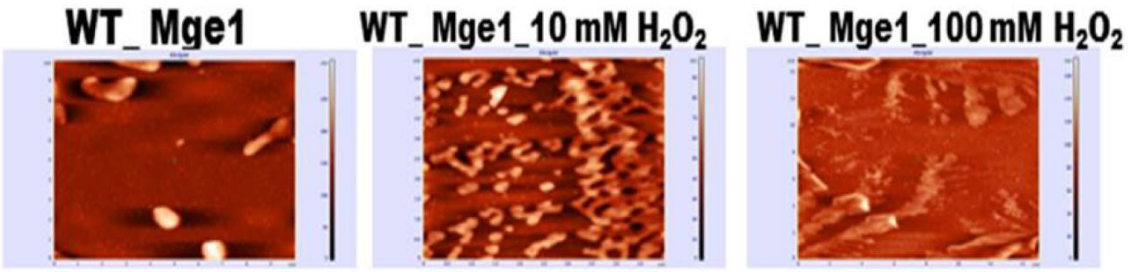

Figure 5.10 Monitoring aggregation of oxidized Mge1 by Atomic Force Microscopy (AFM). *AFM images of recombinant Mge1 protein treated with various concentrations of H_2O_2 (0 (left panel), 10 mM (center panel) and 100 (right panel) mM H_2O_2).*

5.3 Elevated oxidative stress causes aggregation and degradation of Mge1 in intact mitochondria

Our *in vitro* results confirm that elevated oxidative stress causes the aggregation of Mge1. It is interesting to see whether oxidative stress induces the aggregation of Mge1 in the isolated organelle or in cells. We had earlier shown that Mxr2 reduces oxidized Mge1 both *in vitro* and *in vivo (*Allu, Marada et al. 2015). To monitor the aggregation of Mge1 *in vivo*, we isolated mitochondria from wild type and *MXR2*-deleted strains and incubated them with increasing concentrations (0-20 mM) of H_2O_2 for 3 hrs. The total insoluble (aggregated) and 20% of soluble fractions were separated using SDS-PAGE followed by Coomassie staining (**Figure 5.11 A and B**) or western transferred and immuno-blotted against the Mge1 and Aconitase (Aco1) antibodies (**Figure 5.11 C**). Coomassie stained gels show that there is no apparent change in the protein pattern in soluble fractions of wild type and *MXR2* deleted strains. Similarly, we find both soluble fractions contain an equivalent amount of Aco1. However, immunoblot with Mge1 antibody shows a decrease in the amount of Mge1 in soluble fraction of *MXR2* deleted strain when compared to wild type (**Figure 5.11 and E**). In the corresponding insoluble fractions (pellet) from both strains, we observe an increase in the amount of Mge1 with oxidative stress. This oxidative stress effect is more pronounced in case of the *MXR2*-deleted strain. We find that at high oxidative stress, Mge1 levels are low both in the supernatant as well as in the insoluble fraction in the absence of *Mxr2* indicating that most likely it is getting aggregated or degraded. To further test the stability of Mge1 under elevated oxidative stress, mitochondria isolated from wild type and *MXR2*-deletd strains were exposed to 20 mM H_2O_2 for various time intervals (0-3 hrs). The total mitochondrial fractions were resolved on SDS-PAGE, western blotted and probed with Mge1 and porin antibodies (**Figure 5.11 F and G**). We find specific reduction in Mge1 but not porin levels in WT and *MXR2* deleted strain. However, reduction in Mge1 levels are more pronounced in *MXR2* deleted strain when compared to WT type strain. Most interestingly, the temporal decrease in Mge1 level is relatively more rapid in the absence of *MXR2*. This suggests that Mxr2 has a protective function towards Mge1, shielding it from oxidation triggered aggregation and degradation.

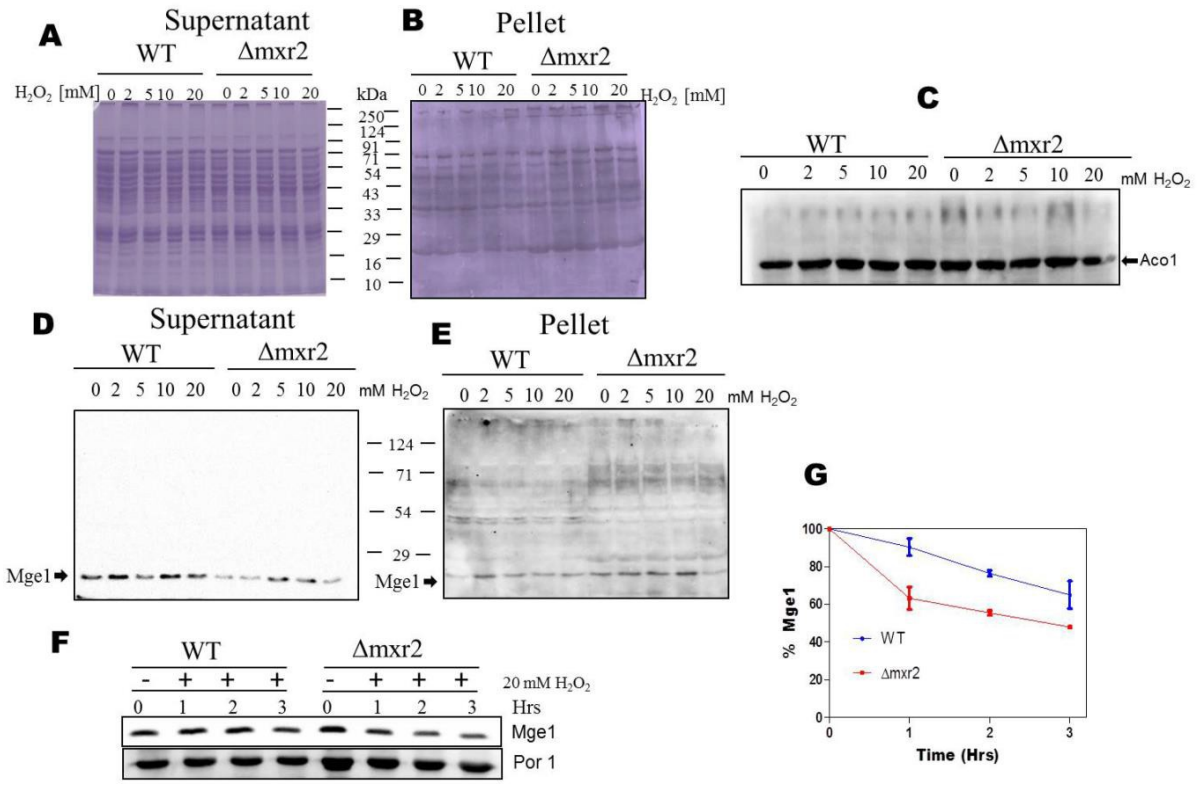

Figure 5.11 Mxr2 protects oxidized Mge1 from aggregation. *Immunoblots of soluble and pellet fractions of H_2O_2 treated mitochondria isolated from wild type and ⊿mxr2 yeast strains as described in the methods section are shown. 20% of soluble fraction (***A and D***) and 100% of insoluble fraction (***B and E***) were separated on SDS-PAGE, western transferred and probed with Mge1 (***D and E***) and with Aconitase1* **(C)** *antibodies.* **Mxr2 protecting the oxidised Mge1 in vivo.** *Mitochondria were isolated from wild type and ⊿mxr2 yeast strains. Mitochondria (1mg/ml) were treated with 0, 2, 5, 10, 20 mM H_2O_2 concentrations in mitochondrial suspension buffer (250 mM sucrose, 10 mM MOPS/KOH pH 7.0, 80 mM KCl, 5 mM $MgCl_2$ 3 mM ATP and 3 mM NADH) for 3 hrs at room temperature. Mitochondria were pellet at 10,000 rpm for 10 mins and mitochondria were solubilised using lysis buffer (0.5% Trition X 100, 200 mM KCl, 30 mM Tris-HCl pH 7.5, 5 mM EDTA) and fractionaton was done by centrifugation at 22,000 rpm for 1 hour. (***F and G***) Amount of Mge1 aggregated protein was analysed by western blotting and quantified by image J.*

5.4 Altered interaction of oxidized Mge1 with Hsp70 and Mxr2

It is of interest to find out how Mxr2 differentiates between oxidized and reduced Mge1. Based on the above studies and those done by Tarrago, et al, we suspect that the hydrophobic patches that get exposed on the Mge1 molecule upon oxidation may invite Mxr2, while, concomitantly promoting its dissociation from Hsp70 (Tarrago, Kaya et al. 2012). To test this possibility, we used increasing concentrations of the denaturant urea to mimic the oxidation-induced exposure of hydrophobic patches and checked its interaction with Mxr2 and Hsp70. A pull-down assay using Ni-NTA beads was performed by treating His-Mge1 with increasing concentrations of urea (up to 5 M), and mitochondrial lysate isolated from a yeast strain expressing Flag-Mxr2. The pulled down Mxr2 and Hsp70 were quantified using Image J software. We note that the

interaction of Mxr2 with native Mge1 is minimal; however, its interaction increases with increase in urea concentration. In contrast, Hsp70 interaction with Mge1 slightly enhances with initial concentration of urea treatment (1-3 M) but decreases from 4 M urea onwards with minimal interaction when Mge1 is treated with 5 M urea (**Figure 5.12 A and B**). To check whether indeed the oxidation of M155 in Mge1 alters its interaction with Hsp70 and Mxr2, we repeated the experiment using the H_2O_2 treated M155L mutant of Mge1, which is resistant to oxidation (**Figure 5.12 C**). We observe some interaction between this M155L mutant and Mxr2 in the control reaction. We attribute this interaction occurs due to the exposure of the hydrophobic leucine residue. Most importantly, we did not see any increase in interaction of M155L mutant with Mxr2, or a decrease in its interaction with Hsp70. This is consistent with the view that wild type Mge1 is susceptible to oxidative stress-induced changes in structure and protein-protein interactions, while the M155L mutant is impervious.

We next asked whether oxidized Mge1 affects the binding of denatured substrates with Hsp70. Heat induced denatured GDH was incubated with Hsp70 and with 0-50 mM H_2O_2 treated Mge1 in buffer as described in methods (**Figure 5.12 D and E**). Predictably, Mge1 shows a decrease in binding with Hsp70 with increase in oxidation. Hsp70 preferentially binds denatured GDH aggregates to higher oxidized Mge1 suggesting that oxidation of Mge1 serves as a harbinger in cellular adaptation towards oxidative.

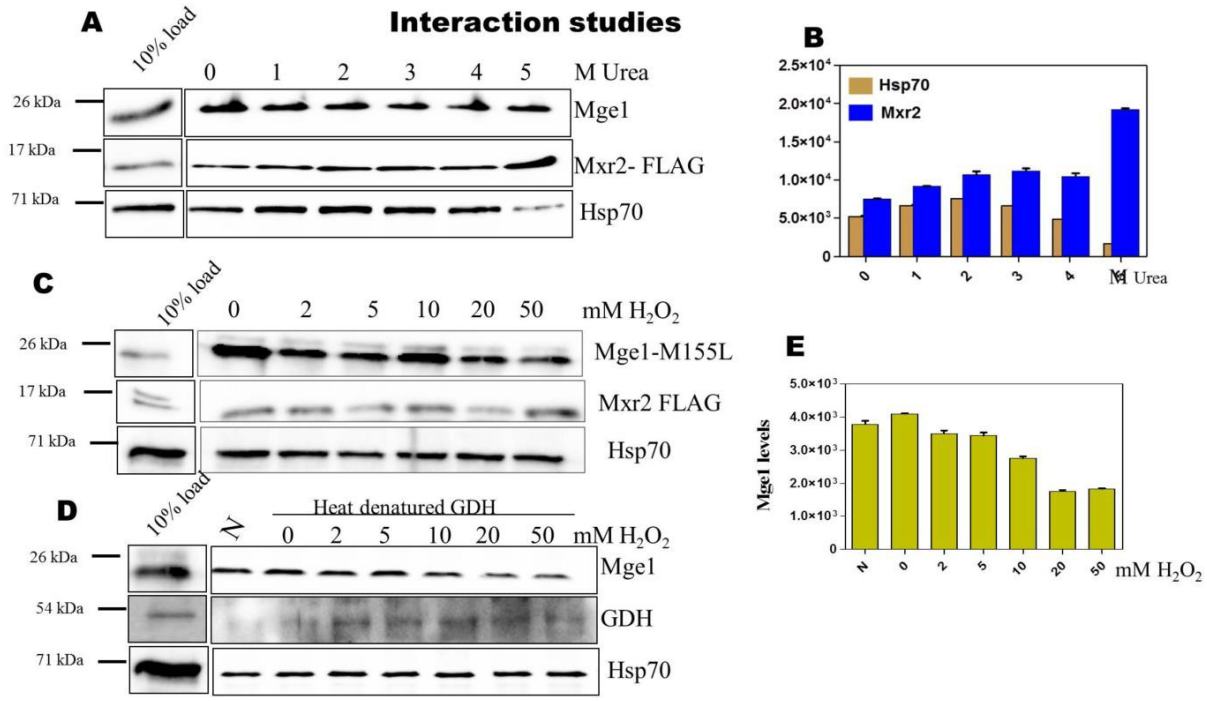

Figure 5.12 Altered interactions of oxidized Mge1 with Hsp70 and Mxr2.

(A) and (B) *His tagged Mge1 protein was denatured using different molar concentrations of urea and incubated with mitochondria lysate obtained from a FLAG-MXR2 expressing yeast cells. Ni affinity chromatography was carried out using Ni-NTA beads as described in the methods section and the eluted proteins were resolved on SDS-PAGE, western transferred and probed with indicated protein specific antibodies as shown (A).* **(B)** *Bar graph depicting quantified levels of Hsp70 and Mxr2 proteins from three independent experiments as described in (A) using Image J software.* **(C).** *Similar to Figure 7(A), Ni pull down assay was carried out except that His tagged Mge1 M155L mutant protein was used instead of His tagged Mge1 and H_2O_2 was used as an oxidizing agent instead of urea.* **(D).** *Immunoprecipitation of denatured glutamate dehydrogenase (GDH) with Hsp70 was carried out in the presence of native and oxidized Mge1 as described in methods. Each reaction mixture containing 15 μg of mHsp70, 30 μg of Mge1 and 30 μg of Hsp70 were incubated at 4° C for 2 hrs in the presence of Hsp70 antibody coupled to protein A sepharose beads. Beads were washed with PBS buffer, proteins resolved on SDS-PAGE and analyzed by western blotting.* **(E).** *Bar graph showing quantified levels of Mge1 protein binding to Hsp70 from three independent experiments using Image J software. 'N' indicates non-denatured GDH.*

5.5 Discussion

Non-physiological cellular ROS levels have pleiotropic effects that include compromised cellular functions and sometimes even cell death (Nakajima, Itakura et al. 2017). Recent work on oxidative stress has revealed that high levels of ROS can be manifested in various disease forms that include cancer, diabetes and neurological diseases (Li, Tan et al. 2015). Our recent studies have uncovered a novel redox mediated pathway that involves Mxr2, Mge1 and Hsp70 (Allu, Marada et al. 2015). These three factors form a new paradigm in mitochondrial redox regulation. Hsp70 plays a pivotal role in protein folding and in import of mitochondrial proteins, besides protecting unfolded proteins during cellular insults. Hence, it is crucial that Hsp70 function be immune to these insults. Any compromise on Hsp70 activity will have an amplified effect. Mge1 is the only co-chaperone of Hsp70 that undergoes structural changes and any derailment in the former's function will negatively affect Hsp70. Keeping in mind the important role of Mge1, the cell appear to have devised a mechanism in the form of Mxr2 to keep Mge1 functional during stress. Slight perturbations in redox levels that induce oxidation of Mge1 155 Met are reversed by Mxr2. However, very high oxidative stress apparently causes irreversible damage to the cell.

The current study is an effort to gain insight into the molecular and structural changes that Mge1 undergoes during oxidation. Thermal stability studies were done at a low and highconcentrations of oxidative stress. Contrary to our expectations, we see that low levels of oxidative stress are tolerated by Mge1, since the thermal unfolding curve is similar to that of the non-stressed Mge1. However, high level of oxidative stress, induced by 100 mM H_2O_2, results in an unfolding of Mge1 protein, accompanied with a downward shift in its Tm value. We attribute the lack of an effect on thermal unfolding by mild oxidative stress to insufficient structural changes. The *in vitro* result at high oxidative stress can be extrapolated to an *in vivo* system wherein we observe irreversible reactions. The unfolding of the Mge1 protein at high oxidative stress is substantiated by the increase in surface area to the solvent. In addition, we deduce a more open conformation from the MD stimulation studies for the oxidized Mge1. MD stimulation studies predict a loss in alpha helicity, movement of helix bundle to beta sheet, increased fluctuations in the region that interact with Hsp70 and formation of new stable intra molecular H bonds in case of oxidized Mge1. These structural alterations the in regulatory region of Mge1 probably leading to the secondary structure conversion between alpha helix and beta sheet along with formation of aggregates during persistent oxidative stress.

Tidow et al (2004) have talked about what they call "chameleon" sequence in protein, where the region switches conformation upon change in the environment conditions (oxidation,

heat, pH). We looked the sequence of Mge1 and find that is for has a chameleon "sequence" (ENTLRKHGIE, residues 120 to 130 in the sequence), and note that is which switchs from α-helical fold into β-sheet conformations. Such oxidation-induced changes in Mge1 structure make it behave like both adaptive and pathogenic aggregates.

Elevated or persistent oxidative stress leads to aggregation even in the presence of Mxr2. This happens as a result of imbalance between the rates of oxidation to reduction of Mge1. Light scattering and fluorescent studies show that oxidized Mge1 can form aggregates while AFM and Congo Red studies indicate that the aggregates are of the amyloid type (**Figure 5.9 and 5.10**). Mitochondrial protein aggregates are associated with myopathies and it is not surprising that oxidized Mge1 forms aggregates as oxidative stress is known to give rise to toxic protein aggregates(Kandimalla, Manczak et al. 2016). Further studies will reveal if Mge1 aggregates have any clinical correlation.

Our previous *in vivo* studies have shown that Mxr2 interacts with oxidized Mge1 and reduces it. In this study, we show that besides its known reducing function, Mxr2 acts like a "chaperone" as it protects oxidized Mge1 from further unfolding. We find that Hsp70 that is noted for its protective function on unfolded proteins does not prefer unfolded Mge1. This is a unique regulation specific to Hsp70-Mge1 mechanism of action and thereby highlights the importance of Mge1 function. Comparing Hsp70 chaperone function with Mxr2, we find that Mxr2 has a greater affinity to unfolded Mge1 than Hsp70. The increase in hydrophobicity observed in case of oxidized Mge1 may be the determining factor for the differences in the affinity. It would be interesting to further probe the reasons for the differences in the affinity juxta positioning the structures of Hsp70, and Mxr2 against unfolded and folded Mge1.

We show in this report that such oxidation (using H_2O_2 as the oxidant) has negative consequences on the secondary, tertiary and quaternary structures of Mge1. The normally active homodimer monomerizes upon Met oxidation (as shown earlier in our studies, unfolds into an inactive form that loses its ability to bind to Hsp70 with any efficiency as oxidative stress increases. While low levels of oxidative stress are tolerated (**see Figure 5.2 at 10 mM H_2O_2**), high oxidative stress leads the molecule to open up, expose buried residues to the surface (**Figure 5.6**), and to produce amyloid type aggregates (**Figure 5.8**). We suspect that this might be aided by the presence of 'chameleon' peptide sequence (ENTLRKHGIE, residues 120 to 130 in the sequence, Figure 1A and B), which switches from α-helical fold into β-sheet conformations (**see Table 1, Figure 2 from Karri S et al 2018, Mitochondrion**). Such

oxidation-induced changes in Mge1 structure make it behave like both adaptive and pathogenic aggregates. These results prove that cellular ROS has dual functions like signaling and pathogenesis (oxidative interface), inactive and unable to act as a co-chaperone. Yeast is known to have two 'protective' enzymes, Mxr1 and Mxr2, which are methionine sulfoxide reductases; the former is located in the cytoplasm while the latter, of current interest, is in the mitochondrion. We have shown that Mxr2 reduces the oxidized form of Mge1 back to its active reduced form, restoring its co-chaperone ability, both *in vitro* and *in vivo*. In the absence of MXR2, elevated ROS levels lead to increased levels of Mge1 in the insoluble fraction that is further aggravated with oxidative stress. Incidentally, we find that *MXR2*-deleted mitochondria exhibit significant amount of insoluble aggregates even in the absence of any external oxidative stress (**Figure 5.11 E**) that is further aggravated with oxidative stress.

We believe that Mxr2 helps in the recycling of oxidized Mge1 thereby limiting the amount of it in the insoluble fraction. Any derailment in this process might have a cascading effect on mitochondrial protein import, protein folding and Fe-S cluster biogenesis.

Our previous *in vivo* studies have shown that Mxr2 interacts with oxidized Mge1 and reduces it. In this study, we show that besides its known reducing function, Mxr2 itself acts as a 'chaperone' as it protects oxidized Mge1 from further unfolding. We find that Hsp70, which is noted for its protective function on unfolded proteins, does not prefer unfolded Mge1. This is a unique regulation orchestrated by Hsp70-Mge1-Mxr2 triad protein complex that impacts response to oxidative stress and the dynamics of aggregated proteins. Our results show that Mxr2 has a greater affinity to unfolded Mge1 and this attribute is protective as their binding pre-empts the oxidative stress induced degradation of Mge. The increase in surface exposure observed in case of oxidized Mge1 may be the determining factor for the differences in the relative affinities of Mxr2 and Hsp70 towards it.

Mitochondrial protein aggregates are associated with myopathies and it is not surprising that oxidized Mge1 forms aggregates as oxidative stress is known to give rise to toxic protein aggregate. Absence of methionine sulfoxide reductases antioxidant system has been shown to be sensitive to oxidative stress and cause a reduced life span in mammalian cells. Further studies will reveal if Mge1 aggregates have any clinical correlation.

Summary of thesis

TIM23 import complex involved in import of major matrix proteins and also involved in assembly of respiratory complex. Mge1, co chaperone, component of import motor (PAM) which is part of TIM 23 complex. PAM complex comprises several chaperones and cochaperone proteins that are conserved across eukaryotes. Our lab and other has studied extensively the role of Mge1 in stress adaptation. Here, we are reporting that Mge1 is co-chaperone in PAM complex which was shown to form complex with Hsp70 and Cox4. Assembly of cytochrome c oxidase is very complex process involving several assembly factories that require multiple steps.

In the first chapter, Mge1 was shown to respond to multiple abiotic stresses. We characterised the underlying mechanisms of adaptive role of Mge1 using budding yeast, *Saccharomyces cerevisiae*. Mutational characterisation of Mge1 revealed that both single mutations M155L and H167L gain in functions like increase in respiratory capacity and enhanced the mitochondria translation. Remarkably, when we mutate the both single mutants and transform, yeast cells showing sensitivity to abiotic stresses and sever growth defect in non-fermentable carbons source. Moreover double mutant causes the defective respiratory assembly at elevated temperatures and decreased mitochondrial translation. Thus, Mge1 might regulate the respiration, and connects the stress adaptation and mitochondria functions. A functional connection between and respiration and CLS revealed that yeast strains having higher respiratory capacity inducing mitophagy efficiently thereby extends the CLS. From transcriptional analysis, double mutant shown specifically down regulate the amino acid and OXPHOS and sterol metabolisms and increased in levels of chaperones and proteases which are prime target for many abiotic stresses. We found that Mge1 is helps in functionally linking between respiration and abiotic stress adaptation. Our findings essentially highlight that yeast cells have co-opted co-chaperones as essential regulators of gene expression under conditions when their folding activity is not required. Furthermore, our work illustrates that essential genes can perform different essential functions in discrete growth conditions.

In second part of my thesis is aimed to dissect the structural and biochemical aspects of mutants of Mge1. In vitro binding data suggesting that both single mutants and double mutant are having similar binding affinity with Hsp70, but they are exhibiting sensitive in presence of ATP with gain in functional activities like ATPase activity, folding and holdase kinetics in additive manner. Biophysical studies reveal that both single mutant showing thermal stability by ~5 ºC whereas double mutant gain in thermal stability by ~10 ºC. From Molecular Dynamics and spectrophometry studies suggesting mutants has adapt distinct topology which are evident from

limited proteolysis assay. This data provide a better understanding the conformational dynamics of Mge1 in contexts of chaperone cycle in mitochondrial matrix.

In third part of work was directed towards the understanding the methionine oxidation induced changes in Mge1 structure. Previous we reported that Mge1 has lone methionine undergoing oxidation both in vivo and in vitro and also reduced to native protein by mitochondrial methionine sulfoxide reductase (Mxr2). However, importance of oxidation events in chaperone cycle is poorly understood. Therefore, structural aspects and interacting components essential in defining the cycle of events in the triad complex (Hsp70-Mge1-Mxr2) proteins were explored. We employed MD simulations and spectroscopic analysis to study the step wise manner of regulation of Mge1under oxidative stress. Methionine sulfoxide induces the local unfolding in C terminus region of Mge1 to timely detach form Hsp70 where precursor proteins are protected from aggregation. We also observed that oxidation increases the surface hydrophobic area of Mge1 there by it causes the formation of amyloid type aggregates. Moreover, in vivo results suggest that stability of Mge1 is governed by Mxr2 protein.

In contrast to invitro results, double mutant showing impairment in import at elevated temperatures. From steady state levels of mitochondrial proteome and BN PAGE analysis suggesting that both single mutants showing increased amount of both import machinery and respiratory complex proteins whereas double mutant showing specifically decreased Cox family proteins without altering the import complex. Analysis of super complex respiratory assembly by BN PAGE, shown that double mutant showing defect in assembly at elevated temperature. These results can be explained by co-immunoprecipitaion assay where double mutant Mge1 impairs the Hsp70-Mge1-Cox4 triad complex which is believed to have role in assembly of complex IV at stress conditions. More importantly respiratory capacity of double mutant greatly affected, single mutants are having respiratory than wild type cells.

Finally, double mutant Mge1 in yeast cells, result in highly compromised growth at multiple abiotic stresses and sever defect in glycerol media. Double mutant Mge1 harbouring yeast cell showed multiple phenotypes at cellular levels including 1) Impairment of import kinetics across inner mitochondria membrane that results in accumulation of pre-proteins in cytosol. 2) Enhanced susceptibility towards to multiple abiotic stresses. 3) Reduction of mitochondria functions namely defect in assembly of respiratory complex and nearly 40 % reduced respiration.

4) Impairment in mitophagy induction under nitrogen starvation without defect in autophagy induction supporting that the mitochondrial functions are impaired.

On the other hand, M155L and H167L variants were found to have enhanced growth phenotype and resistance at permissive conditions. Biochemically, H167L purified variants enhanced ATPase activity and thermal stability when compared to wild type Mge1. Strikingly, the M155L variant also exhibits ATPase and chaperone activity similar to wild type Mge1 and it also showing reduced in vitro import kinetics similar to double mutant Mge1. But, M155L did not showing accumulation cytosolic Hsp60 in vivo. Therefore, it is reasonable to believe that defect growth in double mutant Mge1 is due to consequence of both impairment in respiratory complex assembly and import.

References

Adams, K. L. and J. D. Palmer (2003). "Evolution of mitochondrial gene content: gene loss and transfer to the nucleus." *Mol Phylogenet Evol* **29**(3): 380-395.

Aggeler, R. and R. A. Capaldi (1990). "Yeast cytochrome c oxidase subunit VII is essential for assembly of an active enzyme. Cloning, sequencing, and characterization of the nuclear-encoded gene." *J Biol Chem* **265**(27): 16389-16393.

Albrecht, R., P. Rehling, A. Chacinska, J. Brix, S. A. Cadamuro, R. Volkmer, B. Guiard, N. Pfanner and K. Zeth (2006). "The Tim21 binding domain connects the preprotein translocases of both mitochondrial membranes." *EMBO Rep* **7**(12): 1233-1238.

Alfadda, A. A. and R. M. Sallam (2012). "Reactive oxygen species in health and disease." *J Biomed Biotechnol* **2012**: 936486.

Allen, S., V. Balabanidou, D. P. Sideris, T. Lisowsky and K. Tokatlidis (2005). "Erv1 mediates the Mia40-dependent protein import pathway and provides a functional link to the respiratory chain by shuttling electrons to cytochrome c." *J Mol Biol* **353**(5): 937-944.

Allu, P. K., A. Marada, Y. Boggula, S. Karri, T. Krishnamoorthy and N. B. Sepuri (2015). "Methionine sulfoxide reductase 2 reversibly regulates Mge1, a cochaperone of mitochondrial Hsp70, during oxidative stress." *Mol. Biol. Cell* **26**(3): 406-419.

Auesukaree, C., A. Damnernsawad, M. Kruatrachue, P. Pokethitiyook, C. Boonchird, Y. Kaneko and S. Harashima (2009). "Genome-wide identification of genes involved in tolerance to various environmental stresses in Saccharomyces cerevisiae." *J Appl Genet* **50**(3): 301-310.

Avadhani, N. G., M. C. Sangar, S. Bansal and P. Bajpai (2011). "Bimodal targeting of cytochrome P450s to endoplasmic reticulum and mitochondria: the concept of chimeric signals." *FEBS J* **278**(22): 4218-4229.

Barrientos, A., A. Zambrano and A. Tzagoloff (2004). "Mss51p and Cox14p jointly regulate mitochondrial Cox1p expression in Saccharomyces cerevisiae." *EMBO J* **23**(17): 3472-3482.

Bauer, M. F., C. Sirrenberg, W. Neupert and M. Brunner (1996). "Role of Tim23 as voltage sensor and presequence receptor in protein import into mitochondria." *Cell* **87**(1): 33-41.

Becker, T., S. Pfannschmidt, B. Guiard, D. Stojanovski, D. Milenkovic, S. Kutik, N. Pfanner, C. Meisinger and N. Wiedemann (2008). "Biogenesis of the mitochondrial TOM complex: Mim1 promotes insertion and assembly of signal-anchored receptors." *J Biol Chem* **283**(1): 120-127.

Becker, T., L. S. Wenz, V. Kruger, W. Lehmann, J. M. Muller, L. Goroncy, N. Zufall, T. Lithgow, B. Guiard, A. Chacinska, R. Wagner, C. Meisinger and N. Pfanner (2011). "The mitochondrial import protein Mim1 promotes biogenesis of multispanning outer membrane proteins." *J Cell Biol* **194**(3): 387-395.

Bihlmaier, K., N. Mesecke, N. Terziyska, M. Bien, K. Hell and J. M. Herrmann (2007). "The disulfide relay system of mitochondria is connected to the respiratory chain." *J Cell Biol* **179**(3): 389-395.

Bonawitz, N. D., M. Chatenay-Lapointe, Y. Pan and G. S. Shadel (2007). "Reduced TOR signaling extends chronological life span via increased respiration and upregulation of mitochondrial gene expression." *Cell Metab* **5**(4): 265-277.

Botstein, D., S. A. Chervitz and J. M. Cherry (1997). "Yeast as a model organism." *Science* **277**(5330): 1259-1260.

Bourdon, E. and D. Blache (2001). "The importance of proteins in defense against oxidation." *Antioxid Redox Signal* **3**(2): 293-311.

Bratic, A. and N. G. Larsson (2013). "The role of mitochondria in aging." *J Clin Invest* **123**(3): 951-957.

Burtner, C. R., C. J. Murakami, B. K. Kennedy and M. Kaeberlein (2009). "A molecular mechanism of chronological aging in yeast." *Cell Cycle* **8**(8): 1256-1270.

Cabreiro, F., D. Ackerman, R. Doonan, C. Araiz, P. Back, D. Papp, B. P. Braeckman and D. Gems (2011). "Increased life span from overexpression of superoxide dismutase in Caenorhabditis elegans is not caused by decreased oxidative damage." *Free Radic Biol Med* **51**(8): 1575-1582.

Chacinska, A., M. Lind, A. E. Frazier, J. Dudek, C. Meisinger, A. Geissler, A. Sickmann, H. E. Meyer, K. N. Truscott, B. Guiard, N. Pfanner and P. Rehling (2005). "Mitochondrial presequence translocase: switching between TOM tethering and motor recruitment involves Tim21 and Tim17." *Cell* **120**(6): 817-829.

Chacinska, A., S. Pfannschmidt, N. Wiedemann, V. Kozjak, L. K. Sanjuan Szklarz, A. Schulze-Specking, K. N. Truscott, B. Guiard, C. Meisinger and N. Pfanner (2004). "Essential role of Mia40 in import and assembly of mitochondrial intermembrane space proteins." *EMBO J* **23**(19): 3735-3746.
Chan, D. C. (2012). "Fusion and fission: interlinked processes critical for mitochondrial health." *Annu Rev Genet* **46**: 265-287.
Chen, J., S. M. Young, C. Allen, A. Seeber, M. P. Peli-Gulli, N. Panchaud, A. Waller, O. Ursu, T. Yao, J. E. Golden, J. J. Strouse, M. B. Carter, H. Kang, C. G. Bologa, T. D. Foutz, B. S. Edwards, B. R. Peterson, J. Aube, M. Werner-Washburne, R. J. Loewith, C. De Virgilio and L. A. Sklar (2012). "Identification of a small molecule yeast TORC1 inhibitor with a multiplex screen based on flow cytometry." *ACS Chem Biol* **7**(4): 715-722.
Church, C., B. Goehring, D. Forsha, P. Wazny and R. O. Poyton (2005). "A role for Pet100p in the assembly of yeast cytochrome c oxidase: interaction with a subassembly that accumulates in a pet100 mutant." *J Biol Chem* **280**(3): 1854-1863.
Cui, T. Z., A. Conte, J. L. Fox, V. Zara and D. R. Winge (2014). "Modulation of the respiratory supercomplexes in yeast: enhanced formation of cytochrome oxidase increases the stability and abundance of respiratory supercomplexes." *J Biol Chem* **289**(9): 6133-6141.
Curran, S. P., D. Leuenberger, E. P. Leverich, D. K. Hwang, K. N. Beverly and C. M. Koehler (2004). "The role of Hot13p and redox chemistry in the mitochondrial TIM22 import pathway." *J Biol Chem* **279**(42): 43744-43751.
Dailey, T. A., J. H. Woodruff and H. A. Dailey (2005). "Examination of mitochondrial protein targeting of haem synthetic enzymes: in vivo identification of three functional haem-responsive motifs in 5-aminolaevulinate synthase." *Biochem J* **386**(Pt 2): 381-386.
Danial, N. N. and S. J. Korsmeyer (2004). "Cell death: critical control points." *Cell* **116**(2): 205-219.
Decoster, E., M. Simon, D. Hatat and G. Faye (1990). "The MSS51 gene product is required for the translation of the COX1 mRNA in yeast mitochondria." *Mol Gen Genet* **224**(1): 111-118.
Demuyser, L., E. Swinnen, A. Fiori, B. Herrera-Malaver, K. Vestrepen and P. Van Dijck (2017). "Mitochondrial Cochaperone Mge1 Is Involved in Regulating Susceptibility to Fluconazole in Saccharomyces cerevisiae and Candida Species." *MBio* **8**(4).
Deribe, Y. L., T. Pawson and I. Dikic (2010). "Post-translational modifications in signal integration." *Nat Struct Mol Biol* **17**(6): 666-672.
Dienhart, M. K. and R. A. Stuart (2008). "The yeast Aac2 protein exists in physical association with the cytochrome bc1-COX supercomplex and the TIM23 machinery." *Mol Biol Cell* **19**(9): 3934-3943.
Ding, J., X. Huang, L. Zhang, N. Zhao, D. Yang and K. Zhang (2009). "Tolerance and stress response to ethanol in the yeast Saccharomyces cerevisiae." *Appl Microbiol Biotechnol* **85**(2): 253-263.
Diot, A., K. Morten and J. Poulton (2016). "Mitophagy plays a central role in mitochondrial ageing." *Mamm Genome* **27**(7-8): 381-395.
Dong, Y., D. Zhang, Q. Yu, Q. Zhao, C. Xiao, K. Zhang, C. Jia, S. Chen, B. Zhang, B. Zhang and M. Li (2017). "Loss of Ssq1 leads to mitochondrial dysfunction, activation of autophagy and cell cycle arrest due to iron overload triggered by mitochondrial iron-sulfur cluster assembly defects in Candida albicans." *Int J Biochem Cell Biol* **85**: 44-55.
Dowhan, W., C. R. Bibus and G. Schatz (1985). "The cytoplasmically-made subunit IV is necessary for assembly of cytochrome c oxidase in yeast." *EMBO J* **4**(1): 179-184.
Droge, W. (2002). "Free radicals in the physiological control of cell function." *Physiol Rev* **82**(1): 47-95.
Dunn, C. D., M. S. Lee, F. A. Spencer and R. E. Jensen (2006). "A genomewide screen for petite-negative yeast strains yields a new subunit of the i-AAA protease complex." *Mol Biol Cell* **17**(1): 213-226.
Dutkiewicz, R., J. Marszalek, B. Schilke, E. A. Craig, R. Lill and U. Muhlenhoff (2006). "The Hsp70 chaperone Ssq1p is dispensable for iron-sulfur cluster formation on the scaffold protein Isu1p." *J Biol Chem* **281**(12): 7801-7808.
Ellis, R. J. (1993). "The General Concept of Molecular Chaperones." *Philos. Trans. R. Soc. London Series B-Biological Sciences* **339**(1289): 257-261.
Exner, N., A. K. Lutz, C. Haass and K. F. Winklhofer (2012). "Mitochondrial dysfunction in Parkinson's disease: molecular mechanisms and pathophysiological consequences." *EMBO J* **31**(14): 3038-3062.
Favre, C., P. S. Aguilar and M. C. Carrillo (2008). "Oxidative stress and chronological aging in glycogen-phosphorylase-deleted yeast." *Free Radic Biol Med* **45**(10): 1446-1456.

Feder, M. E. and G. E. Hofmann (1999). "Heat-shock proteins, molecular chaperones, and the stress response: Evolutionary and ecological physiology." *Annual Review of Physiology* **61**: 243-282.

Fontanesi, F., P. Clemente and A. Barrientos (2011). "Cox25 teams up with Mss51, Ssc1, and Cox14 to regulate mitochondrial cytochrome c oxidase subunit 1 expression and assembly in Saccharomyces cerevisiae." *J Biol Chem* **286**(1): 555-566.

Fontanesi, F., I. C. Soto, D. Horn and A. Barrientos (2006). "Assembly of mitochondrial cytochrome c-oxidase, a complicated and highly regulated cellular process." *Am J Physiol Cell Physiol* **291**(6): C1129-1147.

Fontanesi, F., I. C. Soto, D. Horn and A. Barrientos (2010). "Mss51 and Ssc1 facilitate translational regulation of cytochrome c oxidase biogenesis." *Mol Cell Biol* **30**(1): 245-259.

Frazier, A. E., J. Dudek, B. Guiard, W. Voos, Y. Li, M. Lind, C. Meisinger, A. Geissler, A. Sickmann, H. E. Meyer, V. Bilanchone, M. G. Cumsky, K. N. Truscott, N. Pfanner and P. Rehling (2004). "Pam16 has an essential role in the mitochondrial protein import motor." *Nat Struct Mol Biol* **11**(3): 226-233.

Friedman, J. R. and J. Nunnari (2014). "Mitochondrial form and function." *Nature* **505**(7483): 335-343.

Gakh, O., P. Cavadini and G. Isaya (2002). "Mitochondrial processing peptidases." *Biochim Biophys Acta* **1592**(1): 63-77.

Gebert, M., S. G. Schrempp, C. S. Mehnert, A. K. Heisswolf, S. Oeljeklaus, R. Ieva, M. Bohnert, K. von der Malsburg, S. Wiese, T. Kleinschroth, C. Hunte, H. E. Meyer, I. Haferkamp, B. Guiard, B. Warscheid, N. Pfanner and M. van der Laan (2012). "Mgr2 promotes coupling of the mitochondrial presequence translocase to partner complexes." *J Cell Biol* **197**(5): 595-604.

Gebert, N., M. Gebert, S. Oeljeklaus, K. von der Malsburg, D. A. Stroud, B. Kulawiak, C. Wirth, R. P. Zahedi, P. Dolezal, S. Wiese, O. Simon, A. Schulze-Specking, K. N. Truscott, A. Sickmann, P. Rehling, B. Guiard, C. Hunte, B. Warscheid, M. van der Laan, N. Pfanner and N. Wiedemann (2011). "Dual function of Sdh3 in the respiratory chain and TIM22 protein translocase of the mitochondrial inner membrane." *Mol Cell* **44**(5): 811-818.

Georgopoulos, C. and W. J. Welch (1993). "Role of the major heat shock proteins as molecular chaperones." *Annu. Rev. Cell Biol.* **9**: 601-634.

Gerbeth, C., O. Schmidt, S. Rao, A. B. Harbauer, D. Mikropoulou, M. Opalinska, B. Guiard, N. Pfanner and C. Meisinger (2013). "Glucose-induced regulation of protein import receptor Tom22 by cytosolic and mitochondria-bound kinases." *Cell Metab* **18**(4): 578-587.

Gibson, B. R., S. J. Lawrence, J. P. Leclaire, C. D. Powell and K. A. Smart (2007). "Yeast responses to stresses associated with industrial brewery handling." *FEMS Microbiol Rev* **31**(5): 535-569.

Gilkerson, R. W., E. A. Schon, E. Hernandez and M. M. Davidson (2008). "Mitochondrial nucleoids maintain genetic autonomy but allow for functional complementation." *J Cell Biol* **181**(7): 1117-1128.

Gomez, M., R. V. Perez-Gallardo, L. A. Sanchez, A. L. Diaz-Perez, C. Cortes-Rojo, V. Meza Carmen, A. Saavedra-Molina, J. Lara-Romero, S. Jimenez-Sandoval, F. Rodriguez, J. S. Rodriguez-Zavala and J. Campos-Garcia (2014). "Malfunctioning of the iron-sulfur cluster assembly machinery in Saccharomyces cerevisiae produces oxidative stress via an iron-dependent mechanism, causing dysfunction in respiratory complexes." *PLoS One* **9**(10): e111585.

Graef, M. and J. Nunnari (2011). "Mitochondria regulate autophagy by conserved signalling pathways." *EMBO J* **30**(11): 2101-2114.

Grimshaw, J. P., I. Jelesarov, R. K. Siegenthaler and P. Christen (2003). "Thermosensor action of GrpE. The DnaK chaperone system at heat shock temperatures." *J Biol Chem* **278**(21): 19048-19053.

Hamza, I. and H. A. Dailey (2012). "One ring to rule them all: trafficking of heme and heme synthesis intermediates in the metazoans." *Biochim Biophys Acta* **1823**(9): 1617-1632.

Harbauer, A. B., R. P. Zahedi, A. Sickmann, N. Pfanner and C. Meisinger (2014). "The protein import machinery of mitochondria-a regulatory hub in metabolism, stress, and disease." *Cell Metab* **19**(3): 357-372.

Harman, D. (1972). "The biologic clock: the mitochondria?" *J Am Geriatr Soc* **20**(4): 145-147.

Harrison, C. J., M. HayerHartl, M. DiLiberto, F. U. Hartl and J. Kuriyan (1997). "Crystal structure of the nucleotide exchange factor GrpE bound to the ATPase domain of the molecular chaperone DnaK." *Science* **276**(5311): 431-435.

Hawlitschek, G., H. Schneider, B. Schmidt, M. Tropschug, F. U. Hartl and W. Neupert (1988). "Mitochondrial protein import: identification of processing peptidase and of PEP, a processing enhancing protein." *Cell* **53**(5): 795-806.

Hell, K., J. M. Herrmann, E. Pratje, W. Neupert and R. A. Stuart (1998). "Oxa1p, an essential component of the N-tail protein export machinery in mitochondria." *Proc Natl Acad Sci U S A* **95**(5): 2250-2255.

Herczenik, E. and M. F. Gebbink (2008). "Molecular and cellular aspects of protein misfolding and disease." *FASEB J* **22**(7): 2115-2133.

Herrmann, J. M., R. A. Stuart, E. A. Craig and W. Neupert (1994). "Mitochondrial heat shock protein 70, a molecular chaperone for proteins encoded by mitochondrial DNA." *J Cell Biol* **127**(4): 893-902.

Herrmann, L., B. E. Bowler, A. Dong and W. S. Caughey (1995). "The effects of hydrophilic to hydrophobic surface mutations on the denatured state of iso-1-cytochrome c: investigation of aliphatic residues." *Biochemistry* **34**(9): 3040-3047.
Hill, K., K. Model, M. T. Ryan, K. Dietmeier, F. Martin, R. Wagner and N. Pfanner (1998). "Tom40 forms the hydrophilic channel of the mitochondrial import pore for preproteins [see comment]." *Nature* **395**(6701): 516-521.
Horan, S., I. Bourges, J. W. Taanman and B. Meunier (2005). "Analysis of COX2 mutants reveals cytochrome oxidase subassemblies in yeast." *Biochem J* **390**(Pt 3): 703-708.
Hulett, J. M., F. Lueder, N. C. Chan, A. J. Perry, P. Wolynec, V. A. Likic, P. R. Gooley and T. Lithgow (2008). "The transmembrane segment of Tom20 is recognized by Mim1 for docking to the mitochondrial TOM complex." *J Mol Biol* **376**(3): 694-704.
Hutu, D. P., B. Guiard, A. Chacinska, D. Becker, N. Pfanner, P. Rehling and M. van der Laan (2008). "Mitochondrial protein import motor: differential role of Tim44 in the recruitment of Pam17 and J-complex to the presequence translocase." *Mol Biol Cell* **19**(6): 2642-2649.
Isaya, G., D. Miklos and R. A. Rollins (1994). "MIP1, a new yeast gene homologous to the rat mitochondrial intermediate peptidase gene, is required for oxidative metabolism in Saccharomyces cerevisiae." *Mol Cell Biol* **14**(8): 5603-5616.
Ito, A. (1999). "Mitochondrial processing peptidase: multiple-site recognition of precursor proteins." *Biochem Biophys Res Commun* **265**(3): 611-616.

Ishikawa, D., H. Yamamoto, Y. Tamura, K. Moritoh and T. Endo (2004). "Two novel proteins in the mitochondrial outer membrane mediate beta-barrel protein assembly." *J Cell Biol* **166**(5): 621-627.
Jacobson, J. and M. R. Duchen (2004). "Interplay between mitochondria and cellular calcium signalling." *Mol Cell Biochem* **256-257**(1-2): 209-218.
Jahn, T. R. and S. E. Radford (2005). "The Yin and Yang of protein folding." *FEBS J* **272**(23): 5962-5970.
Jan, P. S., K. Esser, E. Pratje and G. Michaelis (2000). "Som1, a third component of the yeast mitochondrial inner membrane peptidase complex that contains Imp1 and Imp2." *Mol Gen Genet* **263**(3): 483-491.
Jazwinski, S. M. (2013). "The retrograde response: when mitochondrial quality control is not enough." *Biochim Biophys Acta* **1833**(2): 400-409.
Jia, L., M. Dienhart, M. Schramp, M. McCauley, K. Hell and R. A. Stuart (2003). "Yeast Oxa1 interacts with mitochondrial ribosomes: the importance of the C-terminal region of Oxa1." *EMBO J* **22**(24): 6438-6447.
Johannsen, D. L. and E. Ravussin (2009). "The role of mitochondria in health and disease." *Curr Opin Pharmacol* **9**(6): 780-786.
Jovaisaite, V., L. Mouchiroud and J. Auwerx (2014). "The mitochondrial unfolded protein response, a conserved stress response pathway with implications in health and disease." *J Exp Biol* **217**(Pt 1): 137-143.
Kaeberlein, M. (2010). "Lessons on longevity from budding yeast." *Nature* **464**(7288): 513-519.
Kandimalla, R., M. Manczak, D. Fry, Y. Suneetha, H. Sesaki and P. H. Reddy (2016). "Reduced dynamin-related protein 1 protects against phosphorylated Tau-induced mitochondrial dysfunction and synaptic damage in Alzheimer's disease." *Hum Mol Genet* **25**(22): 4881-4897.
Kang, P. J., J. Ostermann, J. Shilling, W. Neupert, E. A. Craig and N. Pfanner (1990). "Requirement for hsp70 in the mitochondrial matrix for translocation and folding of precursor proteins." *Nature* **348**(6297): 137-143.
Karbowski, M. and R. J. Youle (2011). "Regulating mitochondrial outer membrane proteins by ubiquitination and proteasomal degradation." *Curr Opin Cell Biol* **23**(4): 476-482.
Karri, S., S. Singh, A. K. Paripati, A. Marada, T. Krishnamoorthy, L. Guruprasad, D. Balasubramanian and N. B. V. Sepuri (2018). "Adaptation of Mge1 to oxidative stress by local unfolding and altered Interaction with mitochondrial Hsp70 and Mxr2." *Mitochondrion*.
Kerr, J. F., A. H. Wyllie and A. R. Currie (1972). "Apoptosis: a basic biological phenomenon with wide-ranging implications in tissue kinetics." *Br J Cancer* **26**(4): 239-257.
Kerscher, O., J. Holder, M. Srinivasan, R. S. Leung and R. E. Jensen (1997). "The Tim54p-Tim22p complex mediates insertion of proteins into the mitochondrial inner membrane." *J Cell Biol* **139**(7): 1663-1675.
Kerscher, O., N. B. Sepuri and R. E. Jensen (2000). "Tim18p is a new component of the Tim54p-Tim22p translocon in the mitochondrial inner membrane." *Mol Biol Cell* **11**(1): 103-116.
Kityk, R., M. Vogel, R. Schlecht, B. Bukau and M. P. Mayer (2015). "Pathways of allosteric regulation in Hsp70 chaperones." *Nat Commun* **6**: 8308.

Kovermann, P., K. N. Truscott, B. Guiard, P. Rehling, N. B. Sepuri, H. Muller, R. E. Jensen, R. Wagner and N. Pfanner (2002). "Tim22, the essential core of the mitochondrial protein insertion complex, forms a voltage-activated and signal-gated channel." *Mol Cell* **9**(2): 363-373.
Kozjak, V., N. Wiedemann, D. Milenkovic, C. Lohaus, H. E. Meyer, B. Guiard, C. Meisinger and N. Pfanner (2003). "An essential role of Sam50 in the protein sorting and assembly machinery of the mitochondrial outer membrane." *J Biol Chem* **278**(49): 48520-48523.
Kulawiak, B., J. Hopker, M. Gebert, B. Guiard, N. Wiedemann and N. Gebert (2013). "The mitochondrial protein import machinery has multiple connections to the respiratory chain." *Biochim Biophys Acta* **1827**(5): 612-626.
Kumar, M. S., P. Y. Reddy, B. Sreedhar and G. B. Reddy (2005). "Alphab-crystallin-assisted reactivation of glucose-6-phosphate dehydrogenase upon refolding." *Biochem J* **391**(Pt 2): 335-341.
Kumar, P., S. Kailasam, S. Chakraborty and M. Bansal (2014). "MolBridge: a program for identifying nonbonded interactions in small molecules and biomolecular structures." *Journal of Applied Crystallography* **47**: 1772-1776.
Lahtvee, P. J., R. Kumar, B. M. Hallstrom and J. Nielsen (2016). "Adaptation to different types of stress converge on mitochondrial metabolism." *Mol Biol Cell* **27**(15): 2505-2514.
Lathrop, J. T. and M. P. Timko (1993). "Regulation by heme of mitochondrial protein transport through a conserved amino acid motif." *Science* **259**(5094): 522-525.
Lazarou, M., S. M. Jin, L. A. Kane and R. J. Youle (2012). "Role of PINK1 binding to the TOM complex and alternate intracellular membranes in recruitment and activation of the E3 ligase Parkin." *Dev Cell* **22**(2): 320-333.
Lemire, B. D. and K. S. Oyedotun (2002). "The Saccharomyces cerevisiae mitochondrial succinate:ubiquinone oxidoreductase." *Biochim Biophys Acta* **1553**(1-2): 102-116.
Li, S., H. Y. Tan, N. Wang, Z. J. Zhang, L. Lao, C. W. Wong and Y. Feng (2015). "The Role of Oxidative Stress and Antioxidants in Liver Diseases." *Int J Mol Sci* **16**(11): 26087-26124.
Lill, R. and U. Muhlenhoff (2008). "Maturation of iron-sulfur proteins in eukaryotes: mechanisms, connected processes, and diseases." *Annu Rev Biochem* **77**: 669-700.
Livnat-Levanon, N. and M. H. Glickman (2011). "Ubiquitin-proteasome system and mitochondria - reciprocity." *Biochim Biophys Acta* **1809**(2): 80-87.
Longo, V. D. and P. Fabrizio (2002). "Regulation of longevity and stress resistance: a molecular strategy conserved from yeast to humans?" *Cell Mol Life Sci* **59**(6): 903-908.
Lopez de Figueroa, P., M. K. Lotz, F. J. Blanco and B. Carames (2015). "Autophagy activation and protection from mitochondrial dysfunction in human chondrocytes." *Arthritis Rheumatol* **67**(4): 966-976.
Ma, M. and L. Z. Liu (2010). "Quantitative transcription dynamic analysis reveals candidate genes and key regulators for ethanol tolerance in Saccharomyces cerevisiae." *BMC Microbiol* **10**: 169.
Mapa, K., M. Sikor, V. Kudryavtsev, K. Waegemann, S. Kalinin, C. A. Seidel, W. Neupert, D. C. Lamb and D. Mokranjac (2010). "The conformational dynamics of the mitochondrial Hsp70 chaperone." *Mol Cell* **38**(1): 89-100.
Marada, A., P. K. Allu, A. Murari, B. PullaReddy, P. Tammineni, V. R. Thiriveedi, J. Danduprolu and N. B. Sepuri (2013). "Mge1, a nucleotide exchange factor of Hsp70, acts as an oxidative sensor to regulate mitochondrial Hsp70 function." *Mol. Biol. Cell* **24**(6): 692-703.
Marada, A., S. Karri, S. Singh, P. K. Allu, Y. Boggula, T. Krishnamoorthy, L. Guruprasad and N. B. V. Sepuri (2016). "A Single Point Mutation in Mitochondrial Hsp70 Cochaperone Mge1 Gains Thermal Stability and Resistance." *Biochemistry* **55**(51): 7065-7072.
Markesbery, W. R. and J. M. Carney (1999). "Oxidative alterations in Alzheimer's disease." *Brain Pathol.* **9**(1): 133-146.
Marom, M., D. Dayan, K. Demishtein-Zohary, D. Mokranjac, W. Neupert and A. Azem (2011). "Direct interaction of mitochondrial targeting presequences with purified components of the TIM23 protein complex." *J Biol Chem* **286**(51): 43809-43815.
Martinez-Caballero, S., S. M. Grigoriev, J. M. Herrmann, M. L. Campo and K. W. Kinnally (2007). "Tim17p regulates the twin pore structure and voltage gating of the mitochondrial protein import complex TIM23." *J Biol Chem* **282**(6): 3584-3593.
Mattson, M. P., M. Gleichmann and A. Cheng (2008). "Mitochondria in neuroplasticity and neurological disorders." *Neuron* **60**(5): 748-766.
Mayer, A., W. Neupert and R. Lill (1995). "Translocation of apocytochrome c across the outer membrane of mitochondria." *J Biol Chem* **270**(21): 12390-12397.

McStay, G. P., C. H. Su and A. Tzagoloff (2013). "Stabilization of Cox1p intermediates by the Cox14p-Coa3p complex." *FEBS Lett* **587**(7): 943-949.
Melero, R., F. Moro, M. A. Perez-Calvo, J. Perales-Calvo, L. Quintana-Gallardo, O. Llorca, A. Muga and J. M. Valpuesta (2015). "Modulation of the chaperone DnaK allosterism by the nucleotide exchange factor GrpE." *J Biol Chem* **290**(16): 10083-10092.
Miao, B., J. E. Davis and E. A. Craig (1997). "Mge1 functions as a nucleotide release factor for Ssc1, a mitochondrial Hsp70 of Saccharomyces cerevisiae." *J Mol Biol* **265**(5): 541-552.
Mick, D. U., K. Wagner, M. van der Laan, A. E. Frazier, I. Perschil, M. Pawlas, H. E. Meyer, B. Warscheid and P. Rehling (2007). "Shy1 couples Cox1 translational regulation to cytochrome c oxidase assembly." *EMBO J* **26**(20): 4347-4358.
Mills, D. A. and J. P. Hosler (2005). "Slow proton transfer through the pathways for pumped protons in cytochrome c oxidase induces suicide inactivation of the enzyme." *Biochemistry* **44**(12): 4656-4666.
Mizushima, N. and M. Komatsu (2011). "Autophagy: renovation of cells and tissues." *Cell* **147**(4): 728-741.
Mokranjac, D., S. A. Paschen, C. Kozany, H. Prokisch, S. C. Hoppins, F. E. Nargang, W. Neupert and K. Hell (2003). "Tim50, a novel component of the TIM23 preprotein translocase of mitochondria." *EMBO J* **22**(4): 816-825.
Mokranjac, D., M. Sichting, W. Neupert and K. Hell (2003). "Tim14, a novel key component of the import motor of the TIM23 protein translocase of mitochondria." *EMBO J* **22**(19): 4945-4956.
Morano, K. A., C. M. Grant and W. S. Moye-Rowley (2012). "The response to heat shock and oxidative stress in Saccharomyces cerevisiae." *Genetics* **190**(4): 1157-1195.
Moro, F. and A. Muga (2006). "Thermal adaptation of the yeast mitochondrial Hsp70 system is regulated by the reversible unfolding of its nucleotide exchange factor." *J. Mol. Biol.* **358**(5): 1367-1377.
Murari, A., V. R. Thiriveedi, F. Mohammad, V. Vengaldas, M. Gorla, P. Tammineni, T. Krishnamoorthy and N. B. Sepuri (2015). "Human mitochondrial MIA40 (CHCHD4) is a component of the Fe-S cluster export machinery." *Biochem J* **471**(2): 231-241.
Nakajima, H., M. Itakura, T. Kubo, A. Kaneshige, N. Harada, T. Izawa, Y. T. Azuma, M. Kuwamura, R. Yamaji and T. Takeuchi (2017). "Glyceraldehyde-3-phosphate Dehydrogenase (GAPDH) Aggregation Causes Mitochondrial Dysfunction during Oxidative Stress-induced Cell Death." *J Biol Chem* **292**(11): 4727-4742.
Nakamura, K., M. Yamaki, M. Sarada, S. Nakayama, C. R. Vibat, R. B. Gennis, T. Nakayashiki, H. Inokuchi, S. Kojima and K. Kita (1996). "Two hydrophobic subunits are essential for the heme b ligation and functional assembly of complex II (succinate-ubiquinone oxidoreductase) from Escherichia coli." *J Biol Chem* **271**(1): 521-527.
Narendra, D. P. and R. J. Youle (2011). "Targeting mitochondrial dysfunction: role for PINK1 and Parkin in mitochondrial quality control." *Antioxid Redox Signal* **14**(10): 1929-1938.
Nargund, A. M., M. W. Pellegrino, C. J. Fiorese, B. M. Baker and C. M. Haynes (2012). "Mitochondrial import efficiency of ATFS-1 regulates mitochondrial UPR activation." *Science* **337**(6094): 587-590.
Nevoigt, E. (2008). "Progress in metabolic engineering of Saccharomyces cerevisiae." *Microbiol Mol Biol Rev* **72**(3): 379-412.
Ocampo, A., J. Liu, E. A. Schroeder, G. S. Shadel and A. Barrientos (2012). "Mitochondrial respiratory thresholds regulate yeast chronological life span and its extension by caloric restriction." *Cell Metab* **16**(1): 55-67.
Ott, M. and J. M. Herrmann (2010). "Co-translational membrane insertion of mitochondrially encoded proteins." *Biochim Biophys Acta* **1803**(6): 767-775.
Pan, Y., E. A. Schroeder, A. Ocampo, A. Barrientos and G. S. Shadel (2011). "Regulation of yeast chronological life span by TORC1 via adaptive mitochondrial ROS signaling." *Cell Metab* **13**(6): 668-678.
Park, S., T. Hanekamp, M. K. Thorsness and P. E. Thorsness (2006). "Yme2p is a mediator of nucleoid structure and number in mitochondria of the yeast Saccharomyces cerevisiae." *Curr Genet* **50**(3): 173-182.
Pellegrino, M. W., A. M. Nargund and C. M. Haynes (2013). "Signaling the mitochondrial unfolded protein response." *Biochim Biophys Acta* **1833**(2): 410-416.
Perez-Martinez, X., S. A. Broadley and T. D. Fox (2003). "Mss51p promotes mitochondrial Cox1p synthesis and interacts with newly synthesized Cox1p." *EMBO J* **22**(21): 5951-5961.
Quiros, P. M., T. Langer and C. Lopez-Otin (2015). "New roles for mitochondrial proteases in health, ageing and disease." *Nat Rev Mol Cell Biol* **16**(6): 345-359.

Quiros, P. M., M. A. Prado, N. Zamboni, D. D'Amico, R. W. Williams, D. Finley, S. P. Gygi and J. Auwerx (2017). "Multi-omics analysis identifies ATF4 as a key regulator of the mitochondrial stress response in mammals." *J Cell Biol* **216**(7): 2027-2045.
Rao, S., O. Schmidt, A. B. Harbauer, B. Schonfisch, B. Guiard, N. Pfanner and C. Meisinger (2012). "Biogenesis of the preprotein translocase of the outer mitochondrial membrane: protein kinase A phosphorylates the precursor of Tom40 and impairs its import." *Mol Biol Cell* **23**(9): 1618-1627.
Regev-Rudzki, N., E. Battat, I. Goldberg and O. Pines (2009). "Dual localization of fumarase is dependent on the integrity of the glyoxylate shunt." *Mol Microbiol* **72**(2): 297-306.
Riistama, S., A. Puustinen, A. Garcia-Horsman, S. Iwata, H. Michel and M. Wikstrom (1996). "Channelling of dioxygen into the respiratory enzyme." *Biochim Biophys Acta* **1275**(1-2): 1-4.
Ristow, M. and S. Schmeisser (2011). "Extending life span by increasing oxidative stress." *Free Radic Biol Med* **51**(2): 327-336.
Robin, M. A., H. K. Anandatheerthavarada, G. Biswas, N. B. Sepuri, D. M. Gordon, D. Pain and N. G. Avadhani (2002). "Bimodal targeting of microsomal CYP2E1 to mitochondria through activation of an N-terminal chimeric signal by cAMP-mediated phosphorylation." *J Biol Chem* **277**(43): 40583-40593.
Rodrigues, M. S., M. M. Reddy and M. Sattler (2008). "Cell cycle regulation by oncogenic tyrosine kinases in myeloid neoplasias: from molecular redox mechanisms to health implications." *Antioxid Redox Signal* **10**(10): 1813-1848.
Rosen, C. G. and G. Weber (1969). "Dimer formation from 1-amino-8-naphthalenesulfonate catalyzed by bovine serum albumin. A new fluorescent molecule with exceptional binding properties." *Biochemistry* **8**(10): 3915-3920.
Rutter, J., D. R. Winge and J. D. Schiffman (2010). "Succinate dehydrogenase - Assembly, regulation and role in human disease." *Mitochondrion* **10**(4): 393-401.

Samokhvalov, V., V. Ignatov and M. Kondrashova (2004). "Reserve carbohydrates maintain the viability of Saccharomyces cerevisiae cells during chronological aging." *Mech Ageing Dev* **125**(3): 229-235.
Santos, M. A., C. Cheesman, V. Costa, P. Moradas-Ferreira and M. F. Tuite (1999). "Selective advantages created by codon ambiguity allowed for the evolution of an alternative genetic code in Candida spp." *Mol Microbiol* **31**(3): 937-947.

Sass, E., S. Karniely and O. Pines (2003). "Folding of fumarase during mitochondrial import determines its dual targeting in yeast." *J Biol Chem* **278**(46): 45109-45116.
Sathananthan, A. H. and A. O. Trounson (2000). "Mitochondrial morphology during preimplantational human embryogenesis." *Hum Reprod* **15 Suppl 2**: 148-159.
Schieber, M. and N. S. Chandel (2014). "ROS function in redox signaling and oxidative stress." *Curr. Biol.* **24**(10): R453-462.
Schiller, D., Y. C. Cheng, Q. Liu, W. Walter and E. A. Craig (2008). "Residues of Tim44 involved in both association with the translocon of the inner mitochondrial membrane and regulation of mitochondrial Hsp70 tethering." *Mol Cell Biol* **28**(13): 4424-4433.
Schmidt, O., A. B. Harbauer, S. Rao, B. Eyrich, R. P. Zahedi, D. Stojanovski, B. Schonfisch, B. Guiard, A. Sickmann, N. Pfanner and C. Meisinger (2011). "Regulation of mitochondrial protein import by cytosolic kinases." *Cell* **144**(2): 227-239.
Schmidt, S., A. Strub, K. Rottgers, N. Zufall and W. Voos (2001). "The two mitochondrial heat shock proteins 70, Ssc1 and Ssq1, compete for the cochaperone Mge1." *J Mol Biol* **313**(1): 13-26.
Schneider, A., M. Behrens, P. Scherer, E. Pratje, G. Michaelis and G. Schatz (1991). "Inner membrane protease I, an enzyme mediating intramitochondrial protein sorting in yeast." *EMBO J* **10**(2): 247-254.
Shadel, G. S. and T. L. Horvath (2015). "Mitochondrial ROS signaling in organismal homeostasis." *Cell* **163**(3): 560-569.
Sideris, D. P., N. Petrakis, N. Katrakili, D. Mikropoulou, A. Gallo, S. Ciofi-Baffoni, L. Banci, I. Bertini and K. Tokatlidis (2009). "A novel intermembrane space-targeting signal docks cysteines onto Mia40 during mitochondrial oxidative folding." *J Cell Biol* **187**(7): 1007-1022.
Siegenthaler, R. K. and P. Christen (2005). "The importance of having thermosensor control in the DnaK chaperone system." *J Biol Chem* **280**(15): 14395-14401.
Sirrenberg, C., M. Endres, H. Folsch, R. A. Stuart, W. Neupert and M. Brunner (1998). "Carrier protein import into mitochondria mediated by the intermembrane proteins Tim10/Mrs11 and Tim12/Mrs5." *Nature* **391**(6670): 912-915.
Stadtman, E. R., H. Van Remmen, A. Richardson, N. B. Wehr and R. L. Levine (2005). "Methionine oxidation and aging." *Biochim Biophys Acta* **1703**(2): 135-140.
Steensels, J., T. Snoek, E. Meersman, M. Picca Nicolino, K. Voordeckers and K. J. Verstrepen (2014). "Improving industrial yeast strains: exploiting natural and artificial diversity." *FEMS Microbiol Rev* **38**(5): 947-995.

Stiburek, L., K. Vesela, H. Hansikova, P. Pecina, M. Tesarova, L. Cerna, J. Houstek and J. Zeman (2005). "Tissue-specific cytochrome c oxidase assembly defects due to mutations in SCO2 and SURF1." *Biochem J* **392**(Pt 3): 625-632.

Strobel, G., A. Zollner, M. Angermayr and W. Bandlow (2002). "Competition of spontaneous protein folding and mitochondrial import causes dual subcellular location of major adenylate kinase." *Mol Biol Cell* **13**(5): 1439-1448.

Strogolova, V., A. Furness, M. Robb-McGrath, J. Garlich and R. A. Stuart (2012). "Rcf1 and Rcf2, members of the hypoxia-induced gene 1 protein family, are critical components of the mitochondrial cytochrome bc1-cytochrome c oxidase supercomplex." *Mol Cell Biol* **32**(8): 1363-1373.

Stuart, R. A., A. Gruhler, I. van der Klei, B. Guiard, H. Koll and W. Neupert (1994). "The requirement of matrix ATP for the import of precursor proteins into the mitochondrial matrix and intermembrane space." *Eur J Biochem* **220**(1): 9-18.

Su, C. H., G. P. McStay and A. Tzagoloff (2014). "The Cox3p assembly module of yeast cytochrome oxidase." *Mol Biol Cell* **25**(7): 965-976.

Szczepanek, K., E. J. Lesnefsky and A. C. Larner (2012). "Multi-tasking: nuclear transcription factors with novel roles in the mitochondria." *Trends Cell Biol* **22**(8): 429-437.

Taanman, J. W. and R. A. Capaldi (1993). "Subunit VIa of yeast cytochrome c oxidase is not necessary for assembly of the enzyme complex but modulates the enzyme activity. Isolation and characterization of the nuclear-coded gene." *J Biol Chem* **268**(25): 18754-18761.

Tarrago, L., A. Kaya, E. Weerapana, S. M. Marino and V. N. Gladyshev (2012). "Methionine sulfoxide reductases preferentially reduce unfolded oxidized proteins and protect cells from oxidative protein unfolding." *J Biol Chem* **287**(29): 24448-24459.

Towpik, J. (2005). "Regulation of mitochondrial translation in yeast." *Cell Mol Biol Lett* **10**(4): 571-594.

Tsukada, M. and Y. Ohsumi (1993). "Isolation and characterization of autophagy-defective mutants of Saccharomyces cerevisiae." *FEBS Lett* **333**(1-2): 169-174.

Tsukihara, T., H. Aoyama, E. Yamashita, T. Tomizaki, H. Yamaguchi, K. Shinzawa-Itoh, R. Nakashima, R. Yaono and S. Yoshikawa (1995). "Structures of metal sites of oxidized bovine heart cytochrome c oxidase at 2.8 A." *Science* **269**(5227): 1069-1074.

Tsukihara, T., H. Aoyama, E. Yamashita, T. Tomizaki, H. Yamaguchi, K. Shinzawa-Itoh, R. Nakashima, R. Yaono and S. Yoshikawa (1996). "The whole structure of the 13-subunit oxidized cytochrome c oxidase at 2.8 A." *Science* **272**(5265): 1136-1144.

van der Laan, M., N. Wiedemann, D. U. Mick, B. Guiard, P. Rehling and N. Pfanner (2006). "A role for Tim21 in membrane-potential-dependent preprotein sorting in mitochondria." *Curr Biol* **16**(22): 2271-2276.

Vanegas, J. M., M. F. Contreras, R. Faller and M. L. Longo (2012). "Role of unsaturated lipid and ergosterol in ethanol tolerance of model yeast biomembranes." *Biophys J* **102**(3): 507-516.

Vevea, J. D., T. C. Swayne, I. R. Boldogh and L. A. Pon (2014). "Inheritance of the fittest mitochondria in yeast." *Trends Cell Biol* **24**(1): 53-60.

Vogel, F., C. Bornhovd, W. Neupert and A. S. Reichert (2006). "Dynamic subcompartmentalization of the mitochondrial inner membrane." *J Cell Biol* **175**(2): 237-247.

Vogt, W. (1995). "Oxidation of methionyl residues in proteins: tools, targets, and reversal." *Free Radic Biol Med* **18**(1): 93-105.

Vogtle, F. N., S. Wortelkamp, R. P. Zahedi, D. Becker, C. Leidhold, K. Gevaert, J. Kellermann, W. Voos, A. Sickmann, N. Pfanner and C. Meisinger (2009). "Global analysis of the mitochondrial N-proteome identifies a processing peptidase critical for protein stability." *Cell* **139**(2): 428-439.

Vongsamphanh, R., P. K. Fortier and D. Ramotar (2001). "Pir1p mediates translocation of the yeast Apn1p endonuclease into the mitochondria to maintain genomic stability." *Mol Cell Biol* **21**(5): 1647-1655.

Voos, W., B. D. Gambill, S. Laloraya, D. Ang, E. A. Craig and N. Pfanner (1994). "Mitochondrial GrpE is present in a complex with hsp70 and preproteins in transit across membranes." *Mol Cell Biol* **14**(10): 6627-6634.

Vukotic, M., S. Oeljeklaus, S. Wiese, F. N. Vogtle, C. Meisinger, H. E. Meyer, A. Zieseniss, D. M. Katschinski, D. C. Jans, S. Jakobs, B. Warscheid, P. Rehling and M. Deckers (2012). "Rcf1 mediates cytochrome oxidase assembly and respirasome formation, revealing heterogeneity of the enzyme complex." *Cell Metab* **15**(3): 336-347.

Wang, W., J. R. Winther and C. Thorpe (2007). "Erv2p: characterization of the redox behavior of a yeast sulfhydryl oxidase." *Biochemistry* **46**(11): 3246-3254.

Waizenegger, T., S. J. Habib, M. Lech, D. Mokranjac, S. A. Paschen, K. Hell, W. Neupert and D. Rapaport (2004). "Tob38, a novel essential component in the biogenesis of beta-barrel proteins of mitochondria." *EMBO Rep* **5**(7): 704-709.

Wallace, D. C. (2007). "Why do we still have a maternally inherited mitochondrial DNA? Insights from evolutionary medicine." *Annu Rev Biochem* **76**: 781-821.

Warner, H. R. (1994). "Superoxide dismutase, aging, and degenerative disease." *Free Radic Biol Med* **17**(3): 249-258.

Weckbecker, D., S. Longen, J. Riemer and J. M. Herrmann (2012). "Atp23 biogenesis reveals a chaperone-like folding activity of Mia40 in the IMS of mitochondria." *EMBO J* **31**(22): 4348-4358.

Wei, H., L. Liu and Q. Chen (2015). "Selective removal of mitochondria via mitophagy: distinct pathways for different mitochondrial stresses." *Biochim Biophys Acta* **1853**(10 Pt B): 2784-2790.

Welch, W. J. (1993). "Heat-Shock Proteins Functioning as Molecular Chaperones - Their Roles in Normal and Stressed Cells." *Philos. Trans. R. Soc. London Series B-Biological Sciences* **339**(1289): 327-333.

Westermann, B., C. Prip-Buus, W. Neupert and E. Schwarz (1995). "The role of the GrpE homologue, Mge1p, in mediating protein import and protein folding in mitochondria." *EMBO J* **14**(14): 3452-3460.

Wiedemann, N., V. Kozjak, T. Prinz, M. T. Ryan, C. Meisinger, N. Pfanner and K. N. Truscott (2003). "Biogenesis of yeast mitochondrial cytochrome c: a unique relationship to the TOM machinery." *J Mol Biol* **327**(2): 465-474.

Wiedemann, N., M. van der Laan, D. P. Hutu, P. Rehling and N. Pfanner (2007). "Sorting switch of mitochondrial presequence translocase involves coupling of motor module to respiratory chain." *J Cell Biol* **179**(6): 1115-1122.

Witte, C., R. E. Jensen, M. P. Yaffe and G. Schatz (1988). "MAS1, a gene essential for yeast mitochondrial assembly, encodes a subunit of the mitochondrial processing protease." *EMBO J* **7**(5): 1439-1447.

Wright, R. M., L. K. Dircks and R. O. Poyton (1986). "Characterization of COX9, the nuclear gene encoding the yeast mitochondrial protein cytochrome c oxidase subunit VIIa. Subunit VIIa lacks a leader peptide and is an essential component of the holoenzyme." *J Biol Chem* **261**(36): 17183-17191.

Wu, C. C., V. Naveen, C. H. Chien, Y. W. Chang and C. D. Hsiao (2012). "Crystal structure of DnaK protein complexed with nucleotide exchange factor GrpE in DnaK chaperone system: insight into intermolecular communication." *J Biol Chem* **287**(25): 21461-21470.

Yankovskaya, V., R. Horsefield, S. Tornroth, C. Luna-Chavez, H. Miyoshi, C. Leger, B. Byrne, G. Cecchini and S. Iwata (2003). "Architecture of succinate dehydrogenase and reactive oxygen species generation." *Science* **299**(5607): 700-704.

Young, O., T. Crotty, R. O'Connell, J. O'Sullivan and A. J. Curran (2010). "Levels of oxidative damage and lipid peroxidation in thyroid neoplasia." *Head Neck* **32**(6): 750-756.

Zara, V., A. Ferramosca, L. Capobianco, K. M. Baltz, O. Randel, J. Rassow, F. Palmieri and P. Papatheodorou (2007). "Biogenesis of yeast dicarboxylate carrier: the carrier signature facilitates translocation.